TECHNISCHE UNIVERSITÄT WIEN

DIPLOMARBEIT

Modelling Tube Output for Medical X-ray Systems depending on Tube Potential and Filtration

zur Erlangung des akademischen Grades

Diplom-Ingenieur/in

im Rahmen des Studiums

Biomedical Engineering

eingereicht von

Alix Péchoultre de Lamartinie
01623351

ausgeführt am

Institut für Medizinische Physik und Biomedizinische Technik der Medizinischen Universität Wien

Atominstitut der Technischen Universität Wien

Betreuer: Ao.Univ.Prof. Dipl.-Ing. Dr.techn. Peter Homolka

Wien, 31.07.2018

(Unterschrift Verfasser/in) (Unterschrift Betreuer/in)

Contents

List of abbreviations 5

Abstract 6

1. Introduction 7

1.1 Dosimetry for radiographic systems 7

1.1.1 Dosimetric quantities 7

1.1.2 Dosimeters 9

1.1.3 Calibration and standards 11

1.2 Radiographic and interventional systems 13

1.2.1 X-ray tubes 13

1.2.1 Classification of x-ray systems 14

1.3 Imaging physics 16

1.3.1 X-ray spectrum 16

1.3.2 Factors influencing x-ray spectra and output 19

1.4 Calculation models of tube output 21

2. Material and Methods 25

2.1 Calculation of absolute dose output 25

2.1.1 Modelling RQR beam qualities 25

2.1.2 Simulation using identical filtration for all kVp 27

2.2 Mathematical modelling of tube output 29

2.2.1 Calculation of Y_{100} for inherent filtration 29

2.2.2 Modelling of dose reduction factors for added filtrations 30

2.2.3 Equivalent copper thickness for Aluminum filters 31

2.2.4 Dose reduction factors as a function of kVp and filter thickness (model 1) 31

Determination of A as a constant 34

Determination of A as a function of filter thickness 35

2.2.5 Determination of DRFs from measurement points in clinical systems (model 1) 42

2.2.6 Parametrization with HVL and homogeneity coefficient (model 2) 45
2.2.7 Determination of DRFs from measurement points in clinical systems (model 2) 49
2.3 Specification of x-ray systems and measurement set up 52
2.3.1 X-ray systems 52
2.3.2 Dosimeter 53
2.3.3 Measurement set-up 53
3. Results 56
3.1 Absolute and relative output derived with XCompW and TASMICS 56
3.2 Deviations obtained with the first model when using XCompW or TASMICS 60
3.3 Output parametrization of clinical systems 61
3.4 Parametrization of DRF as a function of kV and copper thickness 63
3.5 Generic Dose output and DRFs 70
3.6 Parametrization of DRF as a function of HVL and homogeneity coefficient 74
3.7 Comparison of the models parametrizing DRFs 78
4. Discussion 81
4.1 Reference kVp 81
4.2 Choice of measurement points 82
4.2.1 Calculation of output for Inherent filtration 82
4.2.2 Calculation of output with added filtration 84
4.3 Estimation of absolute output 90
4.4 Example of calculations 96
4.5 Comparison of Austrian standards and generic model developed in this work 105
4.6 Limitations of the study 107
4.6.1 Actual vs nomial filter's thickness 107
4.6.2 Shot to shot variation 109
4.7 Recommendations 111
Conclusion 112
Acknowledgments 113

Bibliography 114
Appendix 116
Values of Figure 31 and Figure 32 116
Measurements with clinical systems 117
Precision of the measurements with system 9 120
User guide for the Matlab program 121
List of Tables 123
List of Figures 126

List of abbreviations

QA: Quality Assurance

QS: Quality System

LET: Linear Energy Transfer

WHO: World Health Organization

SI: Système International (d'unité), International System of Units

ICRU: International Commission on Radiation Units and Measurements

HVL: Half Value Layer

MOSFET: Metal Oxide Semiconductor Field Effect Transistors

IAEA: International Atomic Energy Agency

IMS: International Measurement System

PSDL: Primary Standards Dosimetry Laboratory

SSDL: Secondary Standards Dosimetry Laboratory

BIPM: Bureau International des Poids et Mesures

PTCA: Percutaneous Transluminal Coronary Angioplasty

TASMICS: Tungsten Anode Spectral Model using Interpolating Cubic Splines

DRF: Dose reduction Factor

CMPBE: Center for Medical Physics and Biomedical Engineering

Abstract

When working with x-ray systems, it is important to determine the dose output in order to get the organ dose, equivalent dose… Up to now, different programs exist to simulate the dose output, but the calculations are only based on the filtration applied, the kVp, the ripple and the anode angle. As a consequence, the results of such programs are not characteristic of clinical systems but apply to all of them, hence the lack of precision.

The goal of this master thesis is to provide a new program that will estimate the dose output of x-ray systems thanks to a few measurements. Using measurements will characterize the clinical system, and will thus increase the accuracy of the model. This program will work in two major steps: first obtaining a function for the dose output when no filtration is applied, and then for each filtration determining dose reduction factors that should be multiplied to the previous function to get the dose output when a specific filtration is applied. Different models of the dose reduction factor will be proposed, depending on the parameters chosen to describe it (kVp, thickness of copper, HVL or homogeneity coefficient). These models will be compared, and the optimal use will be determined.

1. Introduction

People are exposed to radiation from natural sources constantly, but in some countries such as Japan or the USA the largest contribution to the population dose is coming from medical ionizing radiation. This is due to the large number of x-ray examinations that are performed each year. In 2000 it was estimated that 360 examinations are done for 1000 individuals worldwide each year (UNSCEAR, 2000). This number will probably increase in the next years due to the development of medical facilities in developing countries, where medical radiology services are for now often lacking.

In the field of medical physics and radiation protection, dosimetry is the measurement, calculation and assessment of the ionizing radiation dose absorbed by the human body. (Wikipedia, 2018) As an example, the average dose to the organs and the tissues at risk should be estimated. In QA and QS, dosimetry also aims to evaluate equipment performances.

Researchers are constantly trying to minimize patient exposure, as it has been proven that radiations can have harmful effects for the body. On the other hand, the higher the dose the better the quality to be expected. As a consequence, a compromise should be found to get a readable image without exposing the patient to too high radiation doses. This is the goal of quality assurance: giving a framework to achieve a reasonable image quality without exposing the patient to a too high dose. The basic strategy has been developed by the WHO, and is based on managerial such as technical activities (WHO, 1982), and further requirements are defined by the International Basic Safety Standards for Protection against Ionizing Radiation and for the Safety of Radiation Sources (BSS) (FAO et al., 1996) or in Safety Guide No. RS-G-1.5 (IAEA, 2000b).

1.1 Dosimetry for radiographic systems

1.1.1 Dosimetric quantities

Different quantities are used in medical dosimetry.

- Kerma

The quantity kerma (K) describes the energy transferred from uncharged particle to matter. It is the acronym for Kinetic Energy Released per unit Mass. Its definition is the following:

$$K = \frac{\mathrm{d}E}{\mathrm{d}m} \qquad (1)$$

where E is the energy transferred from indirectly ionizing radiation (uncharged particles such as photons) to charged particles in a mass element d*m* of material. The unit of kerma is Gray (Gy), which corresponds to J/kg in the SI system.

- Absorbed dose

The absorbed dose D is defined as

$$D = \frac{\mathrm{d}\mathcal{E}}{\mathrm{d}m} \qquad (2)$$

where $\mathrm{d}\mathcal{E}$ is the mean energy transferred by ionizing radiation to matter of mass dm. The absorbed dose is also expressed in Gray, or J/kg.

Even if kerma and absorbed dose are expressed in the same unit and are both related to the interaction of radiation with matter, their definitions differ. Volumes where the interactions of interest take place are not equal: in the definition of kerma, this is the place where the energy is transferred from uncharged to charged particles, whereas for absorbed dose it is the place where the kinetic energy of charged particles is spent.

- Organ and tissue dose

The mean absorbed dose in an organ or in a tissue D_T is defined as the ratio of the energy transferred to the organ / tissue $\mathcal{E}_T$ and the mass m_T of the organ / tissue:

$$D_T = \frac{\mathcal{E}_T}{m_T} \qquad (3)$$

This is sometimes only called the organ dose.

- Equivalent dose

Even if the absorbed dose is the same, if different types of ionizing radiation are applied, the stochastic effects might not have the same magnitude. The equivalent dose H_T takes the dependence on LET roughly into account by weighting the organ dose D_T with a radiation weighting factor w_R, R referring to the type of the radiation:

$$H_T = w_R * D_T \qquad (4)$$

The unit of the equivalent dose is the Sievert (Sv), which correspond to J/kg. For high energy photon radiations such as x-ray and gamma radiation, w_R is taken to be unity.

According to ICRU 74 (ICRU Report 74, 2006) and IAEA TRS 457 (IAEA, 2007), the x-ray tube output per mAs Y(d) in a distance d from the focal spot is defined as the quotient of the air kerma $K_a(d)$ from the x-ray tube focal spot by the tube-current exposure–time product, P_{It}. Thus $Y(d) = \frac{K_a(d)}{P_{It}}$. Its unit is J/(kg/C) or Gy/mAs.

When d is equal to 100 cm, the tube output is usually written Y_{100}. The tube-current exposure time product is sometimes also referred as the tube loading.

- HVL

HVL stands for Half Value Layer. It corresponds to the thickness of a material that attenuates a measured quantity (usually the air kerma) to half of its original value in a scatter-free narrow beam geometry, and is usually used to describe the quality of the beam. The first and second HVL should be distinguished: HVL_1 attenuates the initial air kerma by a factor of two, and HVL_2 is the thickness that is needed to attenuate it once again by a factor of two. From these two values, the homogeneity coefficient h can be determined:

$$h = \frac{HVL_1}{HVL_2} \qquad (5)$$

The values of h are between 0 and 1, with higher values indicating a narrower spectrum. For diagnostic radiology, h is usually between 0.7 and 0.9 (IAEA, 2007).

1.1.2 Dosimeters

Dose measurements are essential in quality control and acceptance testing, hence the need of dosimeters. Important properties of these instruments are:

- Sensitivity: the minimum air kerma required to produce a signal output should be low but remain reliable
- Linearity: the dosimeter should exhibit a linear response for a wide range of air kerma (from sub µGy to several hundred mGy). The non-linear behaviour depends on the type of dosimeter and its physical properties. As an example, saturation effects determine the upper value. (IAEA, 2014)
- Energy dependence: the x-ray spectrum is one of the most important quantities affecting the response of a dosimeter.

There are two major types of dosimeters: ionization chambers and solid state dosimeters, which can also be classified into active or passive device. Active devices can display the dose value directly, contrary to passive devices which need a reading device.

- Ionization chambers

This type of dosimeter consists of a chamber filled with air and two electrodes inside. An electric field is formed when a voltage is applied across them. This enables to collect most of the charges created by the ionization of the air within the chamber. The number of collected ions corresponds to the recorded signal. To obtain the energy transferred $\mathcal{E}_{tr}$ from the radiation to the mass of air, this number has to be multiplied with the mean energy required to produce an ion pair in dry air. ($\overline{W}_{air}$ = 33.97eV/ion pair = 33.97 J/C) The air kerma is defined as the ratio of $\mathcal{E}_{tr}$ and the mass of air. In order to obtain the air kerma rate, the recorded signal is the rate of the collection of the ions. Different designs are possible, but the

gap between the two electrodes should always be kept small to prevent ion recombination at high dose.(IAEA, 2014)

- Solid state dosimeters

Different types of solid state dosimeters exist, the most common one being the thermoluminescent and the semiconductor dosimeters. There are two major types of semiconductor dosimeters: silicon diodes (Figure 1) or MOSFETs (Figure 2). Their small size and their ability to respond immediately after the irradiation give them some advantages in many applications.

The silicon diode dosimeter consists of a p-n junction. When ionizing radiation interacts with the semiconductor, electron hole pairs are created and the junction becomes conductive. The higher the rate of ion production is, the higher the current will be. The height of the signal depends on the properties of the radiation, but semiconductor devices can usually produce large signals only from modest amount of radiation. In most cases, p type diodes are chosen because radiation produces less damage in these, than in with n type diodes. (IAEA, 2014)

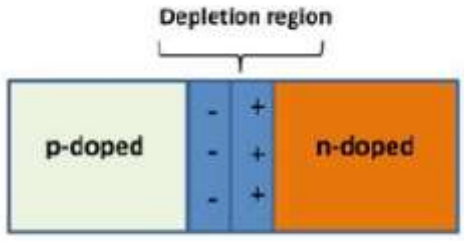

Figure 1 - Cross-sectional diagram of a silicon diodes. From: (IAEA, 2014)

A MOSFET is a silicon transistor. It can measure the threshold voltage, which depends linearly on the absorbed dose. This threshold corresponds to the minimum gate-to-source voltage that is needed to create a conducting path between the source and the drain. When ionizing radiation interacts with the semiconductor, electron hole pairs are created in the SiO_2 region. If a positive voltage is applied at the gate, the positive charge carriers will move toward the SiO_2 – Si border and will be trapped here. The depletion region is then populated by the negative charge carriers, and an electron channel is thus formed, creating a conducting path.

MOSFETs are principally used in patient dosimetry. The major drawback of semiconductor dosimeters is their energy dependence which is more pronounced than for ionization chambers.

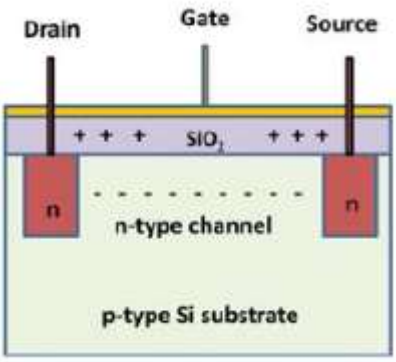

Figure 2 - Cross-sectional section of a MOSFET (IAEA, 2014)

1.1.3 Calibration and standards

It is important to standardize procedures for dose measurements. The instruments need to be calibrated in a way that the measurements are traceable to international standards. This traceability is ensured through the IMS for radiation metrology (Figure 3).

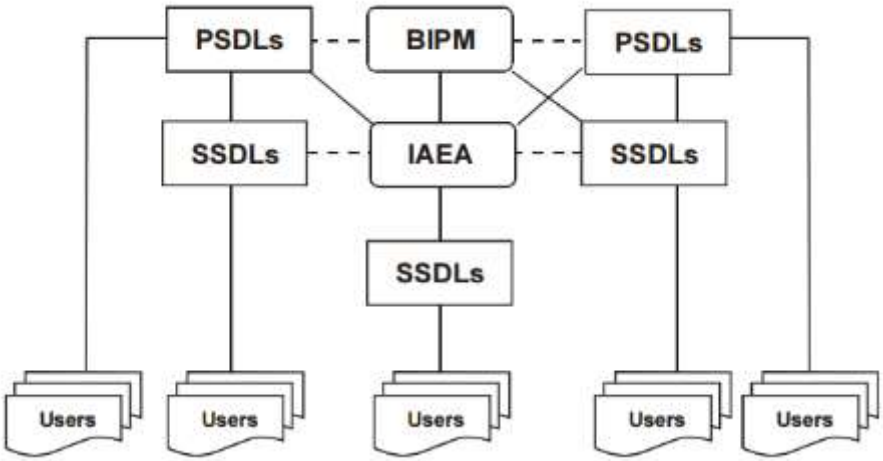

Figure 3 – International Measurement System for radiation dosimetry. The calibration can either be done directly in a PSDL or via a SSPD which is linked to the BIPM, a PSDL or the IAEA/WHO network of SSDLs. The dashed lines indicate intercomparisons of primary and secondary standards (IAEA, 2000a).

A PSDL is a laboratory that tries to develop and improve primary standards in radiation dosimetry, and it provides calibration services for secondary standard instruments. Only about twenty PSDLs exist worldwide, and this is not sufficient to calibrate all the dosimeters of the world, hence the need of SSDLs. These are laboratories which are equipped with secondary standards calibrated in a PSDL. So the goal of SSDLs is to fill the gap between a PSDL and the dosimeter user.

Dosimeters are calibrated in order to fulfil the IEC-61267 standard (IEC, 2005). Depending on the application, different radiation quality series can be used (cf. Table 1) which all consist of several calibration points.

Radiation quality	***Radiation origin***	***Material of an additional filter***	***Application***
RQR	Radiation beam emerging from x-ray assembly	No phantom	General radiography, fluoroscopy and dental applications
RQA	Radiation beam with an added filter	Aluminum	Measurements behind the patient
RQT	Radiation beam with an added filter	copper	CT applications
RQR – M	Radiation beam emerging from x-ray assembly	No phantom	Mammography applications
RQA - M	Radiation beam with an added filter	Aluminum	Mammography studies

Table 1 - radiation qualities for calibrations of diagnostic dosimeters (adapted from (IAEA, 2007))

Table 2 gives the characteristics of the radiation qualities of the RQR series.

Radiation quality	***X ray tube voltage (kV)***	***First HVL (mm Al)***	***Homogeneity coefficient (h)***
RQR 2	40	1.42	0.81
RQR 3	50	1.78	0.76
RQR 4	60	2.19	0.74
RQR 5[a]	70	2.58	0.71
RQR 6	80	3.01	0.69
RQR 7	90	3.48	0.68
RQR 8	100	3.97	0.68
RQR 9	120	5.00	0.68
RQR1 0	150	6.57	0.72

[a] This quality is generally selected as the reference of the RQR series.

Table 2 - Characterization of radiation quality series RQR used for unattenuated beams (according to (IEC, 2005)).

The first step to calibrate a dosimeter is to adjust the x-ray tube voltage to the value of the second column of Table 2. Then the amount of filtration needed to obtain the HVL value given in the third column should be determined. This can simply be done by measuring the attenuation curve. Once the first HVL is fixed, the second HVL can be measured, and the homogeneity coefficient can be calculated. Its value

should lie within 0.03 of the value given in the fourth column. The kVp value can be tweaked a little to comply with HVL and h if this is necessary.

1.2 Radiographic and interventional systems

1.2.1 X-ray tubes

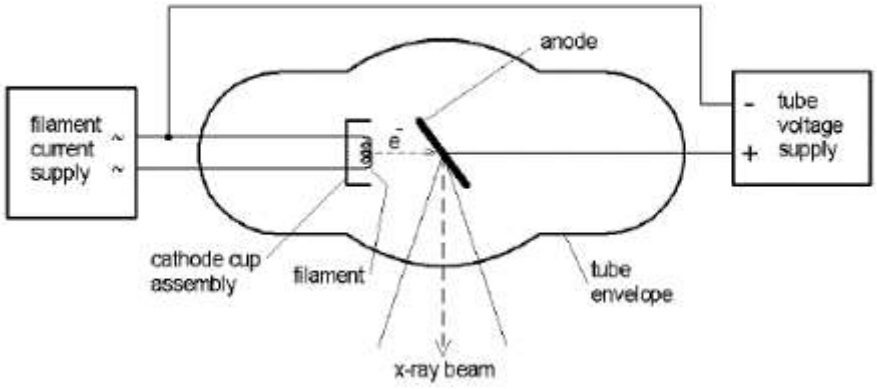

Figure 4 - Components of an x-ray tube (IAEA, 2014)

Figure 4 shows the principal components of an x-ray tube. It consists of:

- an electron source from a heated Tungsten filament. This filament is placed in a focusing cup serving as the tube cathode
- an anode, which corresponds to the target of the electrons
- a tube envelope.

A current heats the filament that will in return emit electrons. The tube current resulting from glow emission is linked to the filament temperature by the Richardson-Dushman law, which gives the saturation current density:

$$j_s = \frac{4\Pi me}{h^3}(kT)^2 e^{\frac{W-\Delta W}{kT}} \text{ where } \Delta W = \sqrt{\frac{e^3 E}{4\,\Pi\varepsilon_0}} \qquad (6)$$

with j_s: surface current density, m: electron mass, e: electron charge, h: Planck constant, W: work function, k: Boltzmann constant, T: temperature of the solid, E: external electrical field strength, ε_0: dielectric vacuum constant. This equation assumes that every electron with an appropriate energy level and direction can pass the surface.

This anode current is typically smaller than 10 mA in fluoroscopy, but it ranges from 100 mA to more than 1000 mA in single exposure mode. The potential difference between anode and cathode

corresponding to the kVp ranges typically from 40 to 125 kVp in radiography, and up to 140 kVp in CT. In mammography, it ranges from 25kVp to 40 kVp.

The major function of the cathode is to send electrons to the anode in a well-defined beam. Usually, electrons do not escape electrical circuits to move into free space. This is only possible if they receive enough energy to escape. The height of this barrier is the work function W. When the filament of the cathode is heated up, the electrons on the surface gain energy. This allows them to move a little away from the surface, thus resulting in emission, called thermionic emission.

The anode has two primary functions:

- converting electronic energy into x-ray radiation
- dissipating the heat that is created during this process.

It is a piece of metal which usually consists of an alloy of Tungsten and Rhenium for radiology applications. Tungsten is the best choice of material due to its high atomic number (Z = 74) leading to a high Bremsstrahlung yield and due to its good thermal properties (melting point of 3422°C, and low evaporation rate). A small proportion of Rhenium is usually added to reduce electron sputter yield. Most anodes are built as rotating anode assemblies to dissipate the heat.

The electronic focal spot is the area of the anode where the radiations are produced. Its dimensions depend on the dimensions of the electron beam coming from the cathode. Small focal spots produce less blurring and give better visibility of details, but large focal spots dissipate more heat. Usually x-ray tubes have two focal spots, which can be chosen depending on the application.

The anode is inclined to the tube axis. The anode angle ranges from 6° to 22° depending on their task, but for most application anode angles between 10° to 16° are used (IAEA, 2014).

The tube envelope is mostly made of glass. It provides an electrical insulation for the cathode and the anode, and ensures a vacuum inside the tube.

1.2.1 Classification of x-ray systems

X-ray systems can be used for imaging of the skeleton, the skull, the thorax, the body and the blood vessel, as well as for interventional procedures. All systems comprise some basic elements:

- an x-ray tube with a generator
- a detection device, usually with an anti-scatter grid
- an image processing chain
- a display unit

- Radiography systems

Radiography systems are mostly used for imaging the thorax and the skeleton, and they acquire single exposures. The x-ray tube and the generator can be used in many configurations, so that the whole body can be imaged (in particular thanks to ceiling support). Until the 1980s, only film-screen systems were implemented, but since then digital imaging has emerged, the two main technologies being either flat panel detectors (direct or indirect) or storage phosphor plates. Digital imaging enables a dose reduction of around 50% for the same image quality (Völk M. et al., 2004). As a consequence, more applications are available for image processing, such as zooming, windowing or filtering(Siemens, 2005). The resolution of flat detectors is around 3.5 lp/mm. This depends on the size of the focal spot that has been chosen. Typical x-ray tubes provide an electrical power up to 80kW and a focal spot of around 1mm (Völk M. et al., 2004). A large focal spot and a large power will be chosen to optimize the image quality in case of highly absorbing body regions, whereas small focal spot is needed to obtain the highest spatial resolution(Siemens, 2005). All systems also contain an Automatic Exposure Control to eliminate under- and overexposure.

- Fluoroscopy systems

Fluoroscopy systems can be used for general radiography, but their major goal remains the imaging of dynamic processes. The most common fluoroscopy examinations are the oesophagus, the stomach, the colon, and if coupled with contrast agents they can realise phlebography (examination of the venous system), myelography (examination of the spinal cord) and vascular imaging. The distance between the source and the image can vary to change the degree of magnification, and the tube angulations can be adjusted to minimize the overlapping of anatomical structures. In order to efficiently perform real-time examinations, the temporal resolution of the detector should be high enough. Fluoroscopy systems are equipped for digital imaging, so that they can all apply post processing techniques.

- Angiography systems

Angiography systems are used for vascular imaging and intervention, but due to the development of CT and MR angiography, they are now mostly only used for real-time guidance and control of interventional procedures, such as PTCA procedures. In these procedures, the electrical power of the x-ray tube can be up to 80kW, and some offers three different focal spots (0.3, 0.6 and 1mm) depending on the dose rate and the level of detail that should be achieved.. To enable depiction of the vascular system, iodinate contrast media are applied using a (mostly arterial, in case of phlebography venous) catheter. As a consequence, the procedure should be performed under sterile conditions. To remove superimposition of bone, digital subtraction angiography is used. This technique gives a final image from the subtraction of pre- and post-contrast images in order to clearly visualize blood vessels in a dense environment. Two different types of system exist: monoplane systems, which consist of one C-arm, and biplane systems, which have two C-arms and can thus simultaneously register projections from two different angles. A

C-arm consists of an x-ray tube and its detector mounted on a C-shaped support. It allows the acquisition of many viewing angles. The rotation can be achieved around three mechanical axes: one parallel to the patient's table, two others perpendicular to each other and to the first axis. The detector should be as close as possible to the patient in order to minimize the dose and to optimize the quality of the image.

- Cardiology systems

Cardiology systems are useful for the diagnosis of cardiac diseases and for coronary intervention. As in angiography, monoplane and biplanes systems can be employed, the latter being more appropriate for paediatric cardiology (Siemens, 2005). Due to the motion of the heart, it is necessary to use higher frame rate. In adult cardiology, 15 to 30 frames/second are used, and up to 60 frames/second for paediatric cardiology (Siemens, 2005). Two focal spot sizes can be used in cardiology: 0.4 and 0.8 mm. The power of the tube can be up to 80 kW. Cardiology systems also offer to acquire and display the patient's vital signs.

1.3 Imaging physics

1.3.1 X-ray spectrum

The bombardment of electrons on a thick target leads to the production of x-rays. These electrons are slowed down because of collisions and scattering events. As a consequence, bremsstrahlung and characteristic radiation are produced.

- Bremsstrahlung

As an accelerated free electron approaches an atomic nucleus, attractive Coulomb forces result in a trajectory alteration. As a consequence, it emits bremsstrahlung, and becomes less energetic. The energy of the photon depends mainly on the charges of the nucleus and the electron and on the distance between them.

A model giving the energy fluence of photon and based only on bremsstrahlung has been developed by Kramers. It describes the thick target as a stack of thin slabs, each of them producing a rectangular distribution of energy fluence Ψ (cf. Figure 5 (a)). According to Kramers' law, the energy fluence Ψ at photon energy E is defined as follows:

$$\Psi(E) = CZI_{tube}(E_0 - E), for\ E < E_0 \quad (7)$$

$$\Psi(E) = 0, for\ E > E_0, \quad (8)$$

where Z is the atomic number of the metal target, I_{tube} is the current of the incident electrons and E_0 is their kinetic energy. By applying a voltage V_0, these electrons are accelerated before striking the material, so that their energy E_0 can be defined as eV_0, with e the electron charge. Kramers' law predicts that the energy fluence Ψ increases with decreasing energy E.

The electron will be slowed down in each layer, so that the maximal kinetic energy will decrease as it progresses inside the target. The superposition of all those rectangular distributions gives rise to a triangular energy fluence distribution shown in Figure 5 (b). This spectrum is called 'ideal spectrum' as it is a simplification. Indeed, quantum mechanics has shown that thin layers do not have rectangular distribution of x-ray energy fluence, and that the energy of the electron decreases continuously and not in a stepwise manner from layer to layer.

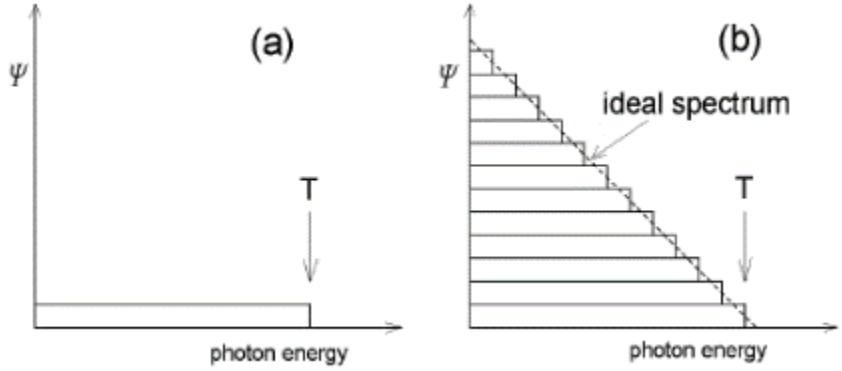

Figure 5 - (a) Distribution of the energy fluence for a thin target bombarded with electrons of kinetic energy T. (b) Triangular spectrum obtained if a thick target is considered as a superposition of thin targets. From: (IAEA, 2014).

By integrating the previous equation over E, the total energy fluence can be approximated:

$$\Psi(E) = CZI_{tube}V_0^2 \qquad (9)$$

Considering this model, the radiation output of an x-ray tube is proportional to the square of the tube voltage. This is only true if spectral changes due to attenuation and emission of characteristic radiation are not taken into account. In addition, contrary to Kramers' law prediction, the exponent changes with the filtration (see 1.3.2). Nevertheless, it can already give a first approximation.

- Characteristic radiation

Characteristic radiations result from the interaction of two electrons. If a fast electron e_1 collides with an electron e_2 of an atomic shell, and if the kinetic energy of e_1 is larger than the binding energy of e_2, then e_2 might be ejected from the atomic shell. The vacancy in the shell is filled with an electron from an outer shell, which might at the same time emit an x-ray photon with an energy equal to the difference of the binding energies of the shells. This radiation along with the binding energies is characteristic for each element, hence the name of characteristic radiation. Table 3 shows the binding energies and the K radiation energies for the materials commonly used in diagnostic radiology.

It should be noted that Auger electrons can also be produced. In this case, instead of characteristic radiation, the excess of energy is given to an electron that is expelled from the shell. The higher the atomic number of the anode is, the smaller the probability of Auger electron is.

Element	Binding energy (keV)		Energies of characteristic x-rays (keV)			
	L shell	K shell	$K_{\alpha 1}$	$K_{\alpha 2}$	$K_{\beta 1}$	$K_{\beta 2}$
Mo	2.87/2.63/2.52	20.00	17.48	17.37	19.61	19.97
Rh	3.41/3.15/3.00	23.22	20.22	20.07	22.72	23.17
W	12.10/11.54/10.21	69.53	59.32	57.98	67.24	69.07

Table 3 - Binding energies and H radiation energies of common anode materials (IAEA, 2014)

- Self-absorption

After being accelerated towards the anode, the electrons are slowed down and stopped inside the anode, typically within tens of micrometres (depending on the tube voltage). So x-rays will be attenuated by the anode material as seen in the Heel effect. Thus, low energy photons are absorbed directly after production in the anode. This partially explains why the spectrum does not have the triangular shape predicted by Kramers model. This self-absorption seems more important for low kVp. The final spectrum is obtained by also taking characteristic radiations into account. If some filtration is added, the spectrum will also be modified. Figure 6 shows that a total filtration of 2.5 mm of Aluminum (which is the minimum required total filtration) leads to the absorption of the L radiation, so that only the K radiation can be seen. It also compares the spectrum predicted by Kramers' law with real unfiltered and real filtered spectra .

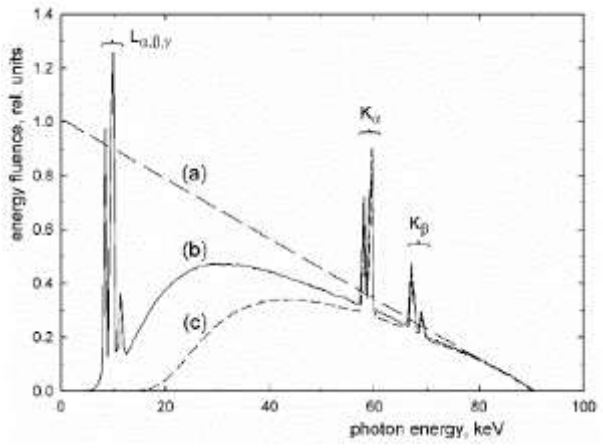

Figure 6 - (a) Ideal bremsstrahlung spectrum for a Tungsten anode and a tube voltage of 90 kVp, (b) actual spectrum includind characteristic x-rays for an inherent filtration of 1mm Be, (c) spectrum filtered with 2.5mm Al eq. From: (IAEA, 2014)

1.3.2 Factors influencing x-ray spectra and output

- Tube voltage

Figure 7 shows that the tube potential affects the maximum photon energy, the average photon energy and the area under the spectra which is related to x-ray output. The following dependence can usually be observed:

$$x\_ray\ output\ \alpha\ (kVp)^{a}, \qquad with\ 1.8 < a < 2.3$$

$$HVL\ \alpha\ (kVp)^{x},\ with\ x \cong 1.1$$ *(for a generator with 2.5mm of Aluminum-equivalent inherent tube filtration)*

a depends on the total filtration and the amount of ripple (Nickoloff E. L. and Berman H. L., 1993).

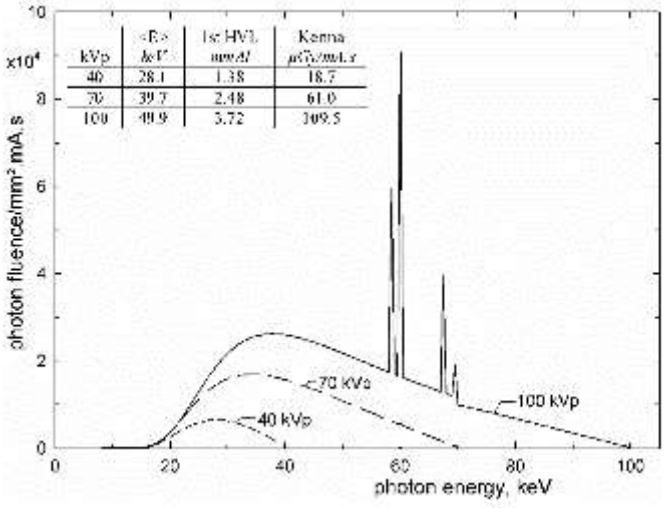

Figure 7 - X-ray spectra for different tube voltages. From: (IAEA, 2014)

- Ripple

The ripple is defined as the percentage of the relative difference of the minimum voltage kV_{min} from the peak voltage:

$$R = \frac{kVp - kV_{min}}{kVp} \qquad (10)$$

Figure 8 plots different spectra for different ripples. This graph shows that the ripple affects the amount of x-ray produced and their energy distribution: an increase in ripple leads to less production of x-ray and a degradation of their energy distribution.

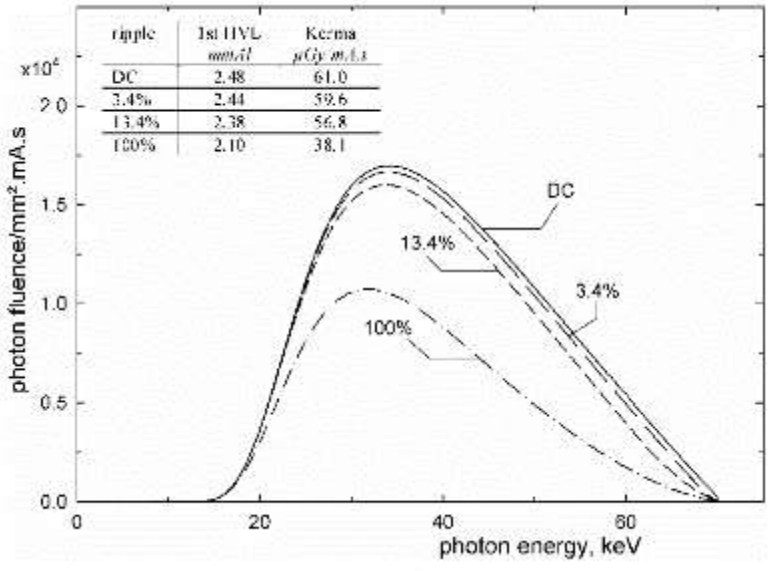

Figure 8 - X-ray spectra for various tube voltage ripple at 70 kVp. From: (IAEA, 2014)

- Anode angle

Different spectra for different anode angles are shown in Figure 9. The anode angle affects mostly the low energy part of the spectrum. The lower it is, the higher the absorption length will be and as a consequence the harder the beam will be. The x-ray output will also decrease.

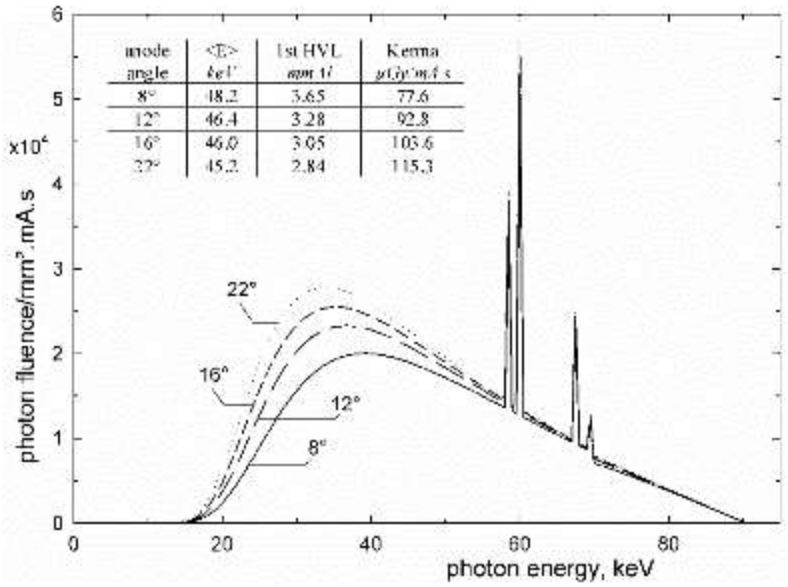

Figure 9 - X-ray spectra for different anode angles. From: (IAEA, 2014)

- Filtration

Photons with very low to low energies exhibit little chances to reach the imaging detector and thus contribute mainly to patient dose. They should be removed to minimize the dose, hence the use of

filtrations. The spectrum will vary depending on the material used as filter and on its thickness, as shown in Figure 10. The thicker the filter is, the lower the x-ray output will be. In diagnostic radiology, the two most common material used as a filtration are Aluminum and copper. Commonly available filters in x-ray devices are 1mm Al, 2 mm Al, sometimes combined with copper as 1 mm Al plus 0.1 mm or 0.2 mm Cu, and pure copper filter sheets from 0.1 to 0.9 mm thickness.

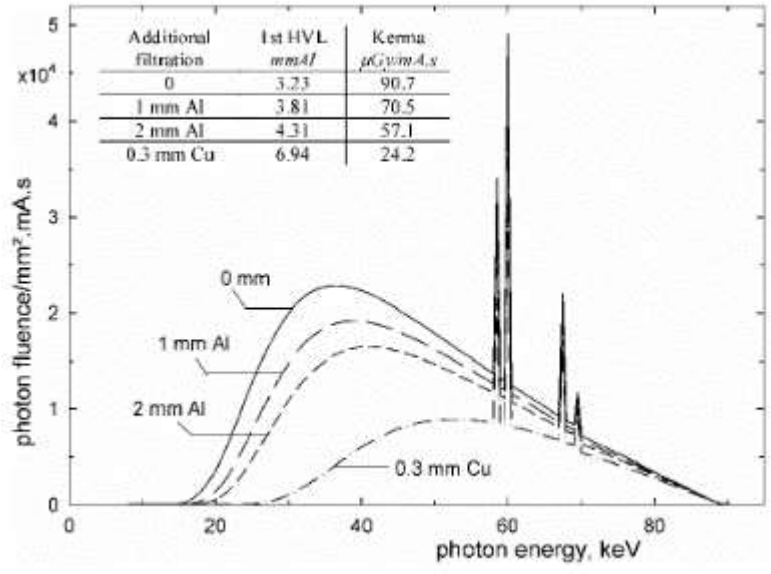

Figure 10- X-ray spectra for different filtrations (IAEA, 2014)

1.4 Calculation models of tube output

Prediction models for x-ray spectra and output can be classified in three major categories: empirical models, semi-empirical models and Monte Carlo simulations.

- Empirical models

Empirical models use measured data to derive x-ray spectra. The first attempt was made by Silberstein (Silberstein L., 1932) who tried to obtain x-ray spectra from measurements of x-ray attenuation curves. Even though lots of efforts have been made to develop this model, errors remain. The principal reason is that attenuation measurements with different detectors will give different values for the same spectrum, due to different response of the detector. Therefore, pure empirical models are normally no longer in use.

- Semi-empirical models

Semi-empirical models combine theoretical equations to calculate the x-ray spectra and adjustments in the parameters of the equations to be coherent with measurements results.

The first semi-empirical model to describe x-ray spectra has been developed by Kramers (H. A. Kramers, 1923):

$$I(\lambda) = \frac{KI_1Z}{\lambda^2}\left(\frac{\lambda}{\lambda_0} - 1\right) \quad (11)$$

where I is the energy fluence, K is a constant, $I_1$is the tube current, Z is the atomic number of the target λ is the wavelength and λ_0 is the shortest emitted wavelength. This model has the advantage of being simple, but it takes only the bremsstrahlung into account and works only for thin targets since it neglects the target's attenuation. As a consequence, this model does not give good agreement with experimental results.

This model has then been improved by Soole (B.W. Soole, 1976). He especially took the target attenuation into account and changed some parameters in the model to be in agreement with the experiments.

Birch and Marshall continued to adjust the parameters of the model so that it fits well with some measured spectra (Birch R. and Marshall M., 1979). The have also used Green's formulation to estimate the characteristic radiation (Green M. and Cosslett V.E., 1968).

Finally, some more improvements have been made by Iles (Iles W. J., 1987) who included a term for electrons backscatter from the target and by Tucker *et al.* (Tucker D. M. et al., 1991) who took the fact that bremsstrahlung and characteristic radiation are not produced at the same depth in the target into account.

The software XCompW is based on this model. It has been developed by Robert Nowotny from the Institute of Medical Physics and Biomedical Engineering in 2002, and can calculate the x-ray spectra along with the kerma and the HVL. As Figure 11 shows, one can change different parameters: kilovoltage (from 20 to 150), ripple, anode angle, distance from emitter to detector, filter material and its thickness. The target material is Tungsten.

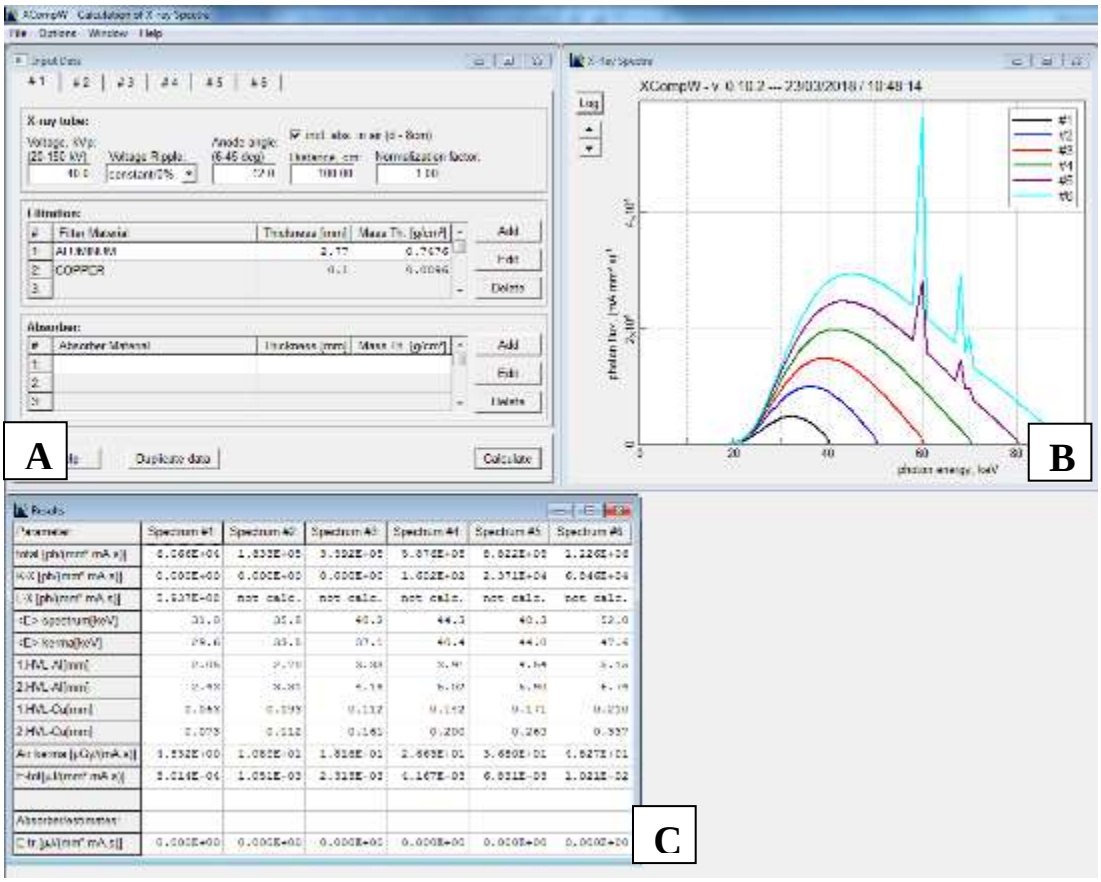

Figure 11- XCompW window. (A) X-ray tube settings. (B) Plotting. (C) Spectrum characteristics

- Monte Carlo simulations

Monte Carlo simulations calculate the x-ray spectra based on a model of transport of electrons and photons in the target and filter. In case of complex geometries, Monte Carlo simulations are the most suitable models. Nevertheless, there are also time consuming because they take into account all the physical processes involved in x-ray generation, even though some of them have no impact on the final spectrum.

TASMICS's model was developed in 2013 by John M. Boone et al. (Hernandez A. M. and Boone J. M., 2014) and is based on such Monte Carlo simulations. It can be used via an Excel sheet or with SPEKTR 3.0, a Matlab program that allows to generate x-ray spectra based on TASMICS. The user can choose different parameters such as the kVp, the ripple, the inherent filtration. For this last parameter, the user can choose among a list of already existing filtrations, but he can also create a new one if needed via another Matlab file, by choosing the material and the thickness. SPEKTR 3.0 has also the advantage to offer other calculations, such as the air kerma and the first or second HVL. Figure 12 shows a screenshot of SPEKTR 3.0, where all parameters can be seen.

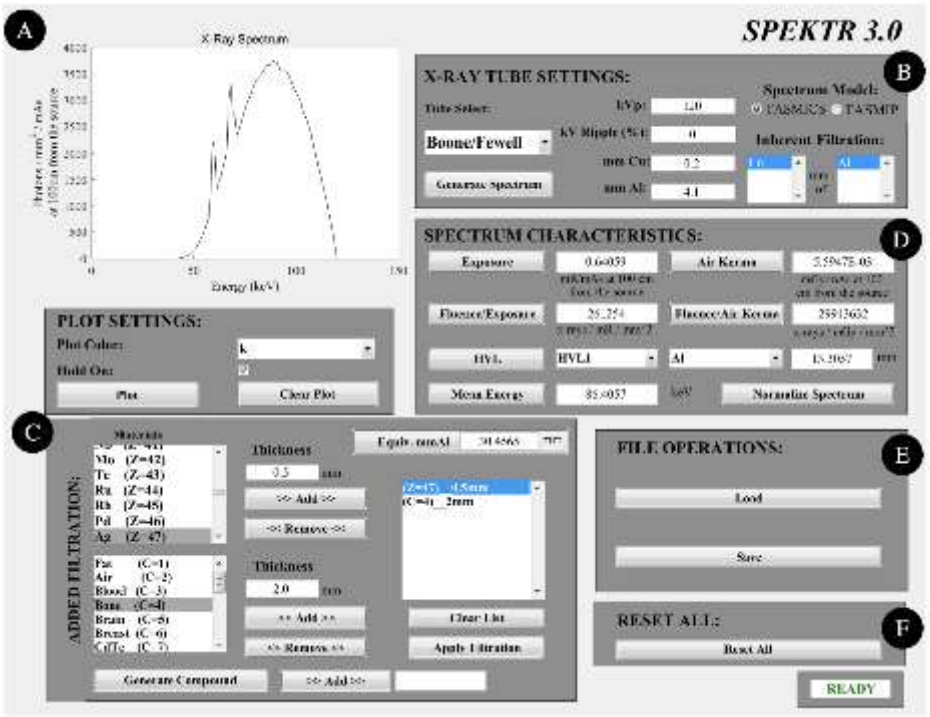

Figure 12 - SPEKTR 3.0 window. (A) Plotting. (B) X-ray tube settings. (C) Added filtration. (D) Spectrum characteristics. (E) File operations. (F) Reset all. Image from (Punnoose J. et al., 2016)

The tube output of an x-ray system is always required to calculate any dosimetric quantities. Yet it depends on different parameters, such as the tube potential, the filtration or the wear on the anode. Hence the need of an accurate model to predict tube output from generic values or a small set of measurements for individual x-ray devices. This thesis presents such a model. It is derived from simulations using semi-empirical spectral modelling. It will be compared with measurements on both new tubes and heavily used tubes, which show more wear and as a consequence have a lower output.

2. Material and Methods

2.1 Calculation of absolute dose output

When calculating tube output with a computer program simulating x-ray tubes and tube assemblies, the inherent filtration must be defined. Since it cannot be modelled exactly, different approaches can be pursued. However, the modelling of the inherent filtration best reproducing the measurements is chosen in the end. The attempts tested were reproducing RQR qualities, and using kVp dependent or independent filtrations.

2.1.1 Modelling RQR beam qualities

Diagnostic radiology dosimeters always have to be calibrated according to the radiation qualities according to the IEC-61267 standard (cf. Table 4). Therefore, standardized radiation qualities are defined that (more or less) mimic output qualities of clinical systems. This series corresponds to the RQR qualities. Other series (not used or referred to in this work) define narrow spectrum qualities, or radiation beams hardened with added aluminium or copper.

Radiation quality	***X-ray tube voltage (kV)***	***First HVL (mm Al)***	***Homogeneity coefficient h***
RQR 2	40	1.42	0.81
RQR 3	50	1.78	0.76
RQR 4	60	2.19	0.74
RQR 5	70	2.58	0.71
RQR 6	80	3.01	0.69
RQR 7	90	3.48	0.68
RQR 8	100	3.97	0.68
RQR 9	120	5.00	0.68
RQR 10	150	6.57	0.72

Table 4 - RQR quality standard

For each computer code (XCompW or TASMICS), the thickness of Aluminum to be added in the simulation as inherent filtration to get the exact same first HVL as the RQR values has been determined (cf. Table 5 and Table 6).

Radiation quality	*X-ray tube voltage (kVp)*	*Inherent filtration to mimic RQR (mm Al)*	*First HVL (mm Al)*	*Homogeneity coefficient h*	*Difference to RQR*
RQR 2	40	2.77	1.42	0.78	-0.03
RQR 3	50	2.65	1.78	0.73	-0.03
RQR 4	60	2.76	2.19	0.71	-0.03
RQR 5	70	2.82	2.58	0.69	-0.02
RQR 6	80	2.86	3.01	0.67	-0.02
RQR 7	90	2.91	3.48	0.66	-0.02
RQR 8	100	2.96	3.97	0.66	-0.02
RQR 9	120	3.09	5.00	0.67	-0.01
RQR 10	150	3.33	6.57	0.71	-0.01

Table 5 - Inherent filtrations resulting in HVLs according to RQR qualities with XcompW

Radiation quality	*X-ray tube voltage (kVp)*	*Inserted filtration to mimic RQR (mm Al)*	*Total inherent filtration to mimic RQR (mm Al)*	*First HVL (mm Al)*	*Homogeneity coefficient h*	*Difference to RQR*
RQR 2	40	1.01	2.61	1.42	0.45	-0.36
RQR 3	50	0.97	2.57	1.78	0.43	-0.33
RQR 4	60	1.13	2.73	2.19	0.42	-0.32
RQR 5	70	1.24	2.84	2.58	0.42	-0.29
RQR 6	80	1.38	2.98	3.01	0.41	-0.28
RQR 7	90	1.56	3.16	3.48	0.41	-0.27
RQR 8	100	1.73	3.33	3.97	0.40	-0.28
RQR 9	120	2.16	3.76	5.00	0.41	-0.27
RQR 10	150	2.65	4.25	6.57	0.41	-031

Table 6 - Inherent filtrations resulting in HVLs according to RQR with SPEKTR 3.0 for TASMICS

Figure 13 shows the HVL calculated along with HVL measured on different systems (cf. 2.3.1 for their description). However, RQR spectra are too hard in terms of HVL for high tube voltages (RQR 9) to mimic spectra found in clinical systems. This comparison is shown in Figure 13. The measurements of the clinical systems indicate that, except for system 3, RQR qualities are close to clinical beam qualities in the lower to medium kVp range, however at higher kVp HVL would be overestimated by RQR (120 kVp: 5.0 mm Al according to RQR 9, between 4.37 to 4.7 mm Al in the clinical systems) Figure 14

shows Y_{100} calculated along with the measured one. One can see that none of the simulations fits the measurements accurately, they only give rough approximations.

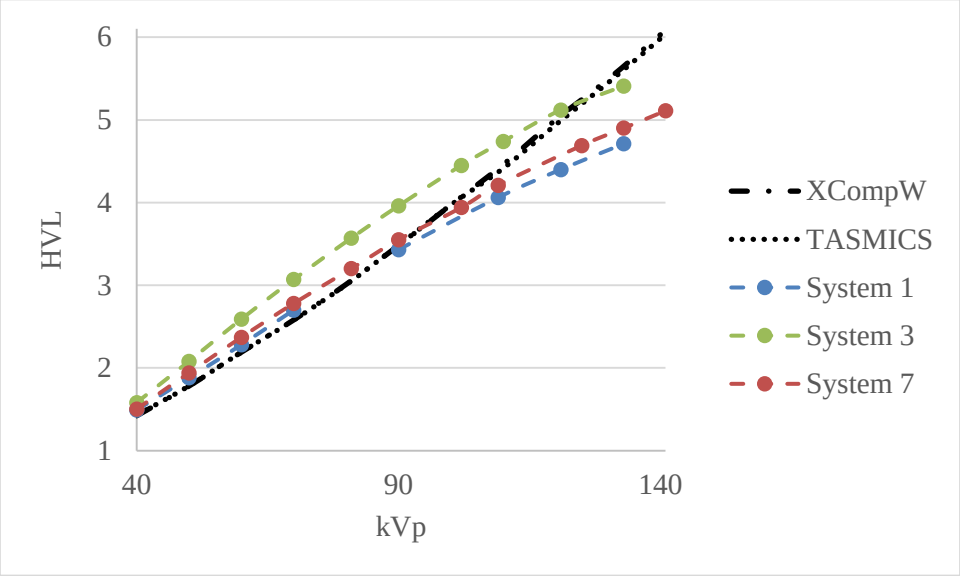

Figure 13 - HVL simulated and measured for the inherent filtration.

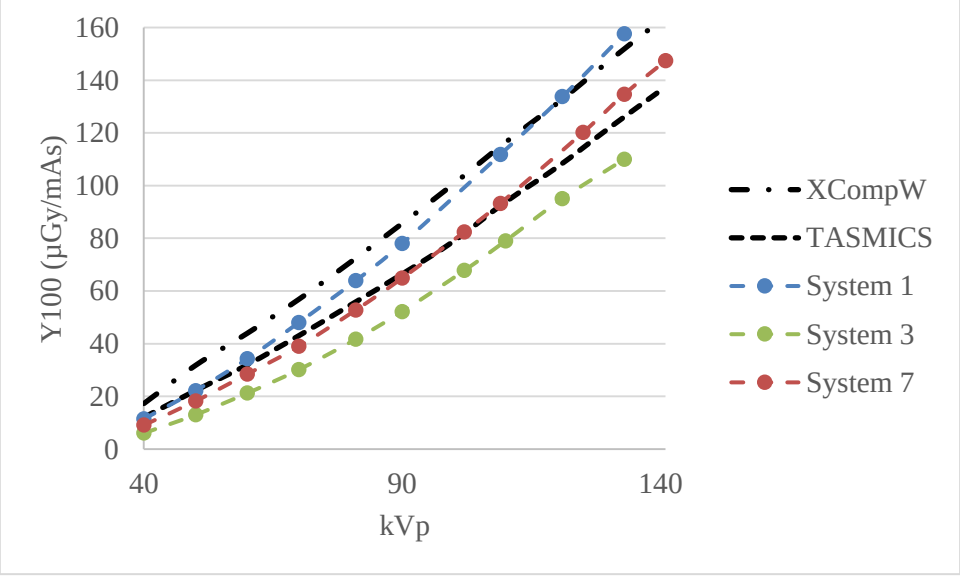

Figure 14 - Y_{100} simulated and measured with kVp dependent inherent filtrations resulting in HVLs according to RQR

2.1.2 Simulation using identical filtration for all kVp

Another idea to improve results is to add a constant filtration for all kVp as inherent filtration to adjust HVL to the values found in actual clinical X-ray machines. According to (RTI Electronics AB, 2010), a total filtration of 2.5mm of Aluminum should give an HVL of 2.76mm Al at 80kVp. For this total filtration, XCompW calculates an HVL of 2.81 mm Al and TASMICS of 2.73 mm Al, respectively. 2.41 mm Al and 2.55 mm Al as total filtration will provide an HVL of 2.76 mm Al at 80 kVp in these

simulations, with XCompW or TASMICS, respectively. Figure 15 compares the HVL for the measurements and the simulations. Y_{100} for the measurements and the simulations are shown in Figure 16. XCompW gives too high results, whereas TASMICS fits the measurements on system 1 but not on the others.

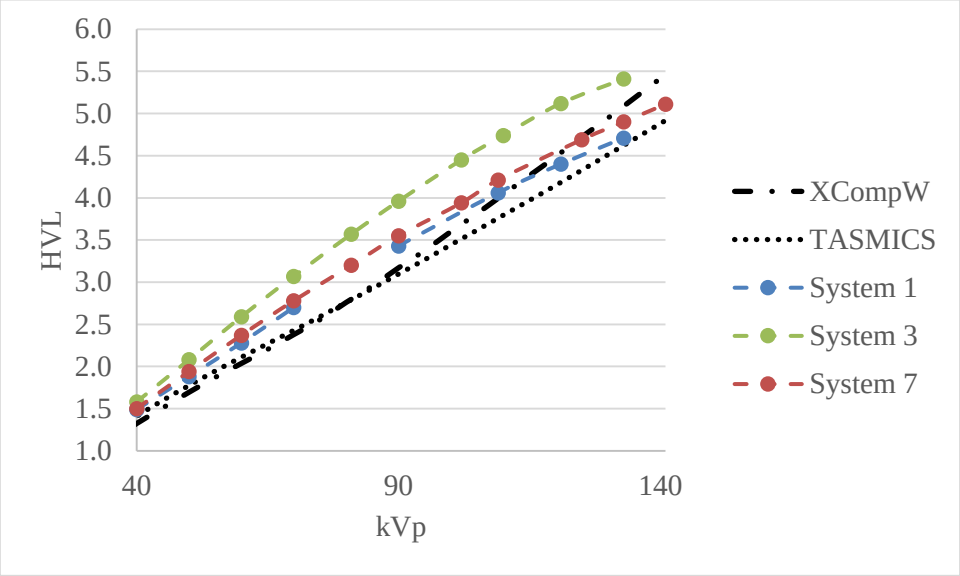

Figure 15 - HVL measured and simulated for a total filtration of 2.41mm Al for XCompW and 2.55mm Al for TASMICS

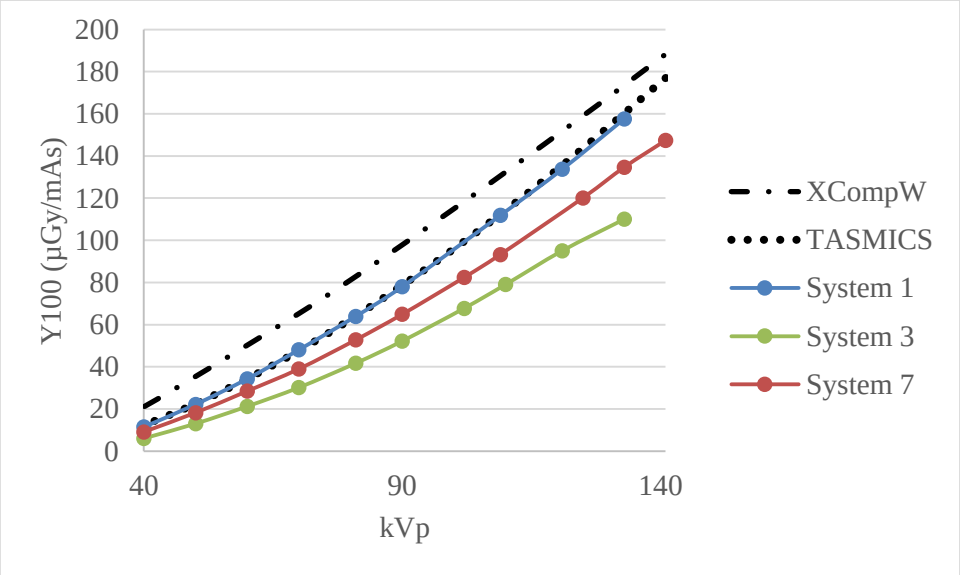

Figure 16 - Y_{100} measured and simulated for a total filtration of 2.41mm Al for XCompW and 2.55mm Al for TASMICS

Both simulations can be used. Nevertheless, the one using a fixed filtration for all kVp has the advantage to better represent the situation in actual x-ray systems, with inherent and additional filtrations, it will thus be used in this work.

2.2 Mathematical modelling of tube output

Tube output is calculated in a two-step approach. First, Y_{100} for inherent filtration is determined. In the second step, dose reduction factors are determined and applied in case an added filtration is used. For the latter – the calculation of the dose reduction factors (DRFs) – two different mathematical models are examined. The programs are written with Matlab (Matlab 2017b, Mathworks, Natick, Massachusetts).

2.2.1 Calculation of Y_{100} for inherent filtration

Step 1: deriving kVp dependence of output with TASMICS

TASMICS has been used to simulate the dose output for kVp values ranging from 30 to 150, with an interval of 5 kVp. The anode angle is set to 16°, the ripple to 0%. As described in 2.1.2, an inherent filtration of 2.55 mm of Aluminum is used for all kVp values.

In this first step, Y_{100} for a clinical system is estimated for the total range of kVp values from a small set of measurements (minimum 3).

According to Kramers' law, Y_{100} can be estimated with $Y_{100} = k * kVp^2$, where k is a constant. It is known that this formula is not precise enough, especially for high kVp where the exponent will be lower as compared to low kVp. Figure 17 shows the power functions that fit the Y_{100} calculated. The exponent is 2.1 for low filtrations and 1.4 for high filtrations, which confirms the previous statement.

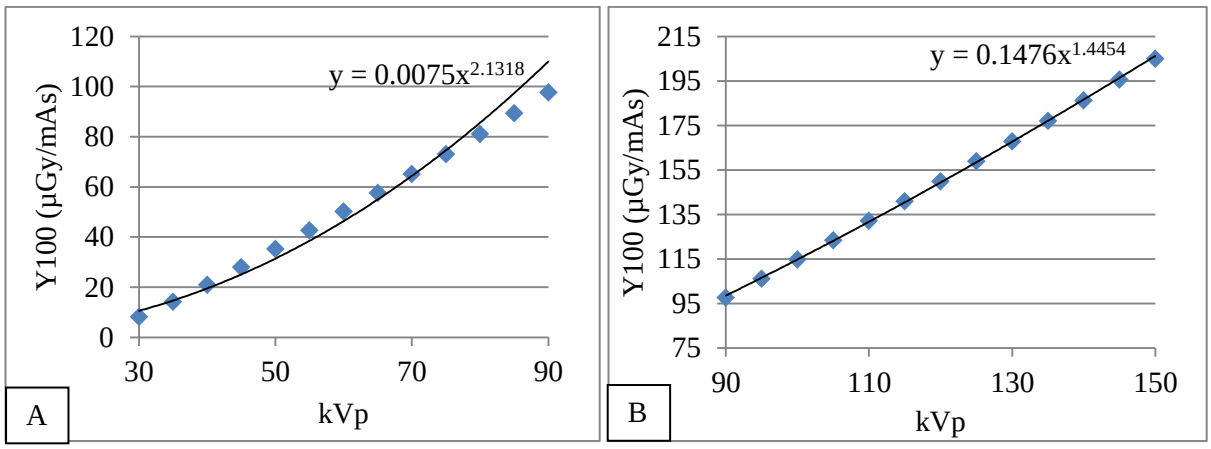

Figure 17 – Low kVp (A) – High kVp (B). Blue points: Y_{100} calculated for inherent filtration

To allow for a dependence on kVp, an exponent with a constant, a linear and a quadratic term is defined as

$$Y_{100} = f(kVp) = c' * kVp^{a+b*kVp+d*kVp^2} \qquad (12)$$

kVp_{ref} refers to a reference kVp, which is usually set to 81.

From the absolute dose output, dose output relative to a reference kVp value usually set to 81 kV is defined via

$$K(kVp) = \frac{f(kVp)}{f(kVp_{ref})} \tag{13}$$

Relative dose output is derived by calculating Y_{100} with TASMICS using a simulation grid of kVp values ranging from 30 to 150 every 5 kVp and dividing by Y_{100} at 81 kVp. Then the parameters a to d are derived according to

$$K(kVp) = c * kVp^{a+b*kVp+d*kVp^2} \tag{14}$$

Since (14) refers to relative output, the normalization factor c is different to c' defined in (12).

Step 2: Deriving individual corrections for clinical systems

Output measurements performed at the clinical system (K_i, i=1 to minimum 3) are used to derive a correction of the kVp dependence of the output calculated with TASMICS. At least three measurement points taken at kVp_i; i =1,2,…,n are used to adapt these simulated values for the actual system. Ratios in output Kerma are calculated as

$$ratio_i = \frac{K_i}{c * kVp^{a+b*kVp_i+d*kVp_i^2}} \tag{15}$$

with K_i indicating the relative dose output from the measurements.

With these ratios, an individual correction function

$$P(kVp) = x_1 + x_2 * kVp + x_3 * kVp^2 \tag{16}$$

is derived with least square fitting. x_1, x_2 and x_3 are three parameters which characterize the output for any individual x-ray system.

Step 3: Calculation of Y_{100}

Absolute output defined as Y_{100} results in

$$Y_{100,0}(kVp) = P(kVp) * f(kVp) * K'_2 \tag{17}$$

with K'_2 representing Y_{100} (absolute output) at the reference kVp.

2.2.2 Modelling of dose reduction factors for added filtrations

TASMICS has been used to simulate the dose output for kVp values ranging from 30 to 150, with an interval of 5 kVp. The anode angle is set to 16°, the ripple to 0%. As described in 2.1.2, an inherent filtration of 2.55 mm of Aluminum is used for all kVp values. Added filtrations used in this simulation range from 0.01mm Cu to 0.9 mm Cu ([0.01; 0.02; 0.03; 0.06; 0.1; 0.2; 0.3; 0.4; 0.5; 0.6; 0.7; 0.8; 0.9]).

0.9 mm Cu has been chosen because it is the highest medical filtration found in current interventional x-ray systems. 0.01 mm Cu has been chosen to represent Aluminum filtrations.

Dose reduction factors are defined as

$$DRF(U,F) = \frac{Y_{100}(U,F)}{Y_{100}(U,0)} \quad (18)$$

where $Y_{100}(U,0)$ corresponds to the yield at tube potential U and inherent filtration.

2.2.3 Equivalent copper thickness for Aluminum filters

Filter thickness is used in terms of copper thickness. In case of aluminium or Al/Cu filtrations, the equivalent copper thickness needs to be derived. TASMICS has been used to calculate the dose output with an added filtration of 1 mmAl at a specific kVp. Then another simulation is done to find which thickness of copper is necessary to obtain the same dose output as in the first case at the same kVp and only with a copper filter.

In this case, the simulations have first been run at 70 kVp. For 1 mm Al, the DRF is 0.661. The closest DRF with only copper filtration has been found with 0.032 mm Cu and is 0.659. Then DRF for other kVp values have been calculated, to ensure that the equivalent copper thickness does not depend too much on kVp. Table 7 shows that it depends slightly on kVp, but the errors always remain low, so 0.032 mm Cu is kept constant for all kVp.

kVp	DRF_{1mmAl}	$DRF_{0.032mmCu}$	*Difference (%)*	DRF_{2mmAl}	$DRF_{0.062mmCu}$	*Difference (%)*
60	0.630	0.625	0.77	0.441	0.438	0.64
70	0.661	0.659	0.37	0.481	0.482	-0.19
90	0.710	0.712	-0.27	0.546	0.554	-1.47
110	0.747	0.753	-0.75	0.598	0.612	-2.38
125	0.770	0.778	-1.04	0.630	0.648	-2.90

Table 7 – Estimation of equivalent copper thickness for Aluminum filter

2.2.4 Dose reduction factors as a function of kVp and filter thickness (model 1)

The goal is to find an appropriate Dose Reduction Factor (DRF) that depends on kVp and the added filtration. Multiplying $Y_{100,0}$ with the appropriate DRF gives the absolute dose output for a specific filtration.

DRF were calculated from the Y_{100} values simulated with TASMICS according to

$$\mathrm{DRF}(U,\mathrm{F}) = \frac{\mathrm{Y}_{100}(\mathrm{U,F})}{\mathrm{Y}_{100}(\mathrm{U,0})} \tag{19}$$

DRF defines a matrix of DRF with U and F values representing tube potentials and copper filter thicknesses used in the simulation. kVp values range from 30 to 150 kVp with an interval of 5 kVp. Figure 18 shows DRF depending on kVp and the thickness of copper.

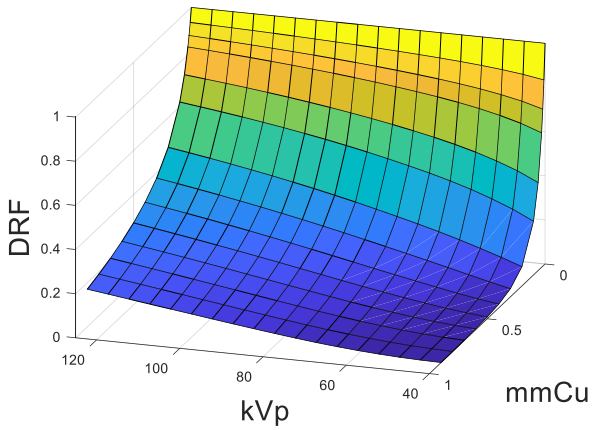

Figure 18 - DRF calculated depending on kVp and thickness of copper

In Figure 19, attenuation factors defined as

$$AF = \frac{1}{DRF} \tag{20}$$

are shown.

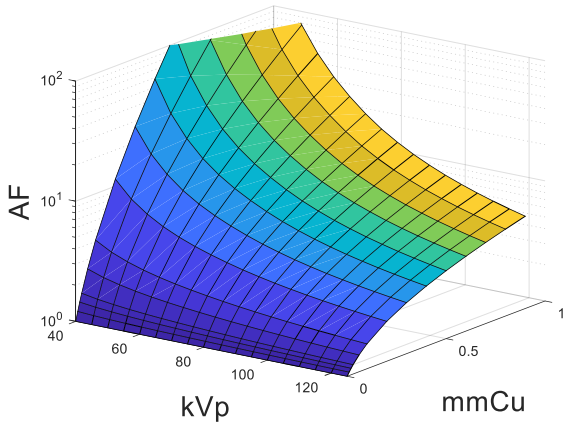

Figure 19 - AF calculated depending on kVp and thickness of copper

From the simulation points, a function of the AF parametrized by the tube potential U and the added filter thickness in mm Cu needs to be defined. This function needs to fulfil these three conditions:

- AF(kVp, 0 mm Cu) = 1
- If kVp increases, AF should decrease strictly monotonically

- If the thickness of copper increases, AF should increase strictly monotonically.

The simplest generic function fulfilling these conditions can be written as:

$$AF_{sim}(U,F) = 1 + A * \frac{F^B}{U^C} \tag{21}$$

where the factor A and the exponents B and C are determined by non-linear least square fitting to simulated values. Then the dose reduction factor is derived as the inverse of the attenuation factor:

$$DRF_{sim}(U,F) = \left(1 + A * \frac{F^B}{U^C}\right)^{-1}. \tag{22}$$

Figure 20 shows the surface that is produced with this fit for the AF. Figure 21 shows the surface that is produced with this fit for the DRF. The blue data points represent the simulation's values. The deviations seem very large, and this is confirmed by Figure 22 which plots the deviations depending on kVp and filter thickness. The error reaches 10^4% and rarely goes beyond 10%. Thus, this model cannot be used in this simple form.

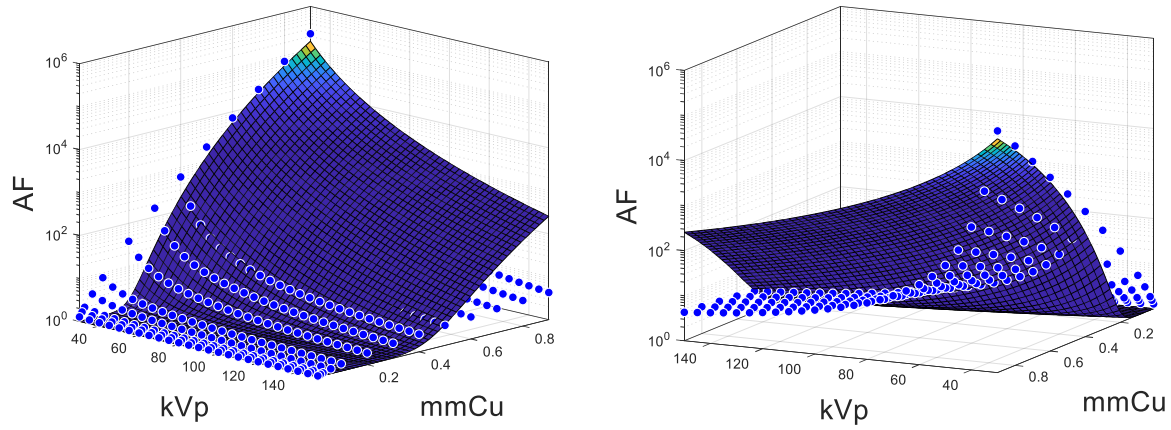

Figure 20 – Surface: AF estimated; blue points: data.

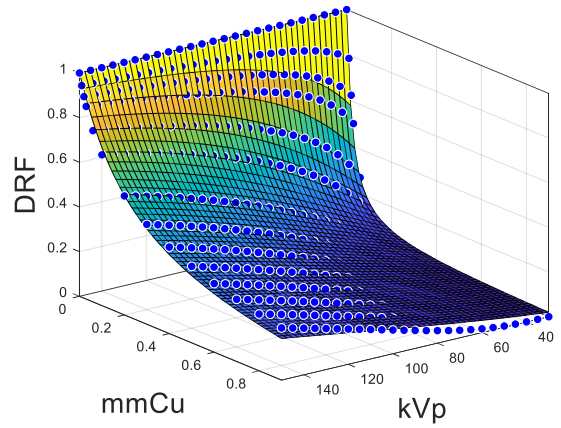

Figure 21 - Surface: DRF estimated; blue points: data.

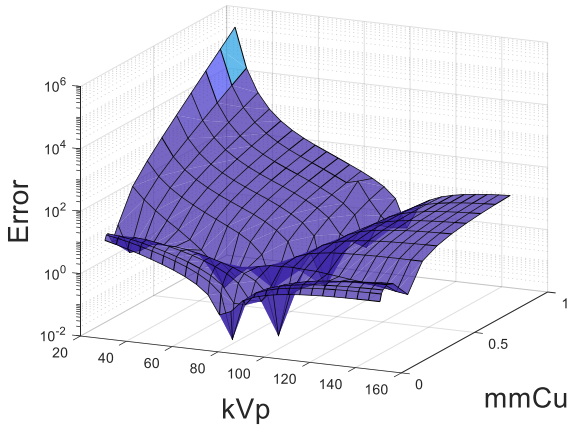

Figure 22 - Errors in percent between the DRF calculated and the fit

To improve the parametrization of the AF and thus of the DRF, A, B and C are defined as functions of the filtration according to

$$AF_{sim}(U,F) = 1 + A(F) * \frac{F^{B(F)}}{U^{C(F)}} \qquad (23)$$

To test the significance of these parameters, p-values have been computed. A low p-value indicates a high significance, and vice-versa. For the parameters of the DRF, the p-values are:

- p-value(A) = $1.1.10^{-13}$
- p-value(B) = $1.0.10^{-243}$
- p-value(C) = $2.0.10^{-181}$.

So even though A has a low p-value, it is much higher than the one of B and C. As a consequence, A does not need to be fitted with the least square fitting. Two solutions remain: either fixing A to a constant for all filtrations, or finding a formula describing A according to the filtration.

Determination of A as a constant

The easiest idea is to fix A according to the value of the first simulation with TASMICS (A=15342), whereas B and C are defined as functions of the filtration. With this in mind, the DRF are simulated for one specific filtration for the whole range of kVp values (from 30 to 150 kVp with an interval of 5 kVp). This defines a vector of DRF. Matlab fits the values of this vector according to

$$DRF_{sim}(U,F) = \left(1 + A * \frac{F^{B(F)}}{U^{C(F)}}\right)^{-1} \qquad (24)$$

with A fixed according to the first simulation, and B(F) and C(F) determined with the least square fitting.

This procedure can be repeated for each filtration, so that it calculates each time a set of parameters (B(F), C(F)) specific for the respective filtration. Figure 23 and Figure 24 show the variation of the

exponents B and C depending on the thickness of copper. C remains between 1 and 2.6, but B varies a lot (from 1.6 to -40) and is negative for high filtrations. However, a negative B violates the assumptions made in the parametrisation model having led to equation 21. As a consequence, it seems more appropriate to use a model where the factor A depends on copper filter thickness.

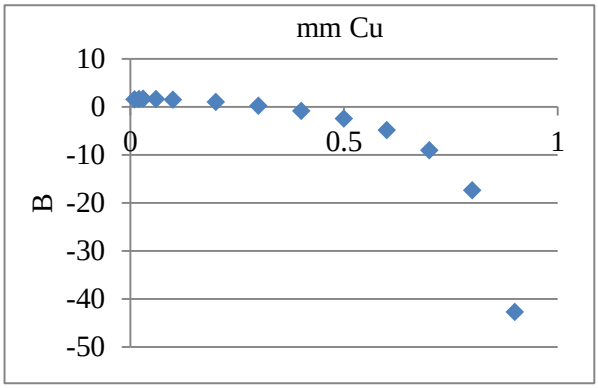

Figure 23 - Dependence of B on filter thickness.

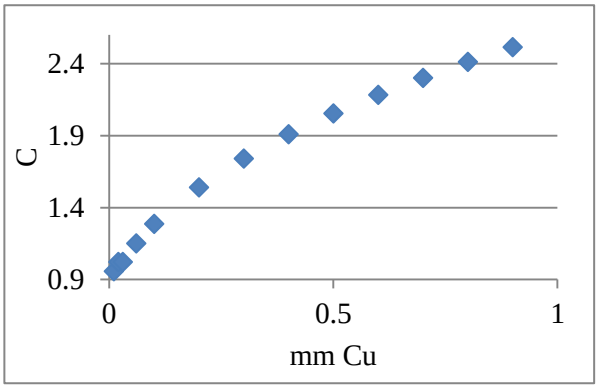

Figure 24- Dependence of C on filter thickness.

Determination of A as a function of filter thickness

The second solution is to find a formula for A depending on the filtration. With this in mind A, B and C are computed for fixed kVp and varying filtration with the least square fitting, so that a formula for A can then be derived.

The filtration varies within ranges of copper thicknesses:

- range 1 represents very low filtrations: 0.01 mm Cu, 0.02 mm Cu and 0.03 mm Cu
- range 2 represents the filtrations used in direct radiography: 0.06 mm Cu, 0.1 mm Cu, 0.2 mm Cu and 0.3 mm Cu
- range 3 represents the low filtrations used for fluoroscopy: 0.4 mm Cu, 0.5 mm Cu,0.6 mm Cu and 0.7 mm Cu
- range 4 represents the high filtrations used for fluoroscopy: 0.7 mmCu, 0.8 mm Cu and 0.9 mm Cu.

For a specific kVp value, all the DRF from one specific range are collected using TASMICS. This gives a vector of DRF for this range of filtration at a specific kVp. As an example, the vector for the range 1 contains 3 values with the DRF for filtrations of 0.01 mm Cu, 0.02 mm Cu and 0.03 mm Cu. Matlab fits the values of this vector according to (22) to determine A, B and C. This computation is repeated for different kVp, namely for 40, 50, 70, 90, 110, 130 and 150 kVp. One obtains in the end a set of parameters A, B and C for each kVp and each filter thickness range. As kVp is fixed, A and C are dependent on each other, so that the parameters of the model are in reality B and $A*U^{-C}$. In the next step,

the parameter $A*U^{-C}$ is broken up into A and C using that C describes a power dependence. By fitting power functions, C can be determined. Then, C is fixed to the power best describing the simulated data allowing determination of A.

$A*U^{-C}$ is plotted as a function of the kVp for each range of filtrations in Figure 25. In each range of filtrations, a fit with a power function has been performed. A large coefficient of determination indicates that A can be described by a constant in each filter range.. According to Figure 25 (A), the fit with a power function gives a coefficient of determination close to 1 (0.9986), so A can be set as a constant for low filtration. On the other hand, Figure 25 (D) shows that this is not the best way for high filtration, as the fit with a power function is lower (R^2=0.9376). As a consequence, A should not be fixed to a constant and a formula describing A according to the filtration needs to be found.

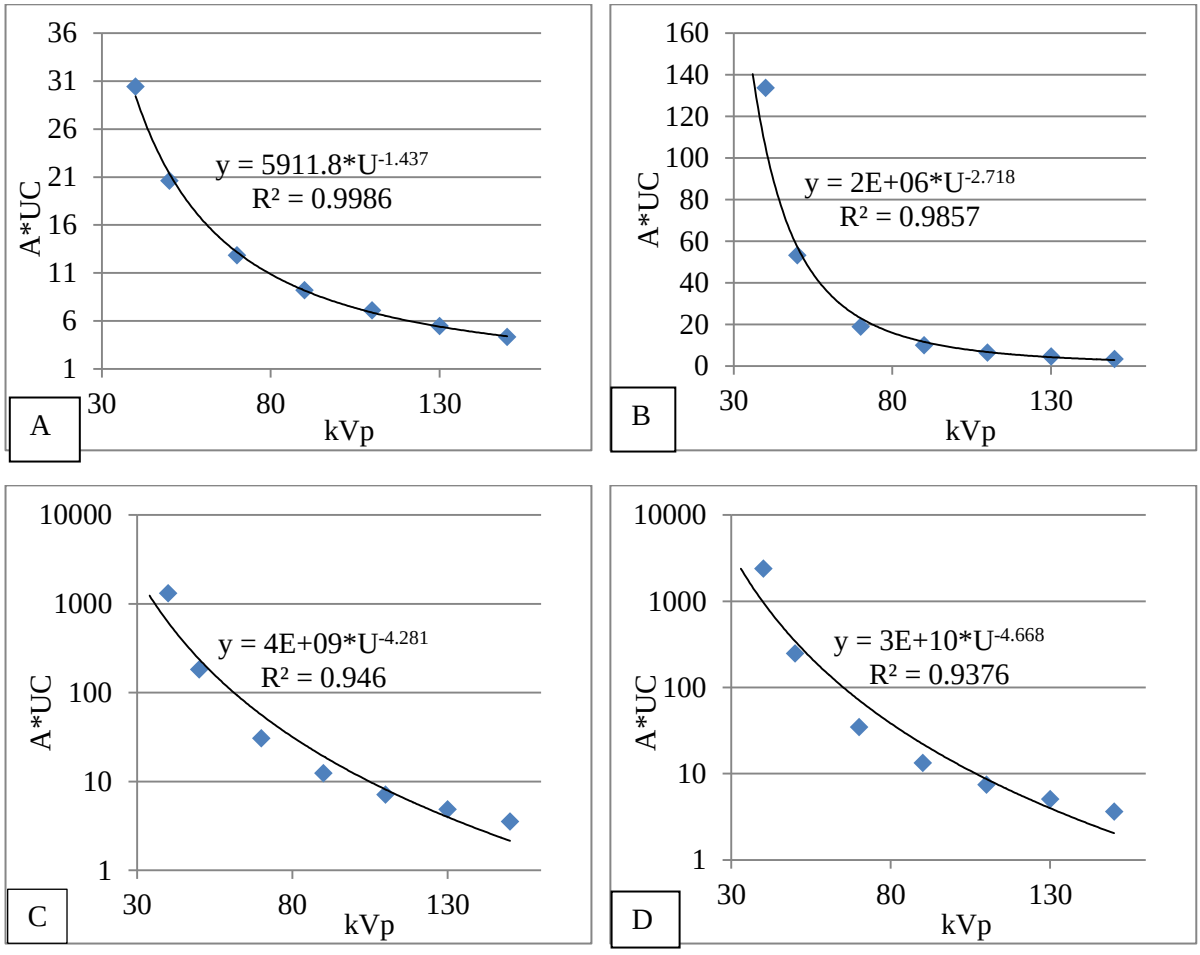

Figure 25 - $A*U^{-C}$ depending on kVp for range 1(A), 2 (B), 3 (C) and 4 (D). Blue points: data, black line: power fit.

With this in mind, a new computation is performed. As previously, kVp is fixed and the filtration varies within the same ranges. A and B are still floating, but this time C is fixed to the value found with the previous power fit, namely 1.437 for the range 1, 2.718 for the range 2, 4.281 for the range 3 and 4.668 for the range 4. This computation allows to determine how A varies for different ranges of filtration,

independently of C. Once again, the computation is performed for different kVp, so that the values of A can be collected for different ranges and for different kVp. Table 8 collects these values and give the average of A for each range. The higher the filtration, the higher A becomes.

kVp	*Range 1*	*Range 2*	*Range 3*	*Range 4*
40	6105	3,02E+06	9,43E+09	7,17E+10
50	5699	2,21E+06	3,41E+09	2,12E+10
70	5754	1,96E+06	2,42E+09	1,42E+10
90	5920	2,05E+06	2,88E+09	1,76E+10
110	6080	2,28E+06	3,91E+09	2,52E+10
130	6212	2,58E+06	5,39E+09	3,66E+10
150	6288	2,91E+06	7,33E+09	5,21E+10
Average	6008	2,43E+06	4,97E+09	3,41E+10

Table 8 – Values of A in the various copper filter thickness ranges

Figure 26 shows the variation of A depending on the filtration at respectively 40, 50, 70, 90, 110, 130 and 150 kVp. The values of A were obtained for range of filtrations. To get these plots, the median of each range has been chosen for the x-axis, namely 0.02 for range 1, 0.15 for range 2, 0.55 for range 3 and 0.8 for range 4. One can see that the shape of the plot is always the same, which shows that A does not depend on kVp. On the other hand, A varies a lot with the filtration (up to seven orders of magnitude), showing once again the need to parametrize A as a function of the filtration.

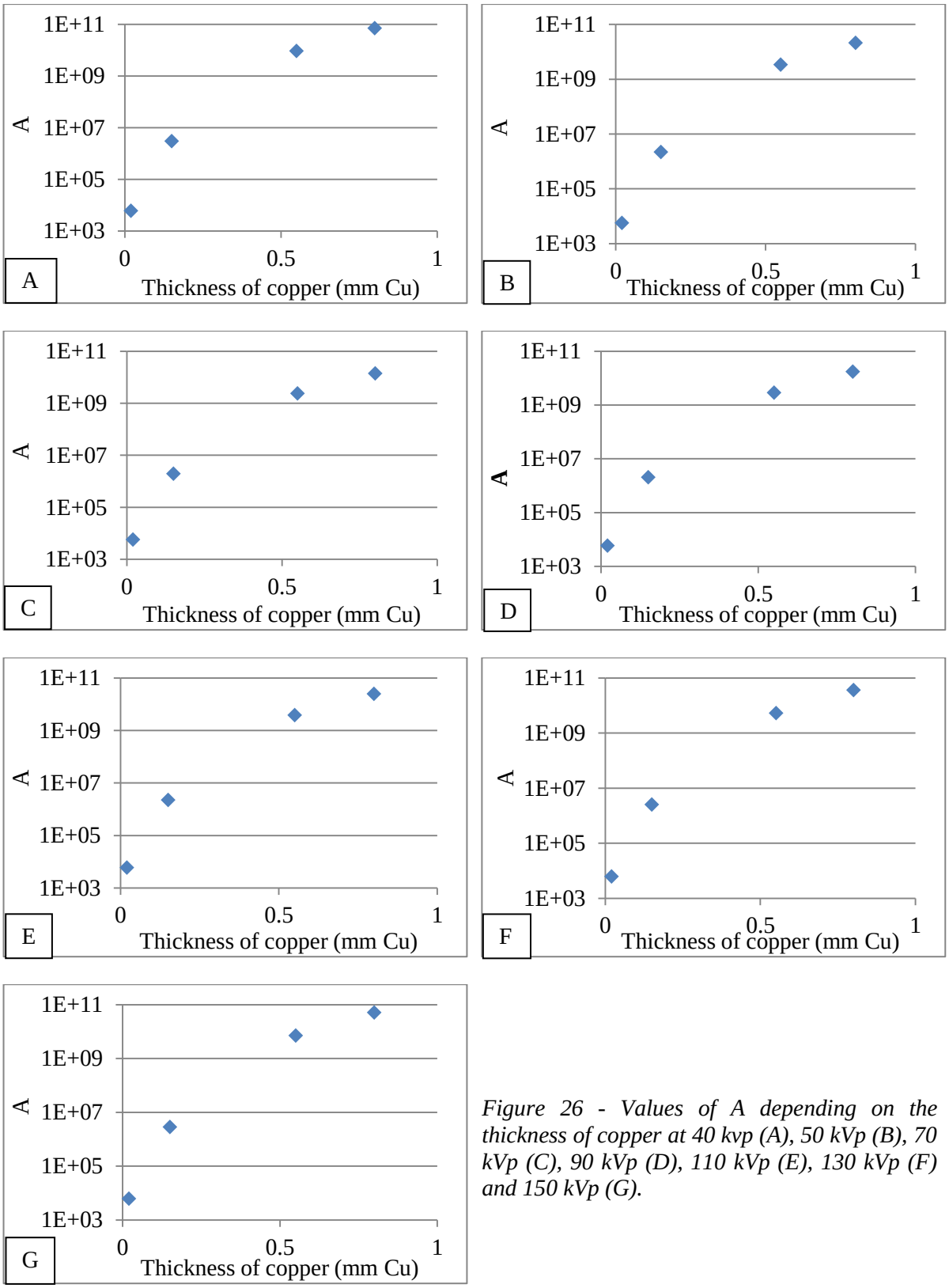

Figure 26 - Values of A depending on the thickness of copper at 40 kvp (A), 50 kVp (B), 70 kVp (C), 90 kVp (D), 110 kVp (E), 130 kVp (F) and 150 kVp (G).

Since the power component of the numerator in (24) is described by B(F), the dependence of A on the filtration must be mathematically different to a power function. To find it, two vectors have been defined in Matlab (cf. Table 9): one containing the medians of each range of filtrations, another containing the average of A for all the kVp in the corresponding range of filtrations.

Ranges	*Copper thickness*	*Average of A*
0.01 & 0.02 & 0.03 mm Cu	0.02	6008
0.06 & 0.1 & 0.2 & 0.3 mm Cu	0.15	2.430E+06
0.4 & 0.5 & 0.6 & 0.7 mm Cu	0.55	4.967E+09
0.7 & 0.8 & 0.9 mm Cu	0.80	3.406E+10

Table 9 - Matrix used in Matlab to parametrize A

Giving the values of A, an exponential fit seems appropriate. In order to determine the formula, the logarithm of A has first been fitted. Figure 27 shows the best fit determined with least square fitting.

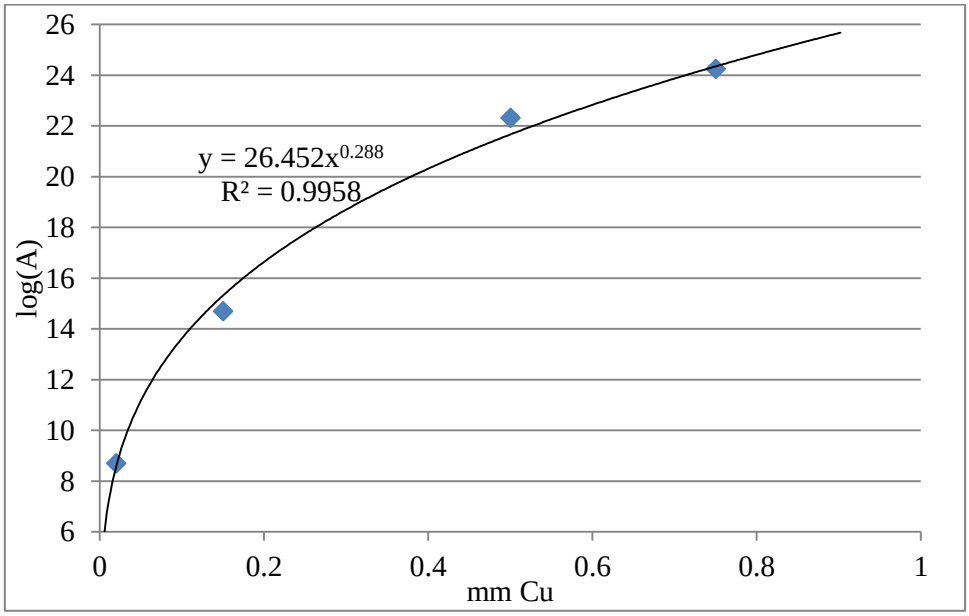

Figure 27 – Blue points: values of log(A); dark line: fit

As a consequence, a two parameters fitting function will be used:

$$A(F) = \exp(26.542 * F^{0.288}) \tag{25}$$

This fit is shown in Figure 28, it has a coefficient of determination of 0.99.

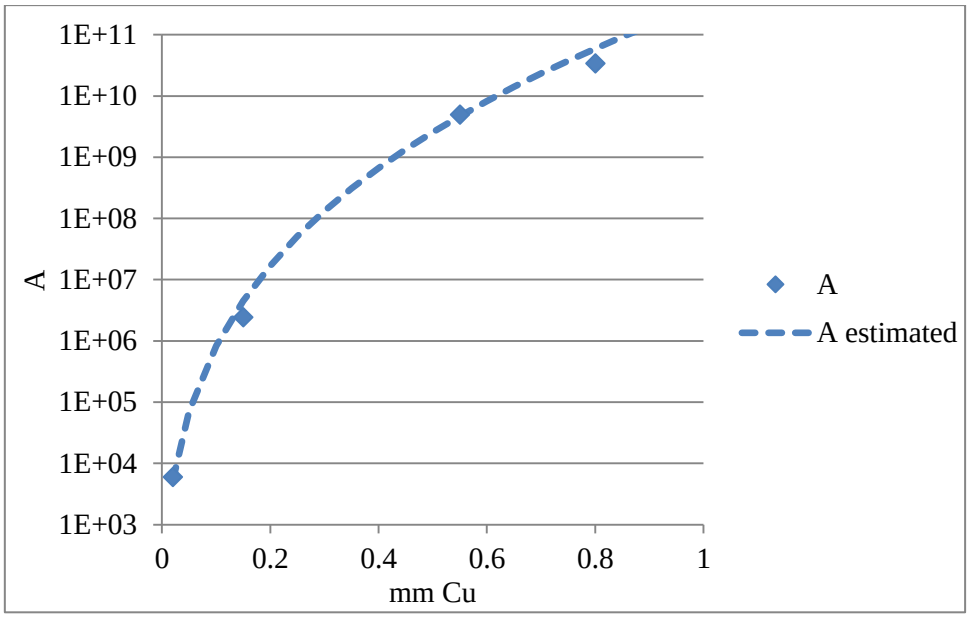

Figure 28 – Exponential fit for A

Now that A is parametrized, B and C also have to be defined as functions of the filtration. With this in mind, the DRF are calculated with TASMICS for a specific filtration for the whole range of kVp values from 30 to 150 kVp with an interval of 5 kVp. This defines a vector of DRF. Matlab fits the values of this vector according to

$$DRF_{sim}(U,F) = \left(1 + A(F) * \frac{F^{B(F)}}{U^{C(F)}}\right)^{-1} \quad (26)$$

with A(F) defined according to (25), and B(F) and C(F) determined with the least square fitting.

This action can be repeated for each filtration, so that it calculates each time a set of parameters (B(F), C(F)) specific for the filtration. Figure 29 and Figure 30 show the variation of respectively the exponents B and C depending on the thickness of copper. C remains between 1 and 2.6, whereas B varies a lot (from 1 to 103). It remains this time always positive, and thus the DRF fulfil the three conditions described previously.

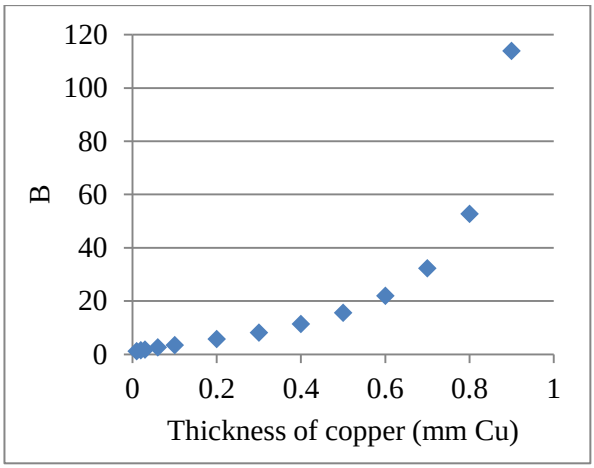

Figure 29 - Dependence of B on filter thickness

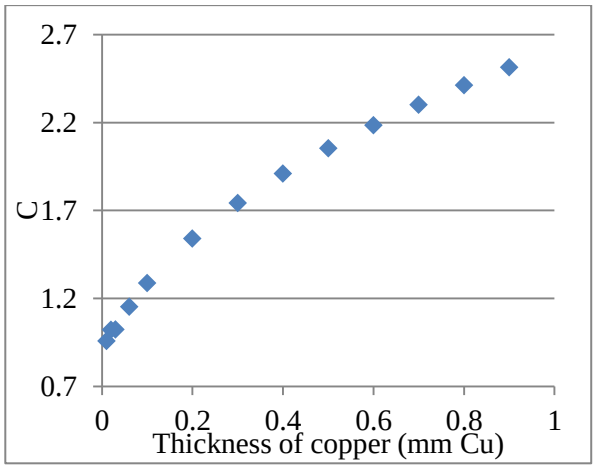

Figure 30 - Dependence of C on filter thickness

- Comparison of DRFs fitted with fixed A vs. filtration dependent A

In order to compare the two approaches, the deviations between the simulated values and the fit are calculated. To obtain the fit, B and C have been derived for each filtration from the data calculated with TASMICS for kVp varying from 30 to 150 kVp with 5 kVp interval. The filtrations used are the same as previously, starting from 0.01 mm Cu up to 0.9 mm Cu.

The deviations between the simulated values and the fit are plotted in Figure 31 and Figure 32 depending on which case they represent. They are shown only in the interesting ranges of kVp, namely from 40 to 125 kVp for low filtrations (up to 0.1 mm Cu) and from 70 to 125 kVp for higher filtrations. Figure 31 (A) and (B) represent the case where A is fixed, and the case where A is defined according to (25), respectively. As can be seen, there is no difference in accuracy between the two cases. The same conclusion can be made with Figure 32 (C) and (D). Nevertheless, even though both models have the same accuracy, letting A vary is physically more relevant, as it results in positive B for all filtrations. As a consequence, A should be defined according to (25), and only this case will be used starting from now.

The errors remain lower than 10%, so that the model is now accurate enough. Some higher deviations can be seen at 70 and 75 kVp for high filtrations, but they are still much lower than in Figure 22. The values can be seen in the Appendix, page 116.

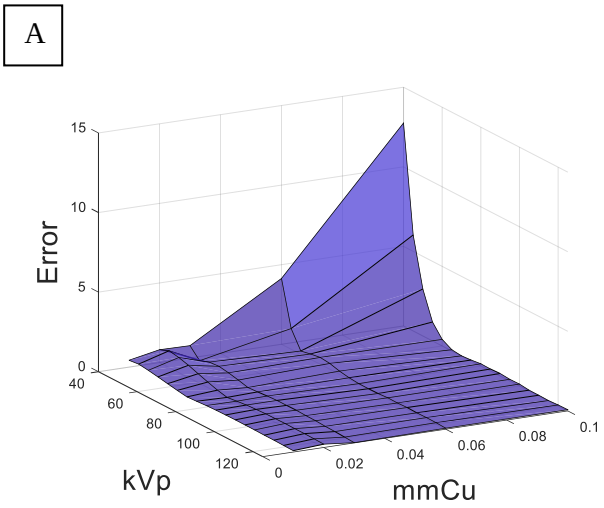

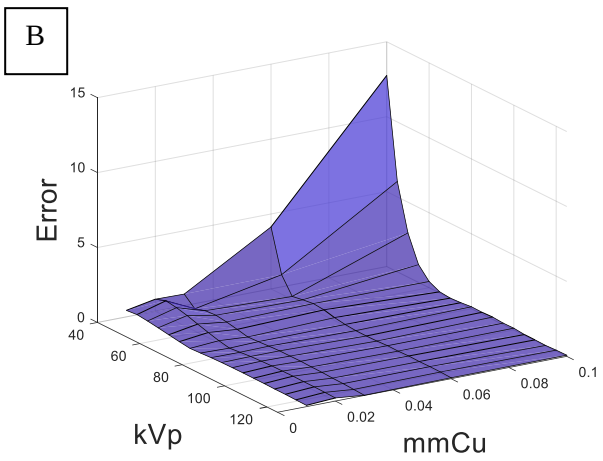

Figure 31 – Errors between the simulated values and the fit for low filtrations and kVp ranging from 40 to 125 kVp when A is fixed (A) and when A is described with (25) (B)

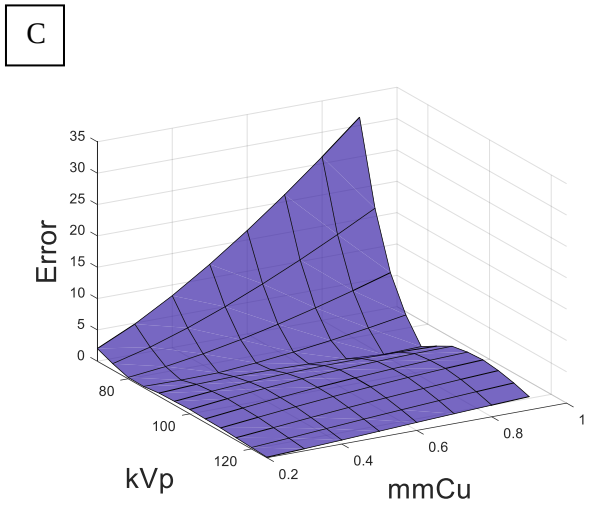

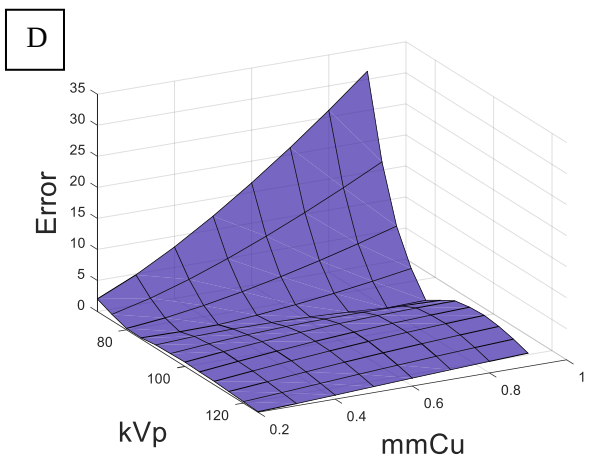

Figure 32 – Errors between the simulated values and the fit for high filtrations and kVp ranging from 70 to 125 kVp when A is fixed (C) and when A is described with (25) (D)

2.2.5 Determination of DRFs from measurement points in clinical systems (model 1)

The implementation of the model is composed of different steps:

- *Step 1:* Calculation of the DRF as a function of kVp for the filtrations for which measured data is available
- *Step 2:* Calculation of the dose output as a function of filter thickness for at least two fixed kVp
- *Step 3:* Calculation of the DRF for all the remaining filtrations

As inputs, it is essential to measure the absolute dose output at at least two kVp values and for at least two filtrations.

Filtration	***kVp***	***Absolute dose output***
Filter 1	U_1	K'_{U_1,f_1}
	U_2	K'_{U_2,f_1}
Filter 2	U_1	K'_{U_1,f_2}
	U_2	K'_{U_2,f_2}

Table 10 - Additional inputs of the first model

Step 1: Calculation of the DRF as a function of kVp for the filtrations for which measured data is available

At least two DRF are calculated from the measurements: $DRF_{U_1,f_i} = \frac{K'_{U_1,f_i}}{Y_{100,0}(U_1)}$ and

$DRF_{U_2,f_i} = \frac{K'_{U_2,f_i}}{Y_{100,0}(U_2)}$. Then the parameters B and C for these filter thicknesses F_{f_i} are determined with least square fitting according to

$$DRF_{meas,F_{f_i}}(U, F_{f_i}) = \left(1 + A(F_{f_i}) * \frac{F_{f_i}^{B(F_{f_i})}}{U^{C(F_{f_i})}}\right)^{-1}. \quad (27)$$

$A(F_{f_i})$ is defined with (25).

The output is then calculated by multiplying $DRF_{meas,F_{f_i}}$ and $Y_{100,0}$:

$$Y_{100,F_{f_i}}(kVp) = DRF_{meas,F_{f_i}}(kVp, F_{f_i}) * Y_{100,0}(kVp) \quad (28)$$

Step 2: Calculation of the dose output as a function of filter thickness for at least two fixed kVp

Figure 33 shows the dose output calculated with TASMICS depending on the filter thickness.

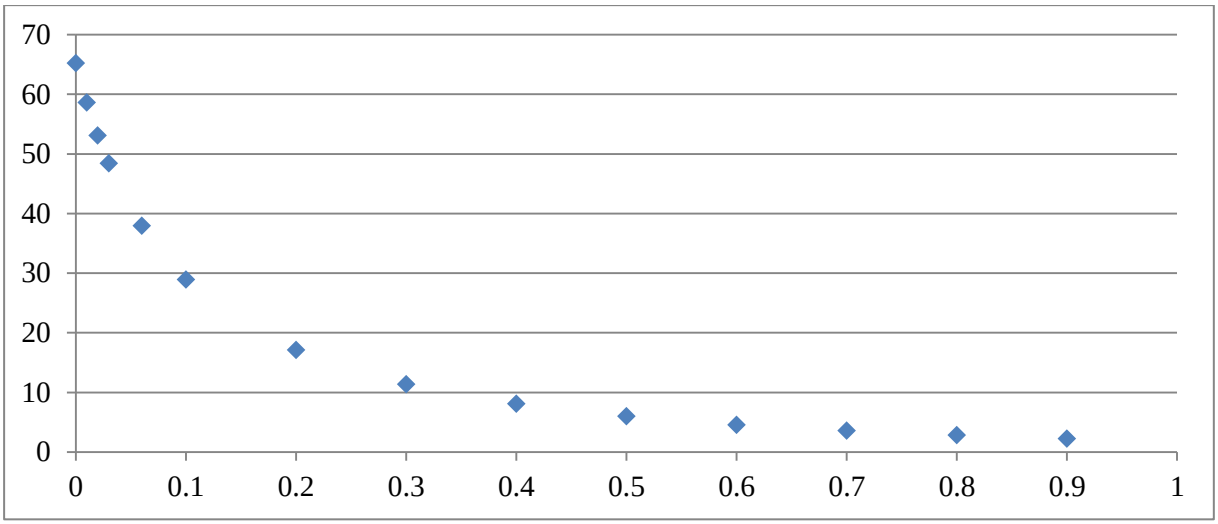

Figure 33 - Dependence of dose output on filter thickness at 70kVp

Dose output at U_1 is fitted using least squares according to

$$f_1(F_{Cu}) = \alpha_1 * (\beta_1 + F_{Cu})^{\lambda_1}, \quad (29)$$

α_1, β_1 and λ_1 are determined by Matlab with the least square fitting.

The same can be done at U_2:

$$f_2(F_{Cu}) = \alpha_2 * (\beta_2 + F_{Cu})^{\lambda_2} . \quad (30)$$

Figure 34 shows the fits for these two functions.

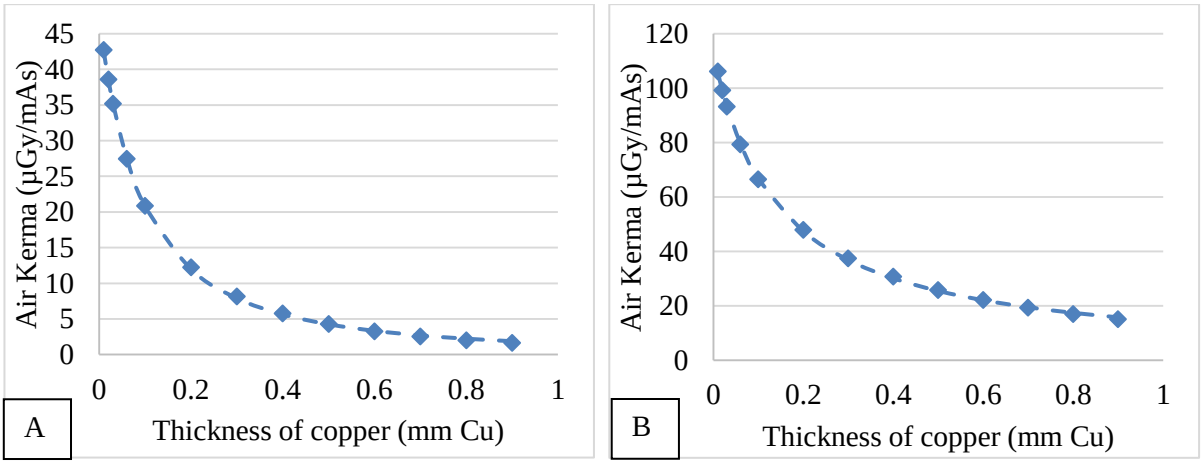

Figure 34 - Dependence of dose output on filter thickness at U_1=70 kVp (A), U_2 = 110 kVp (B). Blue points: data; dashed line: fit from equation (29) for A and from equation (30) for B.

Step 3: Calculation of the DRF for all the remaining filtrations

For any thickness of copper F_{Cu} the DRF can now be calculated at U_1 and U_2:

$$DRF_{U_1} = \frac{f_1(F_{Cu})}{Y_{100,0}(U_1)} \text{ and } F_{U_2} = \frac{f_2(F_{Cu})}{Y_{100,0}(U_2)}.$$

Applying least square fitting, Matlab is used to determine a function that fits these values of the form:

$$DRF_{meas,F_{Cu}}(U, F_{Cu}) = \left(1 + A(F_{Cu}) * \frac{F_{Cu}^{B(F_{Cu})}}{U^{C(F_{Cu})}}\right)^{-1} \quad (31)$$

determining $B(F_{Cu})$ and $C(F_{Cu})$.$A(F_{Cu})$ is defined according to (25) . The values of the final output function are found by multiplying $DRF_{meas,F_{Cu}}$ and $Y_{100,0}$:

$$Y_{100,F_{Cu}} = DRF_{meas,F_{Cu}} * Y_{100,0}. \quad (32)$$

2.2.6 Parametrization with HVL and homogeneity coefficient (model 2)

In this model, the DRF depends on the HVL and the homogeneity coefficient h. These parameters have been chosen because there are physically relevant to describe the dose output of an x-ray system.

XCompW has been used to simulate the dose output for kVp values ranging from 30 to 150, with an interval of 5 kVp. The anode angle is set to 12°, the ripple to 0%. As described in 2.1.2, an inherent filtration of 2.41 mm of Aluminum is used for all kVp values. XCompW has been here preferred than TASMICS, because TASMICS' estimations of the homogeneity coefficient were very low (around 0.5) and can thus not be used.

Step 1: Estimation of h

The homogeneity coefficient cannot be measured, hence the necessity to find a function that estimates it depending on HVL_1 and kVp. The first and second HVL have been simulated with XCompW as described previously. The homogeneity coefficient can thus be derived with

$$h = \frac{HVL_1}{HVL_2}. \quad (33)$$

Figure 35 shows how h varies depending on HVL_1 and kVp.

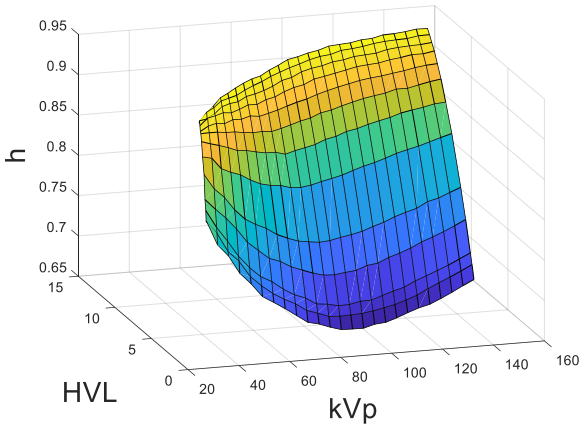

Figure 35 –Homogeneity coefficient simulated.

The values of kVp, HVL_1 and h are stored in three vectors. Thanks to the curve fitting toolbox of Matlab, the user can define a function that fits these vectors. The simplest fit that has been found is

$$h(U, HVL_1) = \left(a * U^b + d * HVL_1^c\right) * U^e, \tag{34}$$

with a, b, c, d, and e parameters determined by the least square fitting.

Figure 36 shows the surface that is produced along with the values that it fits (represented with blue points). The function is physically incorrect. Indeed, for low kVp and high HVL, h is larger than one, which is not possible. Nevertheless, for our range of values, h is always smaller than 1, so the function can still be used. Figure 37 shows that the fit results in a maximal error of 2.42%.

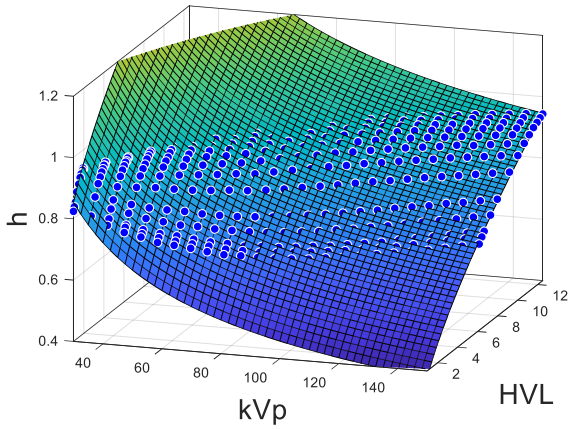

Figure 36 - Estimated function for h depending on HVL and kVp

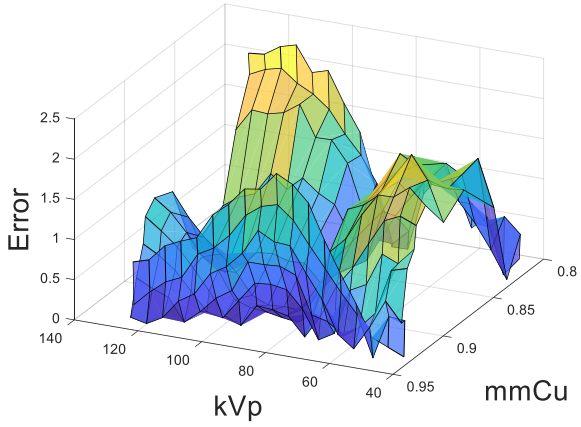

Figure 37 - Error in percent between the simulated homogeneity coefficient and the fit.

Step 2: Estimation of the HVL depending on kVp

According to (E. L. Nickoloff, 1993), a power function can estimate the variation of HVL over the range of kVp values. In order to gain some precision, a linear exponent is chosen, so that the estimation function for the HVL is:

$$HVL(U) = \alpha * U^{\beta+\lambda*U}. \tag{35}$$

Step 3: Estimation the DRF depending on HVL_1 and h

The values of the HVL, h and the DRF have been simulated with XcompW, and are shown in Figure 38. Once again, the curve fitting toolbox of Matlab is used to find a suitable function that fits these values.

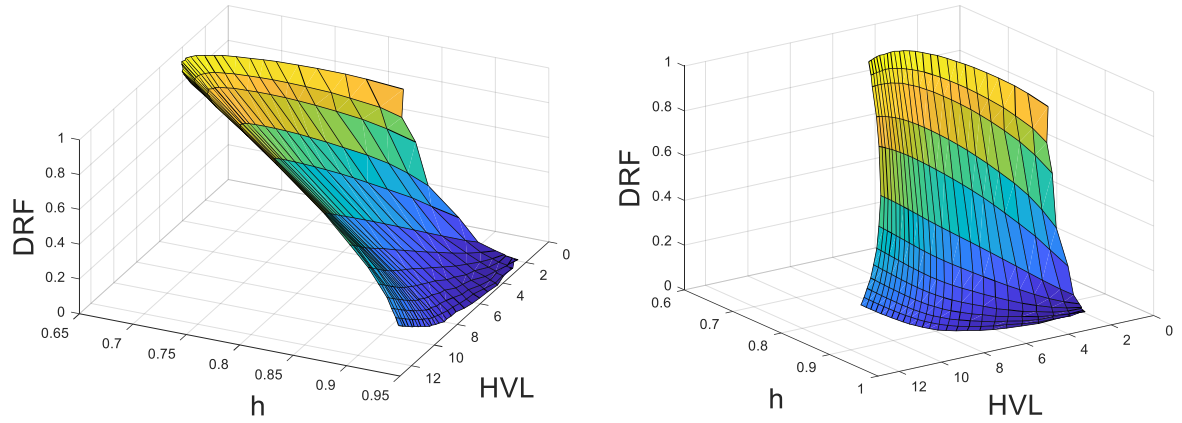

Figure 38 - DRF simulated.

The best fit that has been found is:

$$DRF_{sim}(h, HVL) = A + B * h + C * HVL + (h * HVL)^D \tag{36}$$

with A, B, C and D parameters determined with Matlab with the least square fitting.

In Figure 39, the blue points represent the data from the simulation, and the surface is the fit. One can notice that this estimated DRF is not physically coherent, as it can be larger than one or negative. Figure 40 shows the errors obtained with this fit.

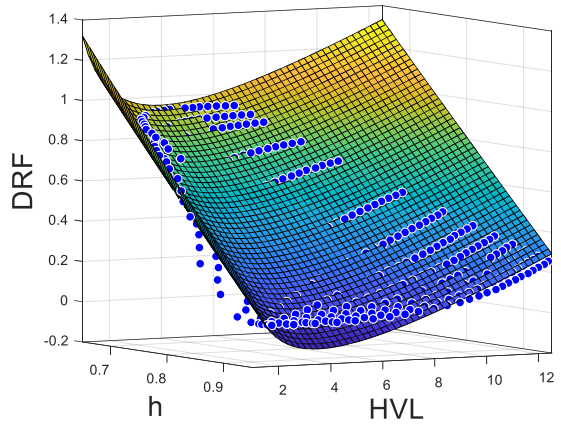

Figure 39 - Surface: DRF estimated; blue points: data.

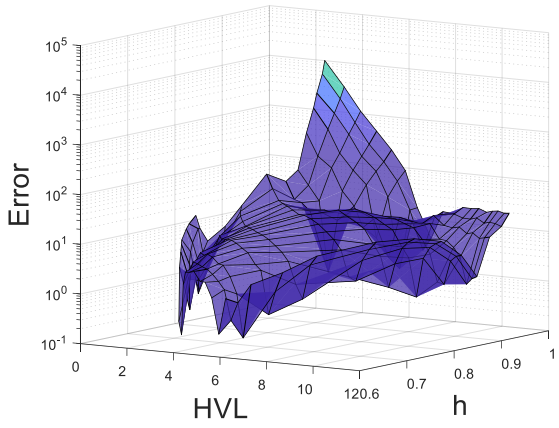

Figure 40 - Errors in percent between the fit and the simulated data.

As they are very large, the same approach as in the first model is applied: A, B, C and D are defined as functions of the filtration:

$$DRF_{sim}(h, HVL) = A(F) + B(F) * h + C(F) * HVL + (h * HVL)^{D(F)}. \quad (37)$$

A set of four parameters (A(F), B(F), C(F) and D(F)) is thus determined for each filtration with the least-square fitting in Matlab.

Figure 41 shows the new errors in percent when the thickness of copper is lower than 0.1mm and for the whole range of kVp. Figure 42 shows the new errors in percent when the thickness of copper is higher than 0.2 mm and for kVp values ranging from 70 to 125 kVp. Apart from a few values, the deviations are lower than 10 %, so the model is accurate.

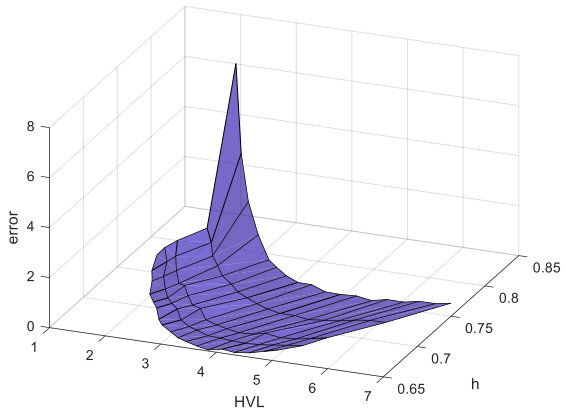

Figure 41- Errors for low filtrations,40 to 125 kVp.

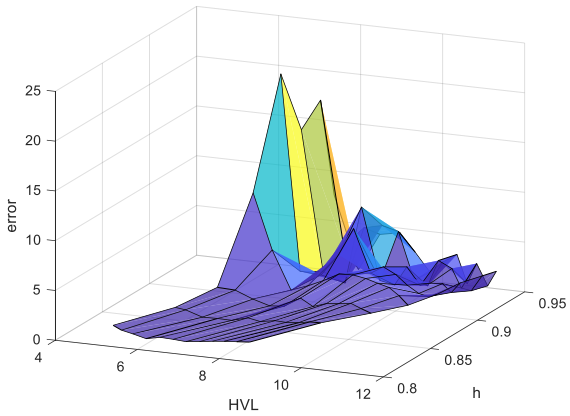

Figure 42- Errors for high filtrations,70 to 125 kVp.

In order to reduce the number of parameters, and thus later the number of measurements, a new computation has been performed where the constant A is fixed to the value of the first simulation, and B, C and D are functions of the filtration:

$$DRF_{sim}(h, HVL) = A + B(F) * h + C(F) * HVL + (h * HVL)^{D(F)}. \quad (38)$$

Figure 43 and Figure 44 show the new errors between the data and the fit. As expected, the deviations are higher than in the previous case. Indeed the overall error is now 2.25%, whereas it used to be 0.8%. Some errors are high, but it remains most of the time lower than 10%, which is precise enough, so A can be fixed.

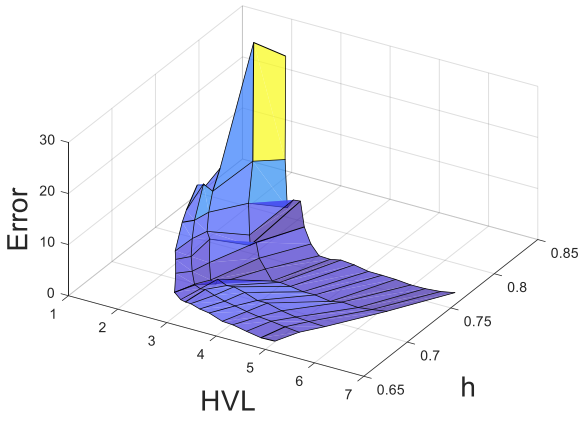

Figure 43 - Errors for low filtrations, A fixed,40 to 125 kVp.

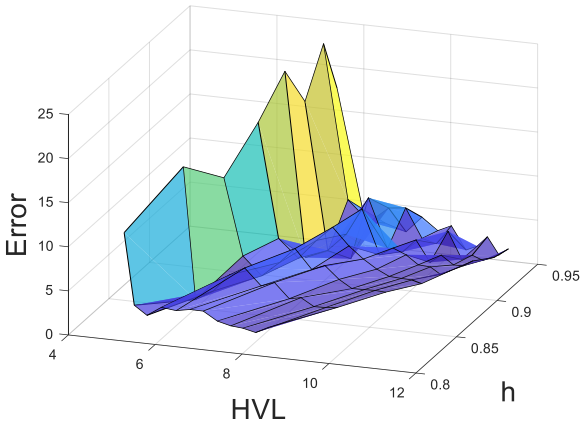

Figure 44 - Errors for high filtrations, A fixed, 70 to 125 kVp.

2.2.7 Determination of DRFs from measurement points in clinical systems (model 2)

The model is composed of different steps:

- *Step 1:* Calculation of the DRF as a function of HVL and homogeneity coefficient for the filtrations for which measurements are performed
- *Step 2:* Estimation of the dose output depending on the thickness of copper at fixed kVp
- *Step 3:* Estimation of the HVL depending on the thickness of copper at fixed kVp
- *Step 4:* Estimation of the dose output for all the other filtrations

As additional inputs, it is essential to measure the absolute dose output and the HVL at at least three kVp values and for at least two filtrations.

Filtration	*kVp*	*Absolute dose output*	*HVL*
Filter 1	U_1	K'_{U_1,f_1}	HVL_{U_1,f_1}
	U_2	K'_{U_2,f_1}	HVL_{U_2,f_1}
	U_3	K'_{U_3,f_1}	HVL_{U_3,f_1}
Filter 2	U_1	K'_{U_1,f_2}	HVL_{U_1,f_2}
	U_2	K'_{U_2,f_2}	HVL_{U_2,f_2}
	U_3	K'_{U_3,f_2}	HVL_{U_3,f_2}

Table 11 – Additional inputs of the second model

Step 1: Calculation of the DRF as a function of HVL and homogeneity coefficient for the filtrations for which measurements are performed

Thanks to HVL_{U_1,f_i}, HVL_{U_2,f_i} and HVL_{U_3,f_i}, α, β and λ (from (35)) are estimated with the least square fitting in Matlab, so that the HVL is known as a function of kVp for Filter *i*.

From K'_{U_1,f_i}, K'_{U_2,f_i} and K'_{U_3,f_i}, three DRF are calculated, and Matlab fits these values according to:

$$DRF_{meas,F_{filter_i}} = A + B(F_{Filter_i}) * h + C(F_{Filter_i}) * HVL + (h * HVL)^{D(F_{Filter_i})} \quad (39)$$

The parameter A is fixed for all the systems with the value from the simulation (A=1.147). B(F_{Filter_i}), C(F_{Filter_i}) and D(F_{Filter_i}) are determined by Matlab with the least square fitting. The values of the final function are found by multiplying $DRF_{meas,F_{Filter_i}}$ with $Y_{100,0}$:

$$Y_{100,F_{Filter_i}} = DRF_{meas,F_{Filter_i}} * Y_{100,0}. \quad (40)$$

Step 2: Estimation of the dose output depending on the thickness of copper at fixed kVp

This step is the same as Step 2 from the previous model.

Step 3: Estimation of the HVL_1 depending on the thickness of copper at fixed kVp

In order to obtain an estimation of the DRF for the other thicknesses of copper, the HVL for all the filtrations are needed. Thanks to the simulation, one can see that it can be estimated with a power function. Figure 45 and Figure 46 show in red the estimation of the HVL at respectively 70 and 110 kVp with a power function when only the values at 0.2 and 0.6 mm of copper are known. The simulation's values are represented with blue points.

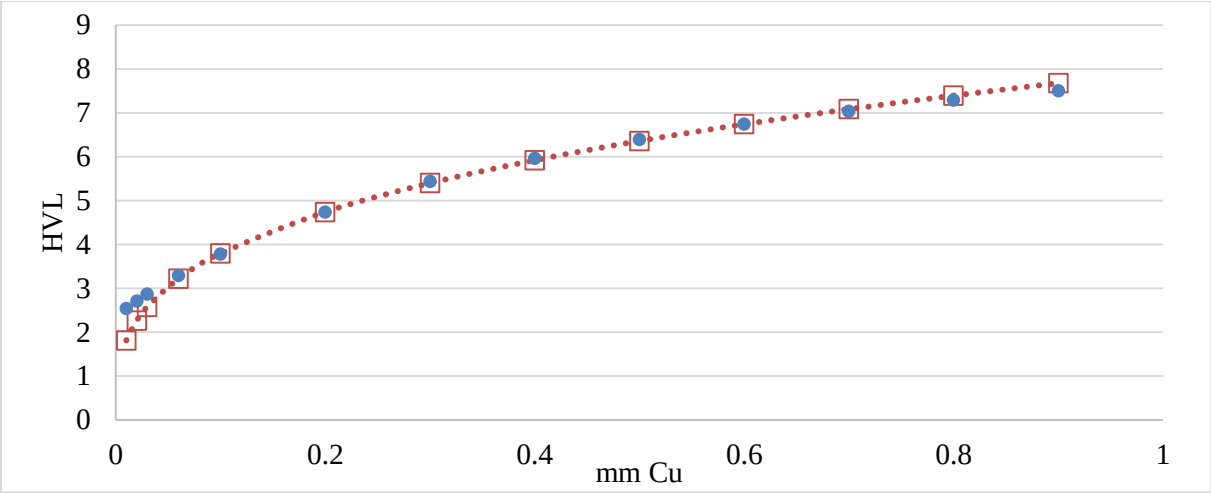

Figure 45 - Dependence of HVL calculated on filter thickness at 70 kVp. Blue circles: simulation's values; red line: fitted power function.

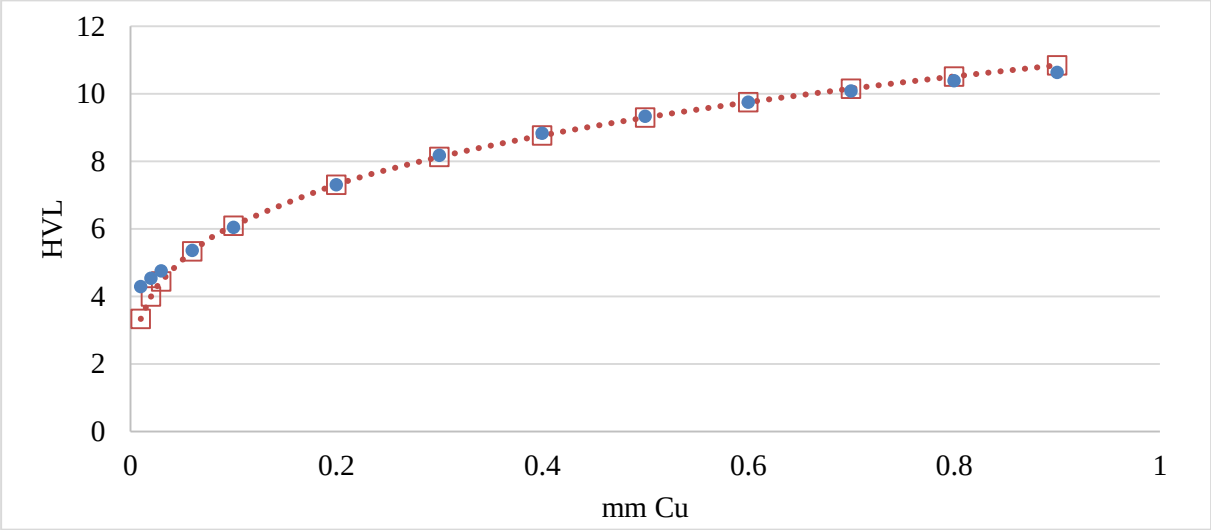

Figure 46 - Dependence of HVL calculated on filter thickness at 70 kVp. Blue circles: simulation's values; red line: fitted power function.

As a consequence, the HVL at U_1 (thanks to HVL_{U_1,f_1} and HVL_{U_1,f_2}), U_2 (thanks to HVL_{U_2,f_1} and HVL_{U_2,f_2}) and U_3 (thanks to HVL_{U_3,f_1} and HVL_{U_3,f_2}) are estimated by power functions, respectively by:

$$f_{U_1}(F_{Cu}) = \lambda_{U_1} * F_{Cu}^{\alpha_{U_1}} \quad (41)$$

$$f_{U_2}(F_{Cu}) = \lambda_{U_2} * F_{Cu}^{\alpha_{U_2}}. \quad (42)$$

$$f_{U_3}(F_{Cu}) = \lambda_{U_3} * F_{Cu}^{\alpha_{U_3}} \quad (43)$$

Step 4: Estimation of the dose output for all the other filtrations

The HVL can first be estimated at U_1, U_2 and U_3 thanks to f_{U_1}, $f_{U_2}$and f_{U_3}. From these three values, Matlab finds a function that estimates the HVL for all kVp values:

$$HVL(U) = \alpha * U^{\beta+\lambda*U}. \quad (44)$$

From Step 2, the dose output at U_1, U_2 and U_3 is also estimated, and thus three DRF are calculated. Knowing those three DRF, the corresponding HVL and homogeneity coefficients, Matlab finds a function that fits the DRF according to:

$$DRF_{meas,F_{Cu}} = A + B(F_{Cu}) * h + C(F_{Cu}) * HVL + (h * HVL)^{D(F_{Cu})}. \quad (45)$$

The parameter A is fixed for all the systems with the value from the simulation. B(F_{Cu}), C(F_{Cu}) and D(F_{Cu}) are determined by Matlab with the least square fitting. The values of the final function are calculated by multiplying $DRF_{meas,F_{Cu}}$ and $Y_{100,0}$:

$$Y_{100,F_{Cu}} = DRF_{meas,F_{Cu}} * Y_{100,0}. \quad (46)$$

2.3 Specification of x-ray systems and measurement set up

2.3.1 X-ray systems

The different systems used for the measurements are described in Table 12.

	Brand	*Name*	*Tube*	*Generator*	*Location*
1	Siemens	Vertix	Biangulix BU 150/12/50R	Polydoros 50 S	CMPBE, 4th floor
2	Siemens	Siremobil Compact L	n/a	n/a	CMPBE, 4th floor
3	Shimadzu	MobileDart Evolution	n/a	n/a	AKH ICU
4	Siemens	Mira Max	n/a	n/a	Kinderklinik
5	Siemens	Aristos	Optitop 150/40/80 HC	Polydoros SX 80	Radiology AKH, 7th floor
6	Siemens	Arcadis Varic	n/a	n/a	CMPBE, 4th floor
7	Philips	Bucky Diagnost CS	n/a	Optimus 50	University of Applied Sciences
8	Siemens	Iconos R200	Optitop 150/40/80	n/a	PTPA/MA39
9	Siemens	Mobilett			CMPBE, 4th floor

Table 12 – Clinical systems

2.3.2 Dosimeter

A calibrated Unfors XI meter (Unfors RaySafe AB, Billdal, Sweden) has been used for the measurements. It can measure:

- the dose with an uncertainty of 5%,
- the kVp with an uncertainty of 2%,
- the HVL with an uncertainty of 10%

The meter has been fixed in the middle of the field to avoid any uncertainties due to a change of position.

2.3.3 Measurement set-up

For all systems, the meter was placed approximately 100 cm away from the focus of the x-ray tube. In case the distance is not exactly 100cm, the results were corrected with the inverse square law. If the system did not provide it, a frame was fixed on the x-ray device to support the filter sheets. Different copper and Aluminum filters have been used, and their thicknesses have been measured to ensure the accuracy of the measurements. For each filter, four locations have been measured with a micrometer screw (Mitutoyo 293, Kawasaki, Japan) and the results were averaged to obtain the overall measured thickness. Table 13 shows nominal and actal thickness of the filters used.

Filtration	***Material***	***Nominal Thickness (mm)***	***Actual thickness (mm)***
1	copper	0.1	0.104
2	copper	0.1	0.107
3	copper	0.1	0.105
4	copper	0.1	0.105
5	copper	0.1	0.104
6	copper	0.1	0.102
7	copper	0.2	0.204
8	copper	0.3	0.305
9	Aluminum	1	0.996
10	Aluminum	1	0.991
11	Aluminum	1	0.99
12	Aluminum	1	1.00

Table 13 - Nominal and actual thicknesses of the filters used

Since actual filter thicknesses varied slightly but measurably from nominal thicknesses, measurements were performed with typically slightly too high filter thicknesses. Filters were stacked to provide thicknesses up to 0.9 mm of copper, 2 mm Al and 1 mm Al plus 0.1 to 0.2 mm of copper (nominal). Table 13 shows actual filter thicknesses used for the determination of DRFs in the clinical systems. In

case built in filters were used (systems 5, 7 and 8) the actual thickness of the filter is assumed to equal to the nominal thickness. These filters are marked with n/a in Table 13.

Systems1	*0.1 mm Cu*	*0.2 mm Cu*	*0.3 mm Cu*	*0.4 mm Cu*	*0.5 mm Cu*	*0.6 mm Cu*	*0.7 mm Cu*	*0.8 mm Cu*	*0.9 mm Cu*	*1 mm Al*	*2 mm Al*	*1 mm Al+0.1 mm Cu*	*1 mm Al+0.2 mm Cu*
1	0.105	0.212	0.316	0.420	0.525	0.621	0.725	0.826	0.930	0.991	1.987	0.991+0.105	0.991+0.212
2	0.105	0.212	0.316	0.420	0.525	0.621	0.725	0.826	0.930	0.991	1.987	0.991+0.105	0.991+0.212
3	0.105	0.212	0.316	0.420	0.525	0.621				0.991		0.991+0.105	0.991+0.212
4	0.105	0.212	0.316	0.420	0.525	0.621				0.991		0.991+0.105	0.991+0.212
5	n/a	n/a	n/a										
6	0.105	0.212	0.316	0.420	0.525	0.621	0.725	0.826	0.930	0.991	1.987	0.991+0.105	0.991+0.212
7	n/a	n/a	n/a	0.405		0.616					1.987	0.991+0.1	0.991+0.2
8	n/a	n/a	n/a	0.405	0.512	0.616	0.720	0.825	0.921	0.991	1.987	0.991+0.1	0.991+0.2
9	0.102	0.204	0.305	0.407	0.509	0.611	0.713	0.816	0.918	0.99	1.99	0.99+0.102	0.99+0.204

Table 14 - Actual filter thicknesses used. Empty case: no measurement performed for this filtration.

3. Results

3.1 Absolute and relative output derived with XCompW and TASMICS

Table 15 shows the parameters describing the dose output calculated with XCompW and TASMICS, respectively, for inherent filtration according to equation (14).

Simulation	*a*	*b*	*c*	*c'*	*d*
XcompW	2.7388	-3.7895E-03	1.7825E-05	1.4814E-02	8.5533E-06
TASMICS	2.9081	-2.8683E-03	6.5961E-06	4.2678E-04	5.5131E-06

Table 15 - Parameters describing Y_{100} calculated for the inherent filtration

In order to determine which computer code should be chosen, the relative output calculated with both codes is compared to the relative output measured on different systems (cf. 2.3.1 for their description) in Figure 47. In the calculations with XcompW, the anode angle was set to 12°, the ripple to 0% and the inherent filtration to 2.41 mm of Aluminum as described in 2.1.2. With TASMICS, the ripple was set to 0% and the inherent filtration to 2.55 mm Al. The anode angle is automatically set to 16° in this case. The errors between the simulation and the measurements have been calculated and gathered in Table 16. For each kVp where measurements have been performed, it compares the minimal, average and maximal errors for the different clinical systems. The number between the brackets indicates the system for which the minimal or maximal value is obtained. In order to get the relative dose output, the absolute dose output is normalized by the absolute dose output at 81 kVp. As a consequence, the relative dose output at 81 kVp is always 1, and the deviations are always zero for this value, as shown in Table 16 TASMICS is always more accurate than XcompW.

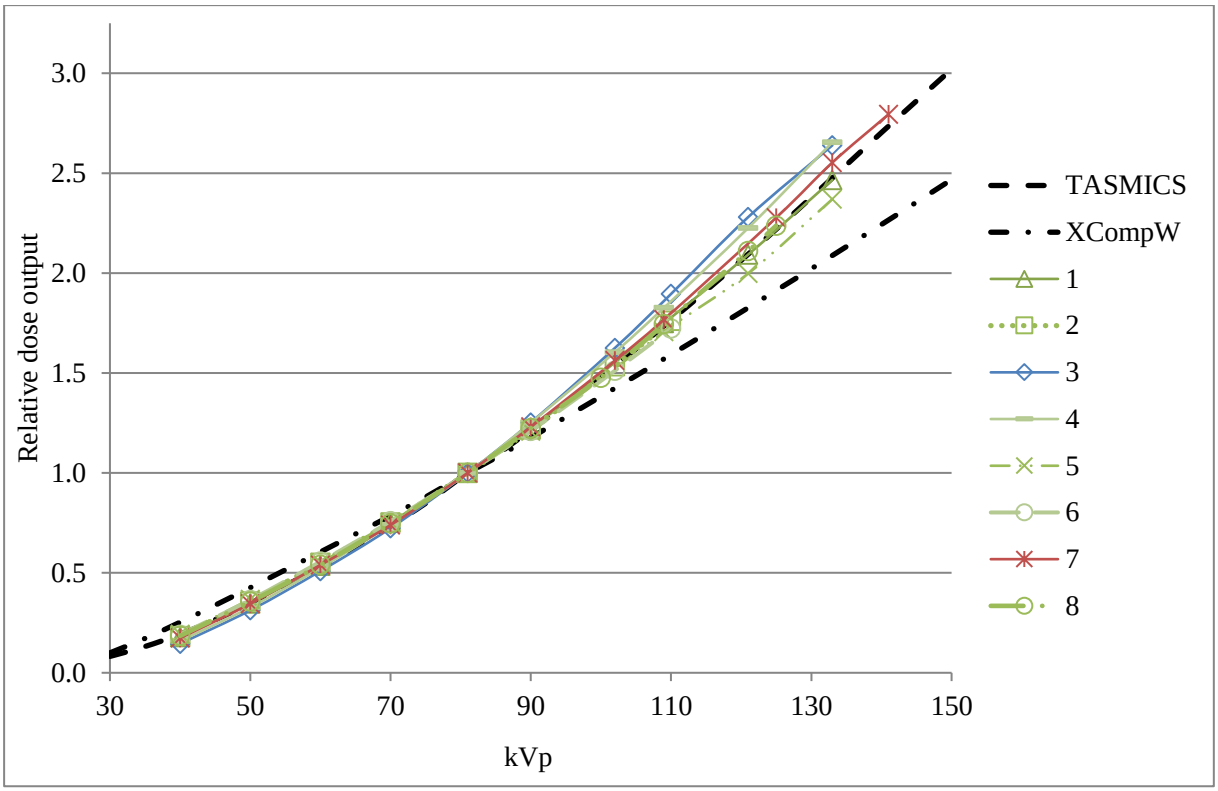

Figure 47 - Relative dose output calculated with TASMICS and XcompW along with those measured on the clinical systems.

	TASMICS			*XCompW*		
kVp	min	average	max	min	average	max
40	-22.8% (3)	-7.0%	2.8% (5)	-41.9% (3)	-30.0%	-22.6% (5)
50	-12.0% (3)	-2.6%	3.6% (5)	-25.7% (3)	-17.8%	-12.6% (5)
60	-6.1% (3)	-0.7%	2.5% (6)	-14.8% (3)	-10.0%	-7.0% (6)
70	-3.4% (3)	-0.5%	1.2% (6)	-7.3% (3)	-4.5%	-3.0% (6)
81	***0.0%***	***0.0%***	***0.0%***	***0.0%***	***0.0%***	***0.0%***
90	-1.2% (5)	0.3%	2.4% (3)	3.8% (5)	5.4%	7.5% (3)
102	-2.2% (6)	1.4%	5.1% (3)	7.5% (6)	11.4%	15.5% (3)
109/110	-3.1% (6)	0.9%	6.7% (3)	9.5% (5)	13.8%	20.5% (3)
121/125	-5.6% (5)	1.5%	7.8% (3)	10.5% (5)	19.2%	26.2% (3)
133	-5.7% (5)	0.9%	5.6% (4)	14.4% (5)	22.4%	28.1% (4)

Table 16 - Minimum, average and maximal deviations in percent for relative dose output between clinical systems and XCompW, or TASMICS, respectively. Numbers in brackets indicate which system has the minimal / maximal deviations.

The absolute dose output of the computer codes is also compared with the absolute dose outputs of the clinical systems in Figure 48. Once again, XcompW always overestimates the dose output, and is thus less accurate than TASMICS, which shows lower deviations.

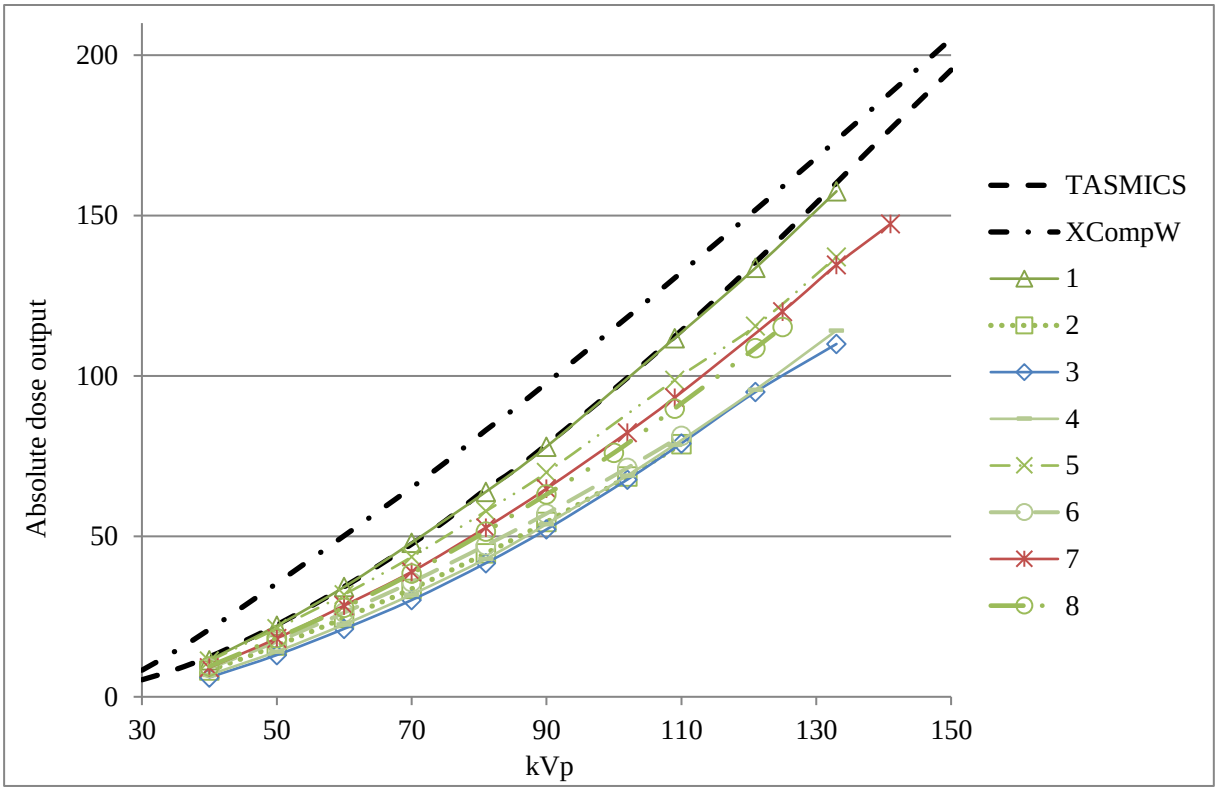

Figure 48 - Absolute dose output calculated with TASMICS and XcompW along with those measured on the clinical systems.

Table 17 shows the value of the absolute dose output for the clinical systems and TASMICS at different kVp. The crosses indicate that no measurements were available for this value. Since some kVp values cannot be set on some systems exactly to the same values (100 or 102, 109 or 110, 121 or 125), some measurements correspond to slightly different settings in Table 17. To indicate to which kVp the measurements refer, underlining has been used to indicate actual kVp values in these cases

	System 1	*System 2*	*System 3*	*System 4*	*System 5*	*System 6*	*System 7*	*System 8*	*TASMICS*
40	11.44	8.21	6.05	6.84	11.18	8.99	9.13	9.52	12.46
50	22.16	15.96	13.02	14.11	21.28	17.21	18.21	18.33	22.42
60	34.26	24.61	21.21	22.56	31.90	26.23	28.45	27.81	34.31
70	48.04	33.65	30.16	31.88	43.59	35.76	38.97	38.46	47.60
81	63.89	44.74	41.68	43.02	57.86	47.20	52.74	51.52	64.70
90	77.98	54.49	52.17	53.81	69.93	57.12	64.88	63.08	78.60
100/102	X	68.64	67.73	69.00	X	71.36	82.37	76.04	95.87
109/110	111.78	78.75	78.99	78.56	98.73	81.32	93.24	89.87	114.17
121/125	133.70	X	95.02	95.73	115.60	X	120.12	108.72	143.61
133	157.57	X	109.98	114.19	137.12	X	134.65	X	160.15

Table 17 - Absolute dose outputs of clinical systems and TASMICS

3.2 Deviations obtained with the first model when using XCompW or TASMICS

Deviations between the measurements and the results of the Matlab program (first model) have also been compared. Average, maximum and minimum deviations with the respective kVp values are shown in Table 17 depending on which computer code is used to run the Matlab program: the first column gives the results when using XCompW, the second when using TASMICS. In each case, the measured absolute dose output at 40, 81 and the highest achievable kVp are given as inputs to the Matlab program. The errors are shown in percent. The minimum deviation is always at 50 kVp, whereas the maximum varies between 90 to 121 kVp. Overall the deviations are rather close for both computer codes, but in average TASMICS is slightly better, it will thus be chosen to run the Matlab program.

Systems	*XcompW*			*TASMICS*		
	Maximum negative deviation	Average	Maximum positive deviation	Maximum negative deviation	Average	Maximum positive deviation
1	-7.05	-1.24	1.66*	-7.70	-1.22	2.46[@]
2	-7.84	-1.85	1.16*	-8.37	-1.97	1.37*
3	-9.14	-1.80	1.10*	-10.49	-1.70	2.28[#]
4	-8.97	-0.94	7.18[&]	-9.90	-0.87	7.87[&]
5	-7.87	-1.02	2.81[&]	-8.28	-1.00	3.32*
6	-7.87	-1.85	1.71*	-7.97	-1.85	1.35[#]
7	-8.83	-0.99	2.39[@]	-9.52	-1.00	3.29[@]
8	-7.72	-0.90	2.72[#]	-8.18	-0.89	3.20[#]

Table 18 – Maximum negative, average and maximum positive deviations in percent for the individual systems. Inherent filtration, XCompW or TASMICS used to run the Matlab program, respectively. Max. negative deviation was always seen at 50 kVp. Max. positive at 90(*), 100 or 102 (#), 109 ([@]) or 121([&]) kVp

3.3 Output parametrization of clinical systems

The individual output of clinical systems without added filtration is described using formula (17) with the parameter set derived from TASMICS shown in Table 15 applying the correction from (16). This corresponds to the first model.

The parameters describing $Y_{100,0}$ for the different machines are provided in Table 19. They have been derived according to (16) with the three measurement points set to: 40, 81, and the maximum kVp of the machines clinically used. This corresponded to 110 kVp in systems 2 and 6, and to 133 kVp for the remaining systems.

Systems	x_1	x_2	x_3
1	0,6308	7,7136E-03	-3,7198E-05
2	0,6432	8,3328E-03	-4,6720E-05
3	0,2076	1,5304E-02	-6,6392E-05
4	0,4047	1,1313E-02	-4,7163E-05
5	0,8013	4,7869E-03	-2,7043E-05
6	0,7151	7,3259E-03	-4,5251E-05
7	0,5716	8,4785E-03	-3,7612E-05
8	0,7075	6,2313E-03	-3,0579E-05

Table 19 - Parameters describing $Y_{100,0}$ for the different systems

Figure 49 shows Y_{100} as a function of kVp. For each system, the estimation from the Matlab program is shown with a dashed line, and the measurement data with points. The red points represent the data given as inputs to the Matlab program. From this plot, one can see that the estimation is accurate, as there is no aberration point. Some points are not exactly aligned with the line, but the errors remain low. This is confirmed by the 'TASMICS' column of Table 18 which gives the deviations between the measurements and the estimation from the Matlab program in percent. They are never higher than 10%.

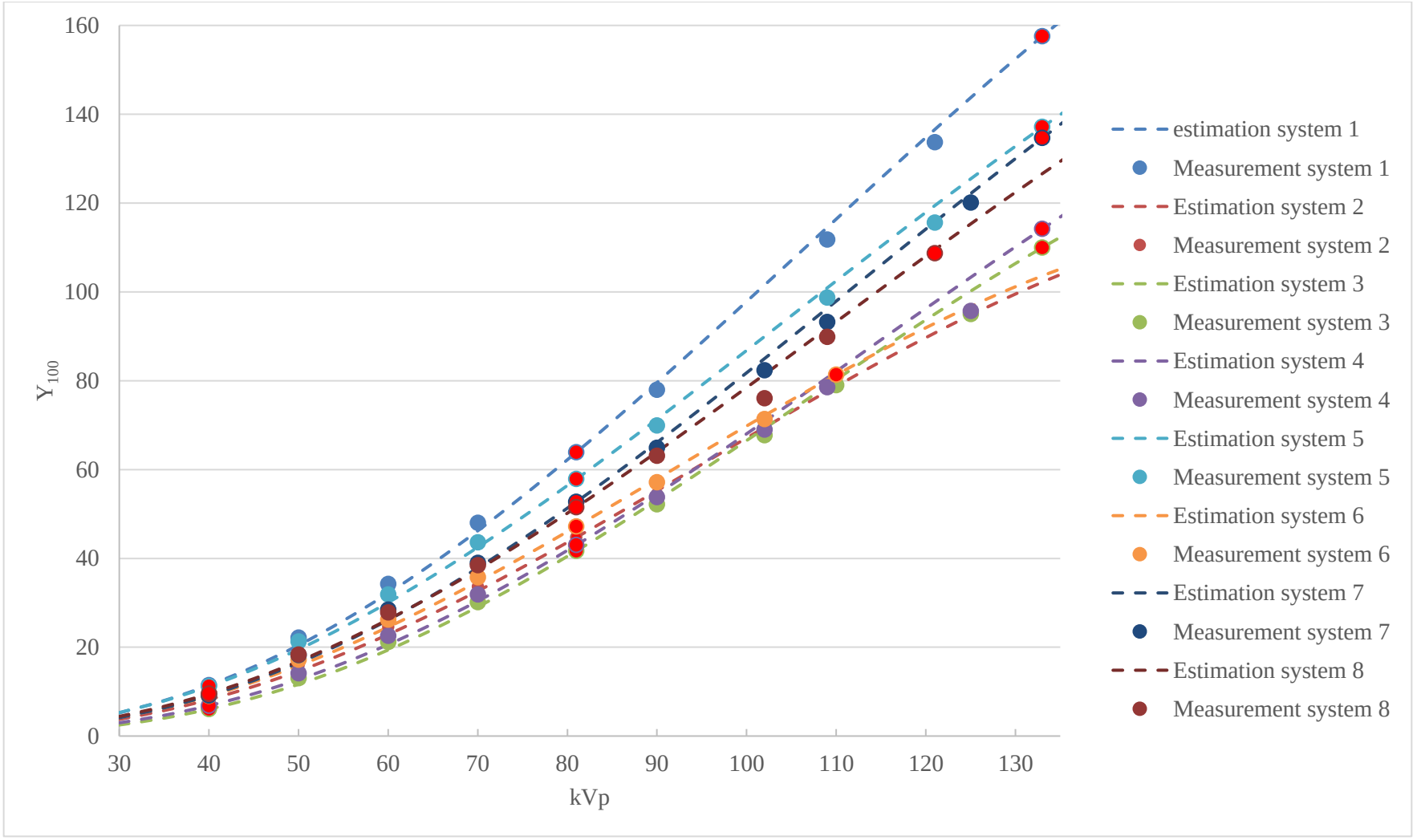

Figure 49 – Y_{100} for the inherent filtration of the clinical systems. Dashed line: estimation from Matlab program; points: measurement data; red points: input of the Matlab program.

3.4 Parametrization of DRF as a function of kV and copper thickness

DRFs calculated with TASMICS were compared to DRFs measured for the clinical systems. Tables 19 and 20 show these values as examples for all systems and TASMICS for 2 kVp points; 70 and 109/110 kVp, respectively. Values calculated with TASMICS are smaller than measured values. This could come from the actual thickness of the filters used, which is always thicker than the nominal one. This is discussed in 4.6.

Systems	*0.1 mm Cu*	*0.2 mm Cu*	*0.3 mm Cu*	*0.4 mm Cu*	*0.5 mm Cu*	*0.6 mm Cu*	*0.7 mm Cu*	*0.8 mm Cu*	*0.9 mm Cu*	*1 mm Al*	*2 mm Al*	*1 mmAl+0.1mm Cu*	*1 mm Al+0.2 mm Cu*
1	0.4622	0.2783	0.1838	0.1306	0.0967	0.0750	0.0581	0.0460	0.0364	0.7500	0.5880	0.3844	0.2388
2	0.4961	0.3061	0.2095	0.1508	0.1132	0.0885	0.0695	0.0559	0.0451	0.7742	0.6238	0.4191	0.2694
3	0.5231	0.3267	0.2228	0.1600	0.1190	0.0922	x	x	x	0.7857	x	0.4358	0.2833
4	0.4886	0.2983	0.2007	0.1432	0.1060	0.0793	x	x	x	0.7651	x	0.4085	0.2584
5	0.4623	0.2790	0.1880	x	x	x	x	x	x	x	x	x	x
6	0.4876	0.2989	0.2021	0.1448	0.1080	0.0849	0.0664	0.0532	0.0428	0.7729	0.6164	0.4109	0.2618
7	0.4770	0.2942	0.1978	0.1422	x	0.0827	x	x	x	x	0.0739	0.4140	0.2644
8	0.4798	0.2930	0.1925	0.1390	0.1029	0.0782	0.0611	0.0487	0.0394	0.7550	0.5933	0.3968	0.2519
TASMICS	0.4376	0.2574	0.1710	0.1214	0.0899	0.0685	0.0534	0.0423	0.0339	0.7249	0.5545	0.3584	0.2201

Table 20 - DRF measured at 70 kVp for clinically used filtrations and TASMICS

Systems	*0.1 mm Cu*	*0.2 mm Cu*	*0.3 mm Cu*	*0.4 mm Cu*	*0.5 mm Cu*	*0.6 mm Cu*	*0.7 mm Cu*	*0.8 mm Cu*	*0.9 mm Cu*	*1 mm Al*	*2 mm Al*	*1 mmAl+0.1mm Cu*	*1 mm Al+0.2 mm Cu*
1	0.5989	0.4330	0.3374	0.2777	0.2347	0.2044	0.1779	0.1581	0.1398	0.8197	0.6945	0.5262	0.3895
2	0.6469	0.4825	0.3847	0.3202	0.2754	0.2402	0.2100	0.1893	0.1693	0.8414	0.7204	0.5673	0.4340
3	0.6562	0.4875	0.3909	0.3242	0.2768	0.2424	x	x	x	0.8431	x	0.5786	0.4413
4	0.6261	0.4562	0.3594	0.2983	0.2530	0.2193	x	x	x	0.8331	x	0.5483	0.4111
5	0.6062	0.4377	0.3428	x	x	x	x	x	x	x	x	x	x
6	0.6348	0.4695	0.3756	0.3137	0.2679	0.2362	0.2077	0.1850	0.1659	0.8434	0.7203	0.5635	0.4283
7	0.6140	0.4479	0.3536	0.2933	x	0.2173	x	x	x	x	0.6896	0.5565	0.4151
8	0.6173	0.4545	0.3530	0.2938	0.2494	0.2142	0.1883	0.1658	0.1478	0.8238	0.6954	0.5461	0.4096
TASMICS	0.5824	0.4191	0.3281	0.2687	0.2263	0.1942	0.1690	0.1486	0.1318	0.7979	0.6615	0.5070	0.3760

Table 21 - DRF measured at 109 or 110 kVp for clinically used filtrations and TASMICS

To assess the accuracy of DRFs derived from a limited set of measurement points, measurements from 0.2 and 0.6 mm copper at 70 and the highest achievable kVp were used to derive DRFs for all kVp values and filtrations according to (25). In case of system 5, 0.2 and 0.3 mm Cu were used, since higher filtrations were not available. When interpreting the results for higher filtrations in this system, this fact should be taken into account. The parameters A, B and C according to equation 25 can be found in tables 21 to 23.

Measured DRFs were compared to values calculated using (25) based on these limited measurements. Table 25 and Table 26 show the differences between measured and calculated values in percent at respectively 70 and 109/110 kVp. The errors are larger at 70 kVp than at 109/110 kVp, especially for the interpolated filtrations (0.7, 0.8 and 0.9 mm Cu) which are not accurate enough.

	0.1 mm Cu	*0.2 mm Cu*	*0.3 mm Cu*	*0.4 mm Cu*	*0.5 mm Cu*	*0.6 mm Cu*	*0.7 mm Cu*	*0.8 mm Cu*	*0.9 mm Cu*	*1 mm Al*	*2 mm Al*	*1 mmAl+0.1 mm Cu*	*1 mm Al+0.2 mm Cu*
A	8,6909E+05	1,7835E+07	1,4108E+08	7,1355E+08	2,7610E+09	8,9137E+09	2,5220E+10	6,4500E+10	1,5224E+11	1,8950E+04	1,6701E+05	2,7129E+06	3,6979E+07

Table 22 - Parameter A describing the DRFs of all systems

Systems	*0.1 mm Cu*	*0.2 mm Cu*	*0.3 mm Cu*	*0.4 mm Cu*	*0.5 mm Cu*	*0.6 mm Cu*	*0.7 mm Cu*	*0.8 mm Cu*	*0.9 mm Cu*	*1 mm Al*	*2 mm Al*	*1 mm Al+0.1mm Cu*	*1 mm Al+0.2 mm Cu*
1	3,6646	6,3186	8,7068	12,0932	16,6963	20,8379	34,7050	57,0256	123,8197	1,9508	2,8026	4,4074	6,8271
2	3,4035	5,7762	8,1007	11,2384	15,4982	19,2243	32,1521	52,7892	114,5444	1,7772	2,5903	4,1000	6,3556
3	3,6385	6,2884	8,8211	12,3237	17,0932	20,9909	35,7770	58,9445	128,2808	1,8934	2,7606	4,3972	6,8821
4	3,7017	6,4315	8,8519	12,3205	17,0388	20,4202	35,5076	58,4017	126,9146	1,9601	2,8252	4,4582	6,9288
5	3,6536	6,1227	8,5512	12,1089	16,7259	23,5389	34,7897	57,1786	124,1776	1,9249	2,7866	4,3994	6,8270
6	3,4080	5,8441	8,0640	11,1691	15,3827	18,6672	31,8503	52,2543	113,3100	1,7945	2,6006	4,0994	6,3358
7	3,6978	6,3631	8,8147	12,2563	16,9361	21,2117	35,2499	57,9500	125,8809	1,9624	2,8249	4,4505	6,9055
8	3,5387	6,0174	8,4319	11,7106	16,1653	20,0667	33,5886	55,1821	119,8005	1,8585	2,6968	4,2617	6,6105
TASMICS	3,3702	5,6357	7,8800	10,8689	14,9183	19,4197	30,7275	50,3095	108,9015	1,7847	2,5792	4,0444	6,2123

Table 23 - Parameter B describing the DRF.

Systems	*0.1 mm Cu*	*0.2 mm Cu*	*0.3 mm Cu*	*0.4 mm Cu*	*0.5 mm Cu*	*0.6 mm Cu*	*0.7 mm Cu*	*0.8 mm Cu*	*0.9 mm Cu*	*1 mm Al*	*2 mm Al*	*1 mm Al+0.1mm Cu*	*1 mm Al+0.2 mm Cu*
1	1,2042	1,3248	1,6130	1,7672	1,9009	2,3057	2,1253	2,2216	2,3097	1,0008	1,1055	1,2805	1,4926
2	1,3683	1,5594	1,8165	1,9869	2,1348	2,5400	2,3833	2,4900	2,5877	1,1599	1,2632	1,4536	1,6837
3	1,2571	1,3903	1,6345	1,7773	1,9012	2,3398	2,1091	2,1983	2,2800	1,0797	1,1679	1,3292	1,5230
4	1,2019	1,3083	1,5968	1,7458	1,8752	2,3725	2,0922	2,1853	2,2705	1,0081	1,1070	1,2777	1,4804
5	1,2115	1,3953	1,6564	1,7661	1,8986	2,0159	2,1211	2,2166	2,3040	1,0223	1,1168	1,2881	1,4944
6	1,3593	1,5251	1,8177	1,9916	2,1426	2,5958	2,3962	2,5049	2,6046	1,1405	1,2506	1,4469	1,6822
7	1,1982	1,3231	1,5993	1,7508	1,8823	2,2833	2,1029	2,1976	2,2842	1,0011	1,1018	1,2752	1,4810
8	1,2805	1,4507	1,7021	1,8622	2,0013	2,4059	2,2346	2,3348	2,4265	1,0822	1,1812	1,3609	1,5774
TASMICS	1,3401	1,5502	1,8131	1,9931	2,1494	2,4460	2,4117	2,5243	2,6273	1,1160	1,2285	1,4302	1,6730

Table 24 - Parameter C describing the DRF

Systems	*0.1 mm Cu*	*0.2 mm Cu*	*0.3 mm Cu*	*0.4 mm Cu*	*0.5 mm Cu*	*0.6 mm Cu*	*0.7 mm Cu*	*0.8 mm Cu*	*0.9 mm Cu*	*1 mm Al*	*2 mm Al*	*1 mm Al+0.1 mm Cu*	*1 mm Al+0.2 mm Cu*
1	1.65%	3.94%	5.11%	8.89%	13.85%	3.94%	25.47%	33.52%	44.60%	3.47%	8.07%	5.58%	8.47%
2	-0.49%	3.02%	2.67%	7.11%	12.32%	3.03%	24.43%	31.80%	41.41%	1.72%	4.55%	3.13%	4.87%
3	-2.34%	3.66%	3.87%	10.09%	17.84%	3.63%	x	x	x	1.62%	x	3.58%	6.37%
4	0.00%	4.86%	4.74%	9.76%	16.30%	4.88%	x	x	x	2.85%	x	4.81%	7.66%
5	1.91%	2.53%	2.52%	x	x	x	x	x	x	x	x	x	x
6	-0.17%	2.90%	3.22%	7.56%	12.99%	2.86%	24.04%	31.49%	41.07%	1.42%	4.90%	3.41%	5.18%
7	1.13%	2.89%	3.46%	7.04%	x	2.94%	x	x	x	x	9.40%	1.86%	2.85%
8	-0.31%	2.28%	4.30%	7.08%	12.65%	2.65%	26.83%	34.60%	43.09%	3.30%	8.04%	4.99%	6.05%

Table 25 - Differences between measured and calculated DRF at 70 kVp.

Systems	*0.1 mm Cu*	*0.2 mm Cu*	*0.3 mm Cu*	*0.4 mm Cu*	*0.5 mm Cu*	*0.6 mm Cu*	*0.7 mm Cu*	*0.8 mm Cu*	*0.9 mm Cu*	*1 mm Al*	*2 mm Al*	*1 mm Al+0.1 mm Cu*	*1 mm Al+0.2 mm Cu*
1	0.46%	-2.41%	-2.65%	-4.18%	-4.96%	-7.00%	-5.71%	-5.78%	-4.26%	2.93%	6.53%	3.83%	3.65%
2	-0.43%	-0.02%	-0.24%	0.26%	0.43%	0.02%	3.58%	3.99%	6.28%	2.48%	6.67%	4.86%	5.39%
3	-1.20%	0.47%	-1.09%	-0.33%	0.46%	-3.78%	x	x	x	2.70%	x	3.71%	4.68%
4	-1.08%	-1.74%	-2.45%	-3.53%	-3.59%	-6.08%	x	x	x	2.31%	x	3.72%	3.64%
5	-0.41%	-2.59%	-3.12%	x	x	x	x	x	x	x	x	x	x
6	0.31%	0.00%	-0.22%	-0.49%	0.03%	0.01%	0.89%	2.27%	4.01%	1.80%	5.93%	4.16%	4.68%
7	-0.15%	-2.16%	-2.96%	-4.35%	x	-6.28%	x	x	x	x	8.55%	0.97%	0.82%
8	0.08%	-1.30%	-1.41%	-2.94%	-3.23%	-5.64%	-2.11%	-0.62%	0.76%	3.33%	7.96%	3.66%	3.26%

Table 26 - Differences between measured and calculated DRF at 109/110 kVp.

3.5 Generic Dose output and DRFs

From the measurements on the eight first clinical systems, generic Y_{100} values were derived for inherent filtration. As generic value of tube output, central values determined from the measurements at a given kVp value defined as

$$CV = \frac{Max\left(Y_{100_{system_1}};Y_{100_{system_2}};\ldots;Y_{100_{system_8}}\right) + Min\left(Y_{100_{system_1}};Y_{100_{system_2}};\ldots;Y_{100_{system_8}}\right)}{2}.$$

provide the best data available. These central values of Y_{100} are shown in Table 27 together with range limits. Thus, CV plus uncertainty provided in Table 27 corresponds to minimal value found in the clinical systems, and CV plus uncertainty to the maximum. Standard deviations are provided in brackets.

$$Uncertainty = CV - Min\left(DRF_{system_1}; DRF_{system_2}; \ldots; DRF_{system_8}\right).$$

kVp	*Generic Y_{100} (µGy/mAs)*
40	8.75 ± 2.7 (1.89)
50	17.59 ± 4.6 (3.19)
60	27.74 ± 6.6 (4.45)
70	39.10 ± 8.9 (6.03)
81	52.78 ± 11.1 (7.72)
90	65.08 ± 12.9 (9.03)
102	75.05 ± 7.3 (5.68)
110	95.17 ± 16.6 (11.99)
121	114.36 ± 19.3 (15.99)
133	133.8 ± 23.8 (19.24)

Table 27 – Generic Y_{100}

From these values, a fit has been realised to obtain a function for the generic dose output (cf. Figure 50) according to (12):

$$Y_{100} = c * kVp^{a+b*kVp+d*kVp^2} \qquad (47)$$

with the parameters given in Table 28.

a	*b*	*c*	*d*
2.4613	-1.2643e-3	1.5184e-3	2.0360e-6

Table 28- Parameters for the generic dose output of the inherent filtration

The deviations between the generic data and the fit are shown in Table 29. The large error at 102 kVp comes from the abnormally low generic data at 102 kVp (cf. Figure 50). Except from this point and the one at 40 kVp, the errors remain close to 0%, the fit is thus accurate.

kVp	*40*	*50*	*60*	*70*	*81*	*90*	*102*	*110*	*121*	*133*
Errors (%)	27.89	4.49	-1.58	-3.24	-3.11	-2.77	7.97	-1.43	-1.62	0.42

Table 29 - Errors in percent between generic data and fit function.

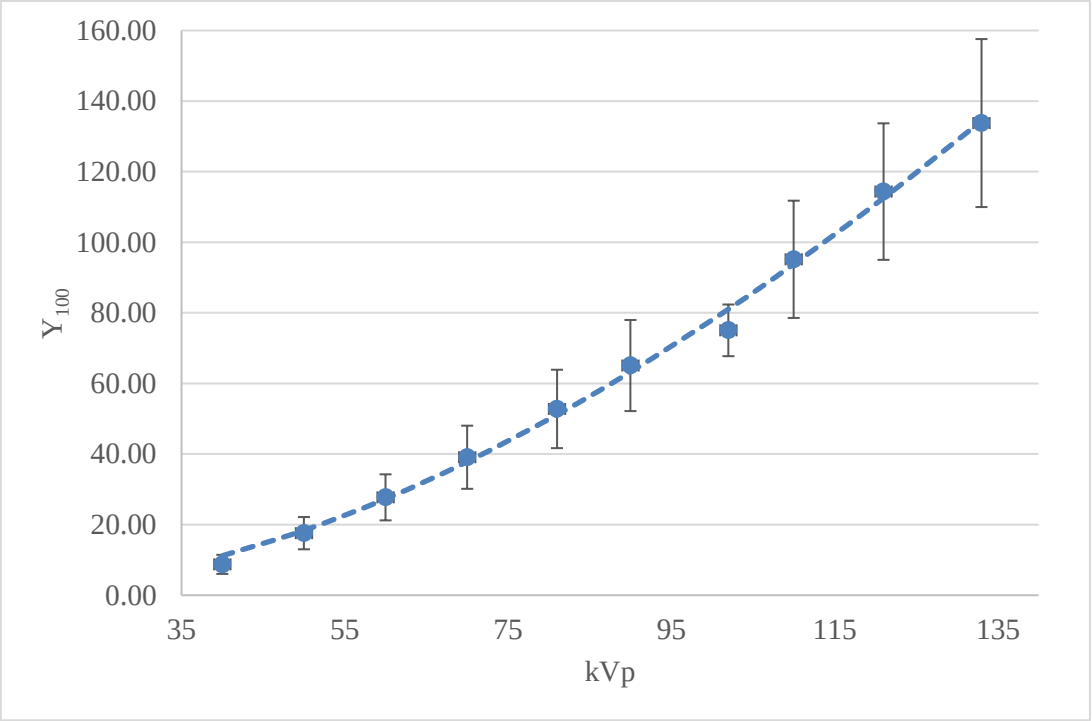

Figure 50 – Function for generic output. Points: generic data; dashed line: fit of the generic data; bars: uncertainties.

The same procedure is applied to obtain generic DRF: DRF have been calculated from the measurements for each kVp and filtration where measurements have been performed. Table 30 shows central values and uncertainties defined by the minimum and maximum values found. Some cases are empty because not enough measurement points were available to calculate the central value.

Alternatively, Table 31 shows the same data calculated with TASMICS. As already seen in Table 20 and Table 21, DRFs calculated with TASMICS are slightly smaller (-11% on average) than seen in the measurements.

Systems	*0.1 mm Cu*	*0.2 mm Cu*	*0.3 mm Cu*	*0.4 mm Cu*	*0.5 mm Cu*	*0.6 mm Cu*	*0.7 mm Cu*	*0.8 mm Cu*	*0.9 mm Cu*	*1 mm Al*	*2 mm Al*	*1 mmAl+0.1mm Cu*	*1 mm Al+0.2 mm Cu*
40	0.278 ±0.010	0.106 ±0.004	0.045 ±0.003										
50	0.368 ±0.016	0.175 ±0.009	0.095 ±0.007								0.498 ±0.003		
60	0.428 ±0.019	0.232 ±0.010	0.146 ±0.011	0.101 ±0.004						0.733 ±0.015	0.560 ±0.019	0.343 ±0.018	0.196 ±0.014
70	0.493 ±0.030	0.302 ±0.024	0.203 ±0.019	0.145 ±0.015	0.108 ±0.011	0.084 ±0.009	0.064 ±0.006	0.051 ±0.005	0.041 ±0.004	0.768 ±0.018	0.606 ±0.018	0.410 ±0.026	0.261 ±0.022
81	0.549 ±0.024	0.365 ±0.019	0.259 ±0.017	0.193 ±0.017	0.152 ±0.014	0.124 ±0.012	0.100 ±0.008	0.084 ±0.007	0.071 ±0.006	0.792 ±0.018	0.640 ±0.019	0.469 ±0.020	0.319 ±0.016
90	0.577 ±0.032	0.395 ±0.027	0.293 ±0.024	0.231 ±0.020	0.187 ±0.017	0.157 ±0.015	0.130 ±0.011	0.112 ±0.009	0.096 ±0.009	0.806 ±0.016	0.666 ±0.018	0.496 ±0.028	0.349 ±0.024
102	0.612 ±0.014	0.440 ±0.013	0.342 ±0.013	0.279 ±0.014	0.232 ±0.013	0.197 ±0.010	0.173 ±0.012	0.151 ±0.011	0.134 ±0.010	0.826 ±0.006	0.694 ±0.016	0.536 ±0.011	0.395 ±0.012
109/110	0.628 ±0.029	0.460 ±0.027	0.364 ±0.027	0.301 ±0.023	0.256 ±0.021	0.223 ±0.019	0.194 ±0.016	0.174 ±0.016	0.155 ±0.015	0.832 ±0.012	0.705 ±0.015	0.552 ±0.026	0.415 ±0.026
121	0.635 ±0.009	0.476 ±0.013	0.381 ±0.007	0.323 ±0.008	0.277 ±0.008	0.245 ±0.006	0.217 ±0.006	0.194 ±0.005	0.175 ±0.005	0.836 ±0.000	0.711 ±0.000	0.560 ±0.025	0.431 ±0.025
133	0.651 ±0.004	0.498 ±0.010	0.410 ±0.008	0.347 ±0.000	0.302 ±0.000	0.271 ±0.000	0.252 ±0.000	0.219 ±0.000	0.199 ±0.000	0.844 ±0.000	0.719 ±0.005	0.587 ±0.008	0.462 ±0.011

Table 30 - Generic DRFs from measurements. Empty cases: not enough measurements available to calculate the central value.

	0.1	*0.2*	*0.3*	*0.4*	*0.5*	*0.6*	*0.7*	*0.8*	*0.9*	*1*	*2*	*1+0,1*	*1+0,2*
40	0.2436	0.0874	0.0369	0.0171	0.0084	0.0043	0.0023	0.0012	0.0007	0.6012	0.3892	0.1725	0.0657
50	0.3258	0.1510	0.0812	0.0474	0.0291	0.0185	0.0121	0.0081	0.0055	0.6590	0.4636	0.2487	0.1216
60	0.3880	0.2076	0.1270	0.0836	0.0577	0.0411	0.0300	0.0223	0.0169	0.6970	0.5153	0.3090	0.1735
70	0.4376	0.2574	0.1710	0.1214	0.0899	0.0685	0.0534	0.0423	0.0339	0.7249	0.5545	0.3584	0.2201
81	0.4810	0.3037	0.2142	0.1605	0.1249	0.0997	0.0812	0.0670	0.0560	0.7478	0.5874	0.4023	0.2642
90	0.5191	0.3458	0.2549	0.1984	0.1597	0.1317	0.1103	0.0937	0.0803	0.7671	0.6157	0.4413	0.3048
102	0.5588	0.3915	0.3002	0.2416	0.2003	0.1696	0.1457	0.1266	0.1110	0.7867	0.6447	0.4825	0.3490
110	0.5824	0.4191	0.3281	0.2687	0.2263	0.1942	0.1690	0.1486	0.1318	0.7979	0.6615	0.5070	0.3760
121	0.6112	0.4537	0.3637	0.3038	0.2602	0.2268	0.2002	0.1784	0.1602	0.8114	0.6820	0.5373	0.4099
133	0.6396	0.4885	0.4000	0.3399	0.2956	0.2612	0.2334	0.2104	0.1910	0.8245	0.7020	0.5673	0.4442

Table 31 – DRF calculated with TASMICS

3.6 Parametrization of DRF as a function of HVL and homogeneity coefficient

Non-linear regression according to (38) results in parameters B, C and D shown in Table 32, Table 33 and Table 34. To obtain these parameters, measurements have been performed with 0.2 mm of copper as first filter and 0.6 mm of Copper as second filter. The measurements have been performed at 70 and 109 or 110 kVp, depending on the system's possibilities. The parameter A is fixed to the simulation's value:

$$A = 1{,}147.$$

Once again, as 0.6 mm of copper was not available for the Aristos system, the second filtration is 0.3 mm of copper. The results for higher filtrations should thus be taken with caution.

Systems	*0.1 mm Cu*	*0.2 mm Cu*	*0.3 mm Cu*	*0.4 mm Cu*	*0.5 mm Cu*	*0.6 mm Cu*	*0.7 mm Cu*	*0.8 mm Cu*	*0.9 mm Cu*	*1 mm Al*	*2 mm Al*	*1 mmAl+0.1mm Cu*	*1 mm Al+0.2 mm Cu*
1	-2.4870	-2.5914	-2.6382	-2.6606	-2.6866	-2.7721	-2.7315	-2.7474	-2.7596	-2.2183	-2.3627	-2.5501	-2.6226
2	-2.4902	-2.5376	-2.3990	-1.9941	-1.9651	-1.9655	-1.8995	-1.8680	-1.8382	-2.0313	-2.3223	-2.5576	-2.5287
3	-2.4676	-2.6661	-2.7616	-2.7926	-2.8109	-2.8796	-2.8348	-2.8433	-2.8503	-2.0609	-2.2909	-2.5671	-2.7200
4	-2.4795	-2.6742	-2.7931	-2.8338	-2.8577	-2.9397	-2.8835	-2.8905	-2.8953	-2.1202	-2.3066	-2.5802	-2.7433
5	-2.5455	-2.6563	-2.5643	-2.2445	-1.9266	-1.8608	-1.7957	-1.7328	-1.6724	-2.0678	-2.3623	-2.6292	-2.6473
6	-2.5068	-2.5544	-2.5523	-2.5154	-2.5171	-2.6669	-2.5890	-2.6278	-2.6607	-2.2305	-2.3848	-2.5627	-2.5847
7	-2.4336	-2.6477	-2.7645	-2.8188	-2.8498	-2.9122	-2.8775	-2.8831	-2.8860	-2.1257	-2.2714	-2.5312	-2.7029
8	-2.5370	-2.7149	-2.7715	-2.7734	-2.7696	-2.8150	-2.7665	-2.7674	-2.7691	-2.1279	-2.3615	-2.6310	-2.7532
TASMICS	-2.3939	-2.3419	-2.0842	-1.9739	-1.9739	-1.9997	-1.9646	-1.9789	-2.1738	-2.1468	-2.2956	-2.4169	-2.2910

Table 32 - Parameter B

Systems	*0.1 mm Cu*	*0.2 mm Cu*	*0.3 mm Cu*	*0.4 mm Cu*	*0.5 mm Cu*	*0.6 mm Cu*	*0.7 mm Cu*	*0.8 mm Cu*	*0.9 mm Cu*	*1 mm Al*	*2 mm Al*	*1 mmAl+0.1mm Cu*	*1 mm Al+0.2 mm Cu*
1	0.0668	0.0564	0.0506	0.0348	0.0178	0.0013	-0.0147	-0.0290	-0.0417	0.0762	0.0670	0.0667	0.0596
2	0.0420	0.0794	0.0898	0.0831	0.0759	0.0728	0.0652	0.0612	0.0578	-0.0297	0.0133	0.0588	0.0852
3	0.0254	0.0197	0.0296	0.0222	0.0131	0.0096	-0.0057	-0.0146	-0.0228	0.0265	0.0216	0.0289	0.0323
4	0.0406	0.0204	0.0141	0.0002	-0.0136	-0.0277	-0.0383	-0.0488	-0.0581	0.0916	0.0547	0.0349	0.0229
5	0.0073	0.0468	0.0639	0.0713	0.0636	0.0562	0.0501	0.0449	0.0405	-0.0501	-0.0168	0.0228	0.0538
6	0.0818	0.0849	0.0816	0.0729	0.0620	0.0441	0.0357	0.0218	0.0083	0.0824	0.0783	0.0846	0.0855
7	0.0678	0.0280	0.0139	-0.0105	-0.0321	-0.0437	-0.0660	-0.0790	-0.0898	0.1252	0.0854	0.0578	0.0316
8	0.0140	0.0180	0.0250	0.0188	0.0105	0.0036	-0.0074	-0.0159	-0.0239	0.0026	0.0062	0.0196	0.0265
TASMICS	0.0929	0.0892	0.0830	0.0710	0.0628	0.0595	0.0505	0.0455	0.0348	0.1031	0.0925	0.0939	0.0904

Table 33 - Parameter C

Systems	*0.1 mm Cu*	*0.2 mm Cu*	*0.3 mm Cu*	*0.4 mm Cu*	*0.5 mm Cu*	*0.6 mm Cu*	*0.7 mm Cu*	*0.8 mm Cu*	*0.9 mm Cu*	*1 mm Al*	*2 mm Al*	*1 mmAl+0.1mm Cu*	*1 mm Al+0.2 mm Cu*
1	-0.0555	-0.0154	0.0111	0.0741	0.1404	0.2160	0.2488	0.2891	0.3218	-0.2003	-0.0917	-0.0448	-0.0207
2	0.0821	-0.0978	-0.2897	-0.7501	-0.7215	-0.7015	-0.6869	-0.6756	-0.6669	0.1615	0.1326	0.0316	-0.1475
3	0.1343	0.1824	0.1635	0.1856	0.2121	0.2362	0.2645	0.2876	0.3081	-0.0142	0.0992	0.1438	0.1535
4	0.0622	0.1630	0.2036	0.2454	0.2828	0.3311	0.3419	0.3646	0.3837	-0.3413	-0.0512	0.1067	0.1722
5	0.1857	0.0529	-0.0818	-0.3606	-0.6803	-0.6805	-0.6904	-0.7076	-0.7309	0.2192	0.2148	0.1516	0.0149
6	-0.0688	-0.1263	-0.1450	-0.1360	-0.0837	0.0596	0.0639	0.1285	0.1824	-0.1603	-0.0827	-0.0773	-0.1253
7	-0.0770	0.1228	0.1911	0.2653	0.3206	0.3573	0.3929	0.4170	0.4360	-0.5634	-0.2283	-0.0060	0.1261
8	0.1699	0.1815	0.1623	0.1752	0.1964	0.2270	0.2455	0.2687	0.2899	0.0682	0.1493	0.1711	0.1617
TASMICS	-0.2371	-0.3587	-0.6599	-0.7199	-0.6165	-0.5347	-0.4682	-0.3901	-0.1472	-0.3728	-0.2501	-0.2644	-0.4353

Table 34 - Parameter D

3.7 Comparison of the models parametrizing DRFs

The two models described in 2.2.2 have also been compared to determine which one should be used. Table 35 shows the minimal, average and maximal errors in percent for each filtration and for each system depending on which model is chosen. The first model refers to the model where the DRF depends on kVp and filter thickness, whereas in the second model the DRF depends on the HVL and the homogeneity coefficient h. The values between the brackets follow the notation: (minimal error; average error; maximal error). They have been obtained by choosing 0.2 mm Cu and 0.6 mm Cu as filters for the inputs of the program. For the first model, measurements were made at 70 and the closest achievable value to 110 kVp, for the second one at 70, 90 and the closest achievable value to 110 kVp. In both case, the absolute value for the inherent filtration has been measured at 40, 81 and the highest achievable kVp (110 or 133 kVp). The measurements on the Aristos system were not possible for a filtration of 0.6 mm Cu, so the second filter is 0.3 mm Cu. The crosses mean that no measurements have been done for this point.

There is not one model which is always better than the other one, but the first model gives overall better results. Indeed the values in bold indicate for one filtration and one clinical system which of the two models has the lowest average error. One can see that, except for the first system, the first model has an overall lower average error than the second one. Moreover, the first model requires fewer inputs than the second one. For these reasons, the first model should be preferred, and will be used for the rest of this report.

System	*1*		*2*		*3*		*4*	
	DRF(kVp,F)	DRF(HVL,h)	DRF(kVp,F)	DRF(HVL,h)	DRF(kVp,F)	DRF(HVL,h)	DRF(kVp,F)	DRF(HVL,h)
1 mm Al	(-2.6;2.0;4.0)	(-2.7;**1.1**;3.6)	(0.5;1.8;3.0)	(0.8;1.8;3.1)	(0.5;2.2;3.8)	(0.4;**1.5**;3.5)	(1.8;3.0;3.9)	(1.5;**2.3**;3.8)
2 mm Al	(-3.1;2.5;4.6)	(-3.4;**1.7**;3.6)	(0.4;2.3;4.6)	(0.3;**2.2**;4.8)	x	x	x	x
1 mm Al+0.1 mm Cu	(-1.4;2.7;4.7)	(-2.2;**2.0**;3.3)	(0.6;2.1;3.0)	(0.3;2.1;3.6)	(0.9;1.9;3.3)	(0.1;**1.3**;3.7)	(0.9;2.5;3.7)	(1.0;**2.2**;3.9)
1 mm Al+0.2 mm Cu	(0.3;2.5;4.3)	(-1.5;**1.6**;3.6)	(0.2;**1.9**;2.9)	(1.1;2.4;3.1)	(0.8;1.9;3.2)	(0.3;**1.8**;2.6)	(1.4;**2.1**;3.1)	(0.5;2.5;3.8)
0.1 mm Cu	(-2.7;0.8;3.2)	(-6.7;**-0.5**;2.1)	(0.2;**2.8**;8.2)	(0.0;3.4;11.5)	(0.4;**2.3**;5.8)	(1.3;2.9;6.0)	(0.6;1.9;4.6)	(0.1;**1.4**;4.9)
0.2 mm Cu	(0;0.3;0.8)	(-1.5;**-0.2**;1.6)	(0.0;**0.4**;1.3)	(0.3; 0.8;1.2)	(0.0;**0.8**;2.0)	(0.4;1.3;2.8)	(0.0;**0.5**;1.5)	(0.4;1.8;3.1)
0.3 mm Cu	(-0.2;**0.3**;1.1**)**	(-2.3;-0.7;2.3)	(0.1;**0.5**;1.1)	(0.0;0.6;2.1)	(0.1;**0.3**;0.5)	(0.8;1.7;2.4)	(0.1;**0.4**;1.0)	(0.8;2.4;3.9)
0.4 mm Cu	(-2.1;**0.0;**4.8)	(-5.4;-0.4;3.9)	(0.2;1.5;4.0)	(0.0;1.5;3.0)	(0.2;**2.4**;6.2)	(0.1;3.0;5.6)	(0.7;**2.0**;4.7)	(1.5;3.9;7.0)
0.5 mm Cu	(-2.5;0.9;9.6)	(-6.6;**0.6**;7.1)	(0.4;**3.6**;9.0)	(0.1;4.0;6.7)	(1.0;**5.5**;13.6)	(1.0;6.1;10.8)	(0.4;**3.9**;10.9)	(0.9;6.2;11.4)
0.6 mm Cu	(-5.9;-3.6;0)	(-6.3;**-0.7**;5.1)	(0.0;**2.7**;7.1)	(0.6;3.7;9.2)	(0.0;**2.5**;5.6)	(0.6;3.1;5.2)	(0.0;**3.4**;7.8)	(1.2;4.6;6.9)
0.7 mm Cu	(-6.6;2.4;20.7)	(-12.4;**2.1**;13.0)	(3.4;**8.6**;20.8)	(2.5;9.4;14.7)	x	x	x	x
0.8 mm Cu	(-3.4;5.2;28.7)	(-9.2;**5.0**;19.0)	(4.0;**11.6**;28.0)	(2.7;12.7;20.1)	x	x	x	x
0.9 mm Cu	(-1.8;8.6;39.3)	(-8.7;**8.4**;25.5)	(6.3;**16.0**;37.4)	(4.7;17.3;27.3)	x	x	x	x

System	*5*		*6*		*7*		*8*	
	DRF(kVp,F)	DRF(HVL,h)	DRF(kVp,F)	DRF(HVL,h)	DRF(kVp,F)	DRF(HVL,h)	DRF(kVp,F)	DRF(HVL,h)
1 mm Al	x	x	(0.3;1.5;3.2)	(0.4;1.5;3.5)	x	x	(-8.0;**0.3**;3.9)	(0.9;4.5;14.6)
2 mm Al	x	x	(0.7;2.2;3.0)	(0.5;**1.8**;4.7)	(0.7;**5.1**;6.9)	(1.0;6.8;19.1)	(-7.6;**1.3**;4.9)	(1.8;5.8;17.5)
1 mm Al+0.1 mm Cu	x	x	(0.3;1.7;2.6)	(0.3;1.7;3.4)	(0.8;**4.4**;16.2)	(0.2;8.8;48.5)	(-2.1;**2.0**;7.6)	(1.4;3.6;8.6)
1 mm Al+0.2 mm Cu	x	x	(0.2;**1.5**;2.2)	(0.5;1.8;3.1)	(0.3;**1.7**;4.0)	(0.3;3.3;16.1)	(-0.6;**1.8**;7.3)	(0.1;3.7;13.4)
0.1 mm Cu	(0.6;**2.2;**4.4)	(0.1;2.7;9.3)	(0.0;**2.2**;6.4)	(0.2;2.9;9.5)	(0.3;2.2;5.7)	(0.3;**2.1**;9.4)	(-5.4;**0.1**;11.6)	(0.0;7.8;40.6)
0.2 mm Cu	(0.0;**0.4**;1.4)	(0.3;1.1;1.6)	(0.0;**0.6**;1.3)	(0.3;0.9;1.4)	(0.0;**0.8**;1.9)	(0.2;2.8;8.3)	(-0.9;**0.4**;0.3)	(0.4;1.5;2.8)
0.3 mm Cu	(0.0;**0.7**;1.3)	(0.2;1.5;2.8)	(0.1;**0.3**;0.5)	(0.4;1.0;2.0)	(0.1;**0.8**;5.0)	(0.5;3.7;14.8)	(0.4;**0.7**;1.6)	(0.0;1.9;3.5)
0.4 mm Cu	x	x	(0.2;**1.7**;4.6)	(0.5;1.8;3.3)	(0.8;2.0;4.0)	(0.7;**1.8**;2.6)	(-1.0;**1.9**;13.7)	(0.7;5.0;20.0)
0.5 mm Cu	x	x	(0.0;**3.4**;9.8)	(0.8;3.7;6.2)	x	x	(-0.8;**1.6**;9.8)	(1.7;4.6;8.0)
0.6 mm Cu	x	x	(0.0;**1.4**;3.5)	(1.0;3.1;5.9)	(0.0;**3.0**;5.3)	(0.6;3.5;5.2)	(-4.4;**-0.5**;4.5)	(1.3;4.0;5.9)
0.7 mm Cu	x	x	(0.9;**7.4**;20.5)	(0.4;7.8;13.5)	x	x	(0.9;**6.0**;23.5)	(0.4;8.8;17.7)
0.8 mm Cu	x	x	(2.3;**10.5**;27.8)	(0.7;10.9;18.7)	x	x	(2.6;**8.9**;31.2)	(1.1;11.3;23.4)
0.9 mm Cu	x	x	(4.0;**14.6**;37.1)	(2.2;15.1;24.5)	x	x	(4.3;**11.9**;39.3)	(2.5;14.0;29.2)

Table 35 - (min, average, max) errors (in %) for the two models

4. Discussion

4.1 Reference kVp

The reference kVp used for the calculation of the dose output for inherent filtration is not fixed and is chosen by the user. It makes sense to use a middle value, such as 70, 80 or 90 kVp. The first model has been tested with three different values (70, 81 and 90 kVp) to estimate the impact of the reference kVp on Y_{100}. The measurement points given as inputs to the Matlab program were done at 40 kVp, kVp_{ref} and the highest measurable kVp. Table 36 shows the minimal, average and maximal deviations from the measurements over the full range of kVp for the inherent filtration at different reference kVp for the different systems. The errors stay close to each other so choosing any of these reference kVp will not influence the results too much. Nevertheless, one can notice that the average errors are slightly higher for 90 kVp (-2.4% error on average, against -1.4% for 81 kVp and 0.7% for 70 kV), so using 70 or 81 kVp will in general give better results. The average error is smaller with 70 kVp, but this reduces the errors for the low kVp (especially at 50 and 60 kVp) and increases for higher kVp. Choosing 81 kVp as reference will give higher error for low kVp, but lower for higher kVp, which are usually of interest. The user is thus advised to use 81 as reference kVp, but can also use 90 or 70 if 81 is not available on the machine.

System	*kVp_{ref} at 70*	*kVp_{ref} at 81*	*kVp_{ref} at 90*
1	(-6.0 1.3 6.5*)	(-7.7 -1.2 2.5@)	(-8.5 -2.4 1.2&)
2	(-6.9 -0.3 3.9*)	(-8.4 -2.0 1.4*)	(-9.2 -2.9 0.5*)
3	(-8.8 0.7 5.7#)	(-10.5 -1.7 2.3#)	(-11.3 -2.8 0.7#)
4	(-7.7 2.3 9.6&)	(-9.9 -0.86 7.9&)	(-10.4 -1.6 7.5&)
5	(-7.2 0.7 4.9*)	(-8.3 -1.0 3.3*)	(-9.0 -2.1 2.4*)
6	(-6.6 -0.2 3.8@)	(-8.0 -1.8 1.3@)	(-8.7 -2.8 0.4@)
7	(-8.3 0.9 6.1#)	(-9.5 -1.0 3.3#)	(-10.3 -2.2 1.9#)

Table 36 – Minimal, average and maximal errors in percent for inherent filtration for different reference kVp. The minimum error is always at 50 kVp. Maximum varies between 90 kVp (*), 100 or 102 kVp (#), 109 kVp (@) and 121 or 125 kVp (&).

4.2 Choice of measurement points

4.2.1 Calculation of output for Inherent filtration

At least three measurements are necessary for the calculation of Y_{100} for inherent filtration. The reference kVp has been discussed in 4.1 and should be chosen in the middle of the kVp range. Ideally, the two other values should be the lowest and highest ones used, namely 40 and 125 kVp if working with the complete kVp range. If other values are chosen, interpolation will introduce larger errors for kVp values lower and higher than the ones used, respectively. As an example, the program has been run for three clinical systems for measurements at 40, 81 and 133 kVp in the first case, 70, 81 and 133 kVp in the second case and 60, 81 and 121/125 kVp in the third case. The results are shown in Table 37. One can see that the interpolation at 40 kVp gives very large error (around 20% or more), interpolation should thus be avoided. As a consequence, the two other measured values should be the lowest and highest values of the range of kVp the user is interested in. However, using 40 kVp as the lowest value does introduce larger errors for 50 to 70 kVp. Since in most cases, these kVp points are frequently used, using 60, 81 and 121/125 kVp representing minimum, typical medium, and maximum kVp values clinically used, may be a good compromise.

	kVp	*40*	*50*	*60*	*70*	*81*	*90*	*109/110*	*121/125*	*133*
System 1	40/81/133	-0,04	-7,70	-6,15	-3,79	-0,01	2,06	2,47	2,16	0,02
	70/81/133	24,30	6,75	2,27	0,00	-0,01	-0,11	-1,29	-0,54	0,02
	60/81/121	17.68	2.84	0.01	-1.01	-0.01	0.46	-0.38	0.00	-0.27
System 3	40/81/133	0,00	-10,49	-8,64	-3,55	0,01	1,79	1,59	0,00	0,02
	70/81/133	27,19	4,02	-0,61	0,02	0,01	-0,12	-1,58	-2,24	0,02
	60/81/125	27.72	4.65	-0.01	0.42	0.01	-0.60	-3.55	-5.29	-4.54
System 7	40/81/133	0,00	-9,52	-8,16	-2,86	-0,01	1,89	3,31	1,72	0,03
	70/81/133	18,52	1,15	-2,00	-0,02	-0,01	0,31	0,58	0,30	0,03
	60/81/125	24.58	4.63	-0.01	0.90	-0.01	-0.19	-0.24	-0.01	0.23

Table 37- Errors in percent for measurements at 40 or 70 kVp, 81 and 133 kVp.

The number of measurement points is not limited to three, and the user can provide more values if available. Table 38 compares results for Y_{100} for inherent of three systems using different kVp measurements:

- three measurement points (40, 81 and 133 kVp), and
- four points available: (40, 50, 81 and 133 kVp) , (40, 60, 81 and 133 kVp) and (60, 70, 80 and 121/125) best representing the clinically used kVp range

The additional points have been chosen at 50 and 60 kVp because this is where the errors are the largest if only three points are measured. For all cases, 81 is the reference kVp.

	kVp values	*40*	*50*	*60*	*70*	*81*	*90*	*109/110*	*121/125*	*133*
System 1	40/81/133	0,0	-7,7	-6,1	-3,8	0,0	2,1	2,5	2,2	0,0
	40/50/81/133	3,6	-4,8	-3,6	-1,6	1,8	3,6	3,2	2,4	-0,3
	40/60/81/133	1,7	-5,6	-3,8	-1,2	2,6	4,5	4,1	2,9	-0,3
	60/70/81/121	17.68	2.84	0.01	-1.01	-0.01	0.46	-0.38	0.00	-0.27
System 3	40/81/133	0,0	-10,5	-8,6	-3,5	0,0	1,8	1,6	0,0	0,0
	40/50/81/133	5,6	-6,5	-5,4	-0,7	2,3	3,6	2,4	0,3	-0,3
	40/60/81/133	2,9	-7,4	-5,3	0,0	3,5	5,0	3,5	1,0	-0,4
	60/70/81/125	27.7	4.7	0.0	0.4	0.0	-0.6	-3.5	-5.3	-4.5
System 7	40/81/133	0,0	-9,5	-8,2	-2,9	0,0	1,9	3,3	1,7	0,0
	40/50/81/133	4,6	-5,9	-5,1	-0,1	2,2	3,7	4,2	1,8	-0,3
	40/60/81/133	2,4	-6,7	-5,0	0,6	3,5	5,1	5,5	2,3	-0,4
	60/70/81/125	24.6	4.5	-0.3	0.6	-0.4	-0.5	-0.4	0.0	0.4

Table 38 – Errors in percent depending on the number of measurement points.

The additional points decrease the errors at 50, 60 and 70 kVp, but they become higher for the other kVp values. As a consequence, additional points at low kVp values should only be used if accurate results are needed for this range of kVp, and are not necessary otherwise.

4.2.2 Calculation of output with added filtration

For the calculation of Y_{100} with a filtration, at least two measurements at two different kVp need to be done for at least two filters. As previously, the user should use the kVp according to the range he is interested in: the first measurement should be done for the lowest value of the range, and the second measurement for the highest to avoid interpolation. Table 39, Table 40 and Table 41 show the errors in percent for respectively system 1, 3 and 7 for different measurement points. One sees that the points that are interpolated always have larger errors, especially for higher filtrations. One the other hand, the middle values are more accurate when using 109 kVp. The user is thus advised to use the lowest and

highest kVp values he is interested in to avoid interpolation, but not to measure the highest / lowest achievable values.

Filtration	*Measurement points*	*70*	*90*	*109*	*121*	*133*
1mmAl+0.1mmCu	90/109	-2.98	1.98	3.48	4.28	3.05
	70/133	-1.85	2.54	3.66	4.28	2.91
0.2 mm Cu	90/109	-1.19	0.00	0.00	1.00	0.40
	70/133	0.00	0.46	-0.01	0.77	0.00
0.6 mm Cu	90/109	8.08	-0.03	-0.01	2.44	3.57
	70/133	0.01	-5.93	-4.70	-1.68	0.01

Table 39 – Errors in percent for the system 1 depending on the kVp chosen for the measurements.

Filtration	*Measurement points*	*70*	*81*	*90*	*110*	*125*
1mmAl+0.1mmCu	81/110	3.69	1.67	0.06	1.46	0.18
	70/125	3.76	1.31	0.58	2.51	1.41
0.2 mm Cu	81/110	0.48	0.01	0.33	0.00	2.45
	70/125	0.00	0.47	1.42	2.05	0.00
0.6 mm Cu	81/110	6.39	0.01	1.75	0.02	1.36
	70/125	0.02	4.78	5.57	2.26	0.01

Table 40 - Errors in percent for the system 3 depending on the kVp chosen for the measurements.

Filtration	*Measurement points*	*40*	*50*	*60*	*70*	*81*	*90*	*102*	*109*	*125*
1mmAl+0.1mmCu	81/109	18.87	5.81	7.42	4.04	2.36	1.02	0.81	0.99	1.76
	70/125	15.39	7.74	8.72	4.92	2.84	1.25	0.85	1.17	2.18
0.2 mm Cu	81/109	x	x	3.97	1.01	0.02	0.34	0.06	0.01	1.50
	70/125	x	x	1.94	0.04	0.25	0.58	0.71	1.02	0.03
0.6 mm Cu	81/109	x	x	x	6.40	0.01	0.90	0.83	0.00	2.44
	70/125	x	x	x	0.00	5.07	5.26	4.41	3.20	0.00

Table 41 - Errors in percent for the system 7 depending on the kVp chosen for the measurements.

The number of measurement points is not limited to two, and computations have been done to check if adding some measurements for middle kVp values improves the results. Table 41 shows the errors in percent at different kVp for the filters 0.2 and 0.6 mm Cu depending on the number of measurement points that are chosen. When no measurement is available to calculate the error, 'X' is written in the

case. Increasing the number of measurement points decrease the errors for the middle values, so that the overall error is decreased. The last column shows the average error for the kVp values in percent. One see that the average is lower when there are three measurement points. The user is thus advised to give as inputs as many measurements as he has to obtain the best accuracy.

Systems	*mmCu*	*Measurement points*	*70*	*81*	*90*	*109/110*	*121/125*	*133*	*Overall error*
1	0.2	70/133	0,0	X	2,51	-3.26	-1,42	0,0	-1.44
		70/109/133	1.18	X	-1,29	-2.05	-0.19	1.23	-0.22
	0.6	70/133	0.01	-7.89	-8.78	-7.86	-3.85	0.01	-4.73
		70/109/133	8.01	-1.91	-3.84	-4.56	-1.30	1.87	-0.29
3	0.2	70/125	0.00	0.50	0.01	0.75	0.00	X	0.25
		70/110/125	0.18	0.73	0.27	0.44	0.32	X	0.39
	0.6	70/125	0.02	5.96	7.20	3.67	0.01	X	3.37
		70/110/125	2.85	3.67	5.22	2.17	1.20	X	3.02
7	0.2	70/125	0.04	0.24	0.59	1.03	0.03	X	0.83
		70/109/125	0.27	0.52	0.27	0.66	0.42	X	0.88
	0.6	70/125	0.00	5.07	5.25	3.20	0.00	X	2.99
		70/109/125	2.46	3.07	3.50	1.85	1.07	X	2.48

Table 42 – Errors in percent depending on the number of measurement points. X: no measurement done for this kVp value.

The choice of the filter used for the measurements is also influencing the accuracy of the results. If the user is looking for Y_{100} with a high filtration, one of the measurements should also be done with a high filter, to avoid bad interpolation. As an example, Table 43 shows the errors obtained if Y_{100} is estimated for 0.4 mm Cu or 1 mm Al + 0.2 mm Cu, when different filters are used for the measurements. It results that adding an additional filter to estimate Y_{100} for a filtration of 0.4 mm Cu is not improving the results. On the other hand, if the user is looking for Y_{100} for a filtration of 1 mm Al + 0.2 mm Cu, it is helpful to add some 1 mm Al +0.1 mm Cu as new filter. To conclude, let the thicknesses of the two first filters be named x_1 and x_2 with $x_1<x_2$, the thickness of the additional third filter x_{new} and the thickness of the filtration the user wants to estimate $x_{searched}$. Adding a new filter improves the results if

$$x_{searched} < x_1 \text{ and } x_{new} < x_1$$

or

$$x_{searched} > x_2 \text{ and } x_{new} > x_2.$$

Filtration to estimate		*Filters used*	*70*	*81*	*90*	*109/110*	*121/125*	*133*
0.4	System 1	0.2 Cu/0.6 Cu	4.77	0.38	-0.42	-1.83	-1.42	-2.06
		0.2 Cu/0.3 Cu/0.6 Cu	4.27	0.02	-0.69	-1.96	-1.49	-2.07
		1Al+0.1Cu/0.2Cu/0.6Cu	6.53	1.18	-0.21	-2.56	-2.59	-3.57
	System 3	0.2 Cu/0.6 Cu	6.16	2.95	1.47	1.25	0.15	X
		0.2 Cu/0.3 Cu/0.6 Cu	6.08	2.95	1.51	1.36	0.31	X
		1Al+0.1Cu/0.2Cu/0.6Cu	9.46	4.98	2.71	1.21	0.55	X
	System 7	0.2 Cu/0.6 Cu	3.99	X	0.85	1.21	X	X
		0.2 Cu/0.3 Cu/0.6 Cu	3.76	X	1.01	1.33	X	X
		1Al+0.1Cu/0.2Cu/0.6Cu	8.57	X	0.81	1.31	X	X
1+0.2	System 1	0.2 Cu/0.6 Cu	-0.12	X	1.81	2.49	3.97	2.60
		0.2 Cu/0.3 Cu/0.6 Cu	-0.46	X	1.61	2.39	3.92	2.59
		1Al+0.1Cu/0.2Cu/0.6Cu	1.10	X	1.89	1.85	2.99	1.38
	System 3	0.2 Cu/0.6 Cu	1.63	0.46	1.66	2.94	1.98	X
		0.2 Cu/0.3 Cu/0.6 Cu	1.69	0.46	1.69	3.03	2.09	X
		1Al+0.1Cu/0.2Cu/0.6Cu	0.59	1.86	2.50	2.86	1.42	X
	System 7	0.2 Cu/0.6 Cu	4.37	2.66	1.34	0.52	1.14	0.70
		0.2 Cu/0.3 Cu/0.6 Cu	4.52	2.79	1.45	0.44	1.08	0.65
		1Al+0.1Cu/0.2Cu/0.6Cu	1.32	0.77	0.23	0.37	0.23	0.50

Table 43 – Influence on the number of filters used for the measurements

4.3 Estimation of absolute output

In many cases measurements for the total range of kVp and all filtrations will not be available to assist dosimetric calculations of e.g. patient doses. In this case the medical physicist may need to resort to either generic values, or work with a rather limited dataset.

- Generic values

Generic values are described in 3.5. No measurement is necessary to obtain Y_{100} in this case. In Figure 51, these values have been used to calculate Y_{100} with 0.3 mm Cu as filtration, and are compared with the measurements of system 1, 3 and 7. Depending on the system, the generic values might not be accurate.

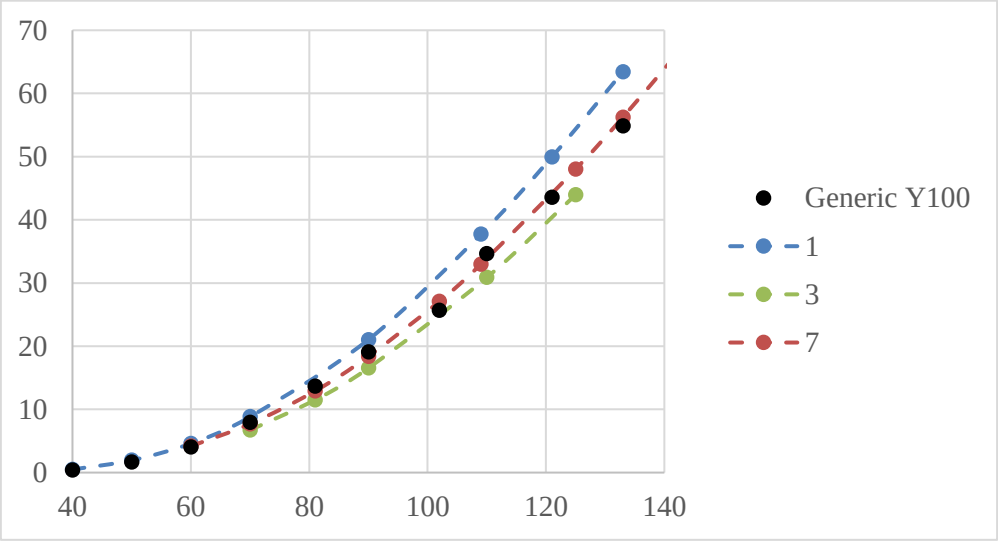

Figure 51 – Generic Y_{100} compared with measurement for 0.3 mm Cu.

- Working with a limited dataset

If there is not enough measurements available to work with the Matlab program, it is also possible to use the values from TASMICS and to correct them with one single measurement. The idea is to use the values provided by TASMICS to obtain the absolute dose output for all the kVp values, and to scale them with the measurement point. As the dose output of the inherent filtration is needed to obtain the dose output with filtration (it is multiplied with the DRF), the measurement point should be done for the inherent filtration. Let's consider the user can only measure the dose output at 70 kVp for the inherent filtration. The results are plotted in Figure 52 for system 1, 3 and 7. Depending on the system used, large errors (up to 10%) can already be seen for high kVp. For the additional filtration, one can use the DRF obtained with TASMICS. They are multiplied with the absolute dose output of the inherent filtration obtained after scaling. This results in the absolute output with filtration. As an example, Figure 53 plots the results for a filtration of 0.3 mm Cu. As the estimation of the inherent Y_{100} was already inaccurate for some systems, the errors become even larger when a filtration is added. As a consequence,

the error goes up to 26% for system 3. On the other hand, it remains lower than 7% for system 1, showing that this method is appropriate only for a few systems.

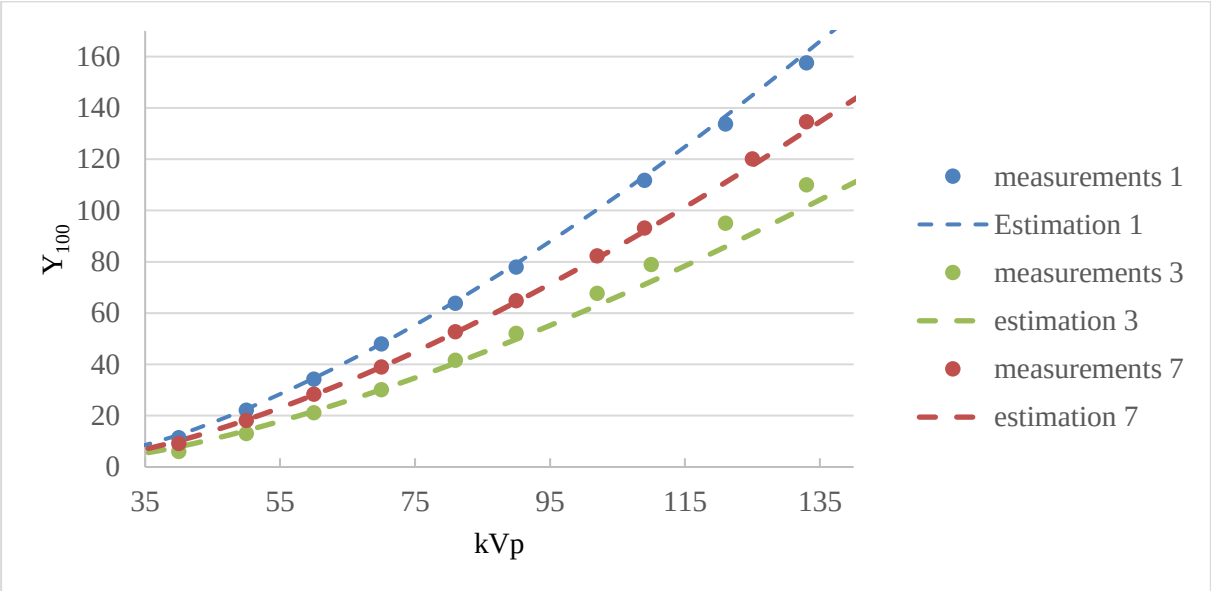

Figure 52 – Y_{100} obtained from scaling the TASMICS values, inherent filtration.

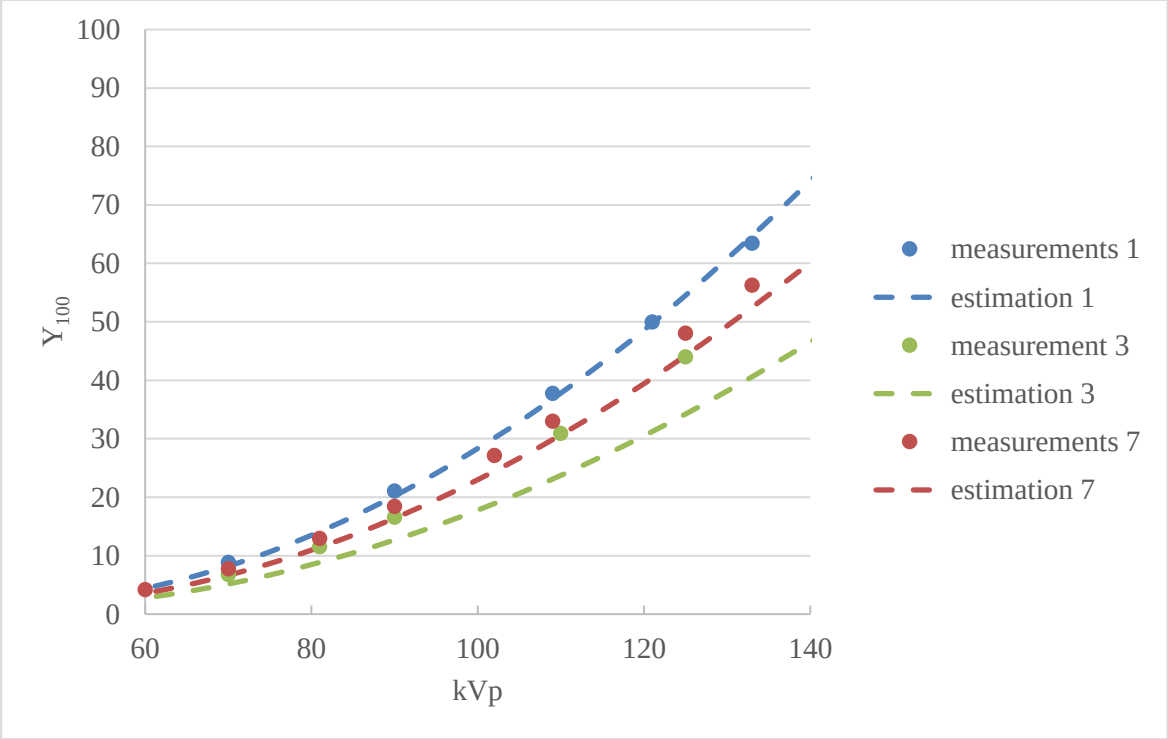

Figure 53 – Y_{100} obtained from scaling the TASMICS values, 0.3 mm Cu.

- Application of the parametrization model (model 1)

As an example, Figure 54 plots Y_{100} for a filtration of 0.3 mm Cu calculated with the Matlab program. In this case, the measurements are realised at 40, 81 and the highest achievable kVp for the inherent

filtration, and 70 and the highest achievable kVp for two filters (0.2 and 0.6 mm Cu). The results are plotted for system 1, 3 and 7. The results are very accurate, with a maximal error of 1.1% for system 1 at 70 kVp.

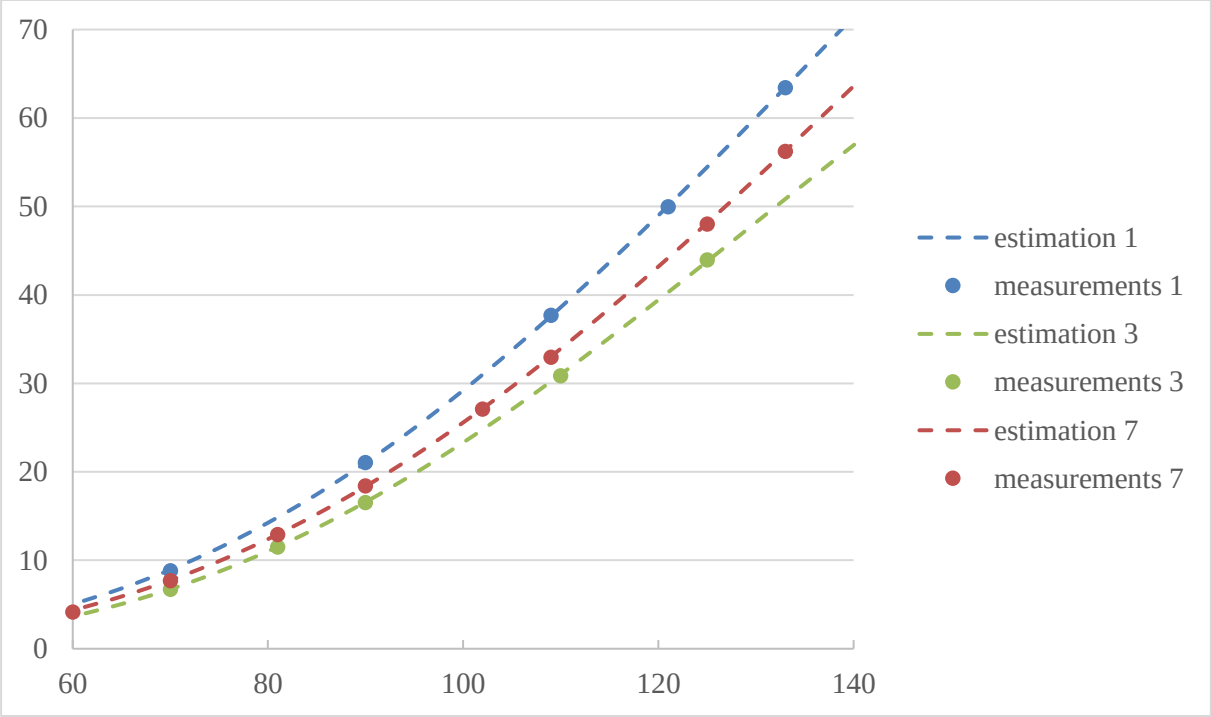

Figure 54 – Y_{100} calculated with Matlab, 0.3 mm Cu.

- Comparison of the results

The results of these three methods have been compared to the measurements results, and Table 44 shows the deviations for 0.3 mm Cu of filtration for system 1, 3 and 7. Using the Matlab program is always the best choice, as the deviations are always lower for all kVp and all systems. Using the generic values or the scaled TASMICS values might in both cases not be accurate, this depends on the system. Thereby, system 3 shows large deviation for both cases, whereas scaling the TASMICS results is more appropriate for system 1 and using the generic values is more appropriate for system 3. The bad results of the limited dataset might come from the DRF calculated with TASMICS. As discussed previously, they are too low compared to the measurements DRF, and thus introduce errors. The generic model is based on the calculation of the central value of the DRF from the measurements. As a consequence, the systems showing the highest / lowest DRF cannot be used with the generic model, as their DRF will be too far from the central value. No preference can be given to separate between those two methods when a filtration is applied. Figure 55 compares generic and limited dataset models for the inherent filtration. In this case, it is obvious that the limited dataset model is better, as the generic model is only accurate for system 7. The user is thus advised to use the limited dataset rather than the generic model if he is looking for the dose output of the inherent filtration.

kVp	*System 1*			*System 3*			*System 7*		
	Generic values	Limited dataset	Matlab program	Generic values	Limited dataset	Matlab program	Generic values	Limited dataset	Matlab program
40	-18.88	7.97	107.26	X	X	X	X	X	X
50	-14.00	5.70	28.28	X	X	X	X	X	X
60	-12.28	4.50	9.86	X	X	X	-3.08	14.41	4.94
70	-9,99	7,01	1,11	18,32	23,27	0,19	3,14	13,56	0,51
81	x	x	x	18,84	26,38	0,15	5,96	11,82	0,18
90	-9,22	3,88	-0,03	15,42	23,28	0,23	3,81	10,84	0,23
109/110	-8,12	2,38	-0,26	12,25	23,13	0,49	5,12	10,67	0,21
121/125	-12,76	0,55	0,24	3.70	22,15	0,37	-5.06	7,90	0,21
133	-13,51	-1,62	0,03	x	x	x	-2,45	8,12	0,05

Table 44 – Errors in percent – Comparison of the different method to calculate Y_{100}.

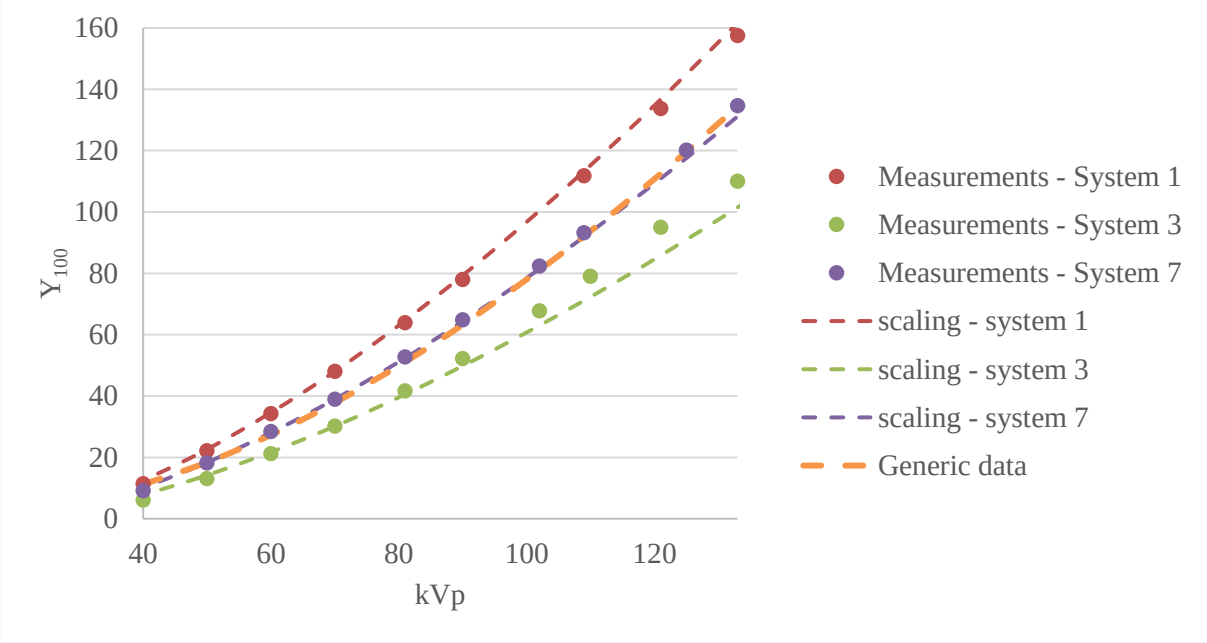

Figure 55 – Comparison of generic and limited dataset model.

- Improvement of the results

The previous result means using the DRF from TASMICS is the reason for this poor fit. In order to improve the results, two solutions are tested:

- First case: the generic DRF are used instead of the ones from TASMICS
- Second case: one additional measurement point at the filtration of interest is available

In the first case, the estimation of the absolute dose output for the inherent filtration with a limited dataset is kept the same. The difference is in the use of DRF: in the first case, DRF calculated with TASMICS were used. This new approach will use the DRF from the generic model, as it has been shown previously that those DRF were more accurate than the DRF calculated with TASMICS. The process is the same, only the DRF change. Once again, the errors between the measurements and the limited dataset model with generic DRF are collected. They can be seen in Table 45. For system 1, the errors were already low when using the DRF from TASMICS, and they are now a bit higher. On the other hand, the errors for system 3 and 7 are now greatly reduced, the user is thus advised to use the limited dataset with the generic DRF. The values are also compared to the values of the generic model in Table 44. It now seems that the limited dataset model with generic DRF is overall better than the generic model. It makes sense, as the DRF used are the same in both models, and the dose output for the inherent filtration is better estimated with the limited dataset model, as seen with Figure 55.

kVp	*System 1*	*System 3*	*System 7*
40	16.61%	X	X
50	10.64%	X	X
60	9.51%	X	-1.86%
70	10.60%	-8.74%	2.80%
81	X	-10.93%	2.63%
90	10.65%	-11.69%	2.64%
102	X	X	-0.82%
109/110	11.24%	-14.69%	3.22%
121/125	2.79%	-26.68%	-13.26%
133	0.42%	X	-8.12%

Table 45 - Y_{100} for a filtration of 0.3 mm Cu determined with the limited dataset used with generic DRF – Errors between this model and the measurements.

In the second case, one measurement point is available for the filtration of interest. The absolute dose output obtained from the limited dataset model is thus scaled to correct it thanks to the known measurement point. Let's consider the user has done a measurement at 90 kVp with a filtration of 0.3 mm Cu. The previous dose output (obtained with the limited dataset model) is scaled so that the result

at 90 kVp is now correct. Table 46 shows the errors in this new case. As mentioned, the errors at 90 kVp is always 0. The errors are much lower than in Table 44, and the model now gives accurate results. The user is thus advised to use this scaled limited dataset model.

kVp	*System 1*	*System 3*	*System 7*
40	1.13%	X	X
50	1.89%	X	X
60	0.64%	X	4.00%
70	3.25%	-0.02%	3.05%
81	X	4.03%	4.86%
90	0.00%	0.00%	0.00%
109/110	-4.29%	-0.21%	-4.33%
121/125	-1.21%	-1.48%	-3.30%
133	0.32%	X	1.68%

Table 46 – Errors between measurements and scaled limited dataset model, when a measurement is done at 0.3 mm Cu, 90 kVp (used for scaling).

The same procedure can be applied to the limited dataset model with generic DRF. The results are shown in Table 47. The errors are very low, except for high kVp and 40 kVp where they are higher than when using the scaled limited dataset model with DRF from TASMICS. The user should thus use this model instead of the previous one only if he is not interested in high kVp values. He can in any case use the scaled limited dataset with DRF from TASMICS which results in low errors.

kVp	*System 1*	*System 3*	*System 7*
40	5.39%	X	X
50	-0.01%	X	X
60	-1.03%	X	-4.38%
70	-0.05%	3.33%	0.16%
81	X	0.86%	-0.01%
90	0.00%	0.00%	0.00%
109/110	X	-3.40%	-3.37%
121/125	0.53%	-16.98%	0.57%
133	-7.11%	X	-15.48%

Table 47 - Errors between measurements and scaled limited dataset model with generic DRF, when a measurement is done at 0.3 mm Cu, 90 kVp (used for scaling).

4.4 Example of calculations

- Mobilett

In order to test the model, it has been run for a system 9. The measurements for the inherent filtration are done at 50, 81 and 121 kVp. Two additional filters are used: 0.1 mm Cu and 0.3 mm Cu, with measurements at 70 and 121 kVp.

Figure 56 shows estimated (dashed line) and measured (points) Y_{100} for the filtrations usually used with this Mobilett. Table 48 shows the errors in percent for all the kVp where measurements have been done. One can see that the interpolated values at the extremities of the kVp range always give large errors, especially for high filtrations. Nevertheless, except for the inherent filtration, kVp lower than 60 are usually not used, so the extremely high errors found in Table 48 are not an issue for doctors and physicists. For the usual kVp range, errors are always lower than 6 %, the model is thus accurate.

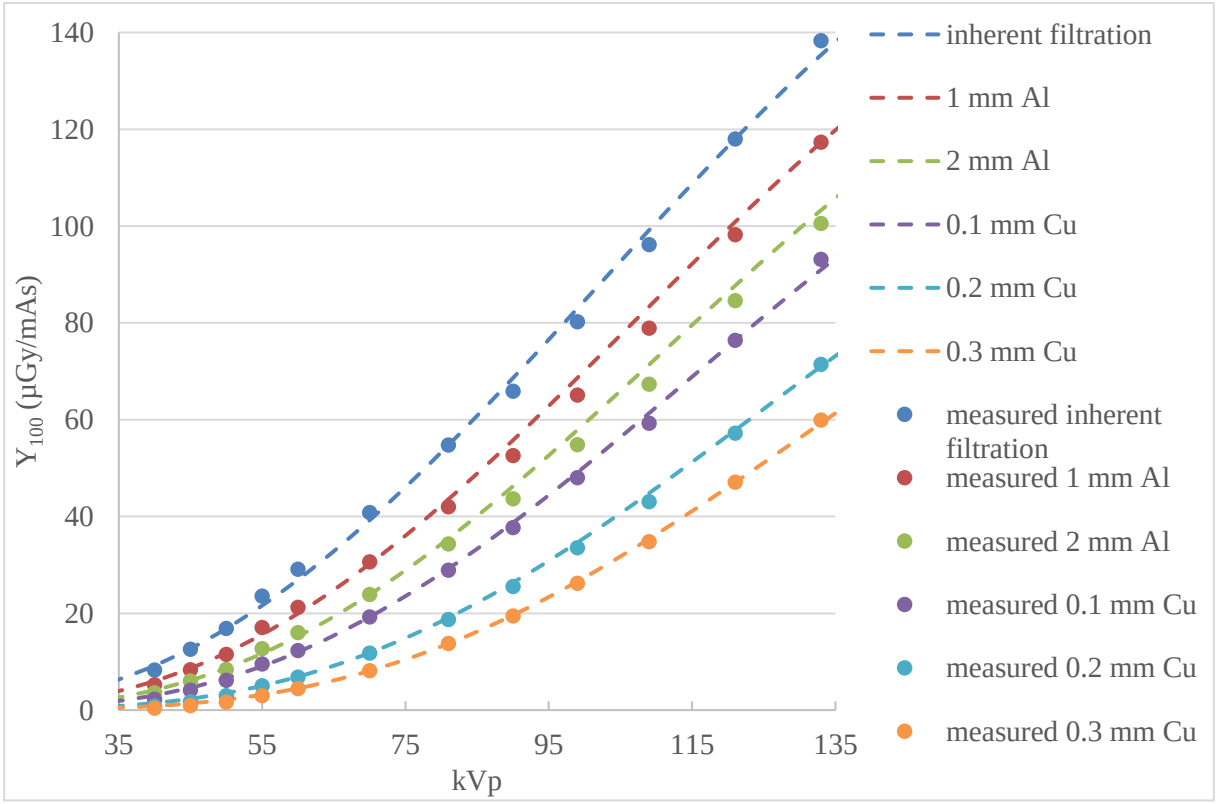

Figure 56 – Estimated (dashed line) and measured (points) Y_{100} for different filtrations. Estimations based on measurements at 50, 70, 81 and 121 kVp

kVp	*Inherent filtration*	*1 mm Al*	*2 mm Al*	*0,1 mm Cu*	*0,2 mm Cu*	*0,3 mm Cu*
40	11,30	15,62	16,73	37,66	74,87	114,87
45	1,24	3,82	2,75	12,69	34,11	49,68
50	0,00	2,95	2,96	7,39	19,44	30,52
55	-8,34	8,38	7,81	4,34	0,46	5,96
60	-7,44	6,03	4,71	2,28	1,18	2,08
70	-3,82	1,42	0,11	0,00	0,59	0,03
81	0,01	3,83	3,18	1,22	1,84	0,05
90	4,10	6,02	6,00	2,72	3,08	0,86
99	3,48	5,47	5,60	2,29	3,35	1,48
109	3,15	5,67	5,99	3,60	4,15	1,71
121	0,00	2,72	3,64	0,00	1,06	0,01
133	-2,13	0,05	2,71	2,27	0,60	1,00

Table 48 – Errors in percent between the estimated and measured Y_{100}

The Matlab program also allows to determine Y_{100} for higher filtration, even if they are usually not used. Figure 57 shows Y_{100} estimated and measured for a filtration of 0.5 mm Cu and 0.9 mm Cu. The deviations are in Table 49. Once again, the results for kVp lower than 70 are not relevant for physicists. 0.5 mm Cu still gives good results, as the errors are lower than 10% except at 70 kVp. On the other hand, 0.9 mm Cu has larger errors and only the higher kVp values give errors lower than 10%. Table 49 also shows the errors if the generic model is used to estimate Y_{100} for these two filtrations. It results that, for this system, using the generic model is more appropriate than using the interpolated values from the Matlab model.

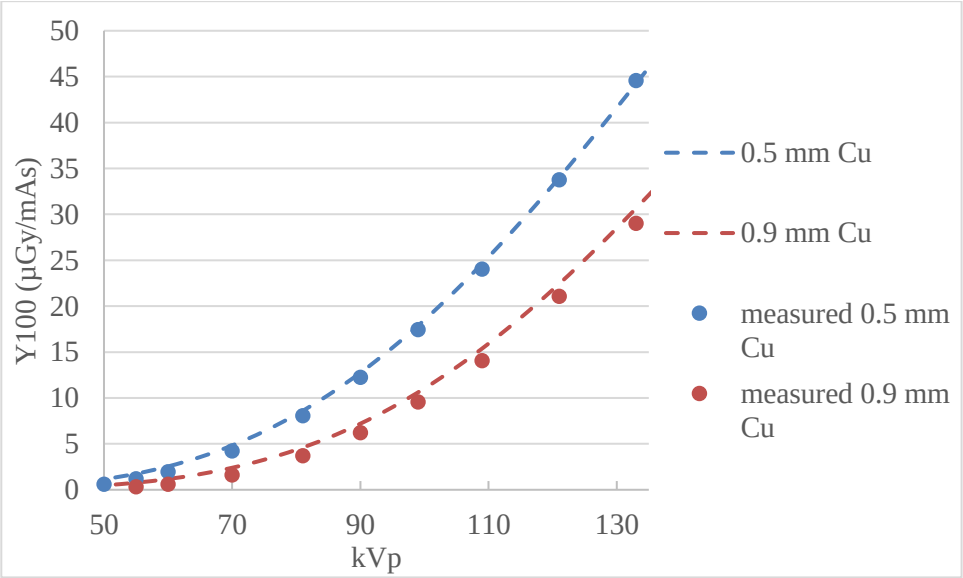

Figure 57 – Y_{100} estimated (dashed line) and measured (points) for higher filtrations

kVp	*0.5 mm Cu*		*0.9 mm Cu*	
	Matlab model	Generic model	Matlab model	Generic model
50	99,29	X	X	X
55	47,21	X	154,81	X
60	29,81	X	100,33	X
70	14,50	-0,04	50,23	-0,19
81	6,72	-0,66	24,55	1,54
90	4,34	-0,48	16,22	1,17
99	2,63	X	11,03	X
109	2,52	1,32	9,57	4,73
121	0,67	-6,00	6,54	-4,75
133	0,74	-9,38	5,69	-8,06

Table 49 – Errors in percent between estimated and measured Y_{100} for the Matlab and the generic model

- System 7

The model has also been tested with system 7. The measurements for the inherent filtration are done at 70, 90 and 125 kVp. Two additional filters are used: 1 mm Al + 0.1 mm Cu and 0.3 mm Cu, with measurements at 70 and 125 kVp.

Figure 58 shows estimated (dashed line) and measured (points) Y_{100} for the filtrations usually used with system 7. Table 50 shows the errors in percent for all the kVp where measurements have been done. Once again, large errors are seen for interpolated values, but otherwise the model is accurate with errors lower than 10 %.

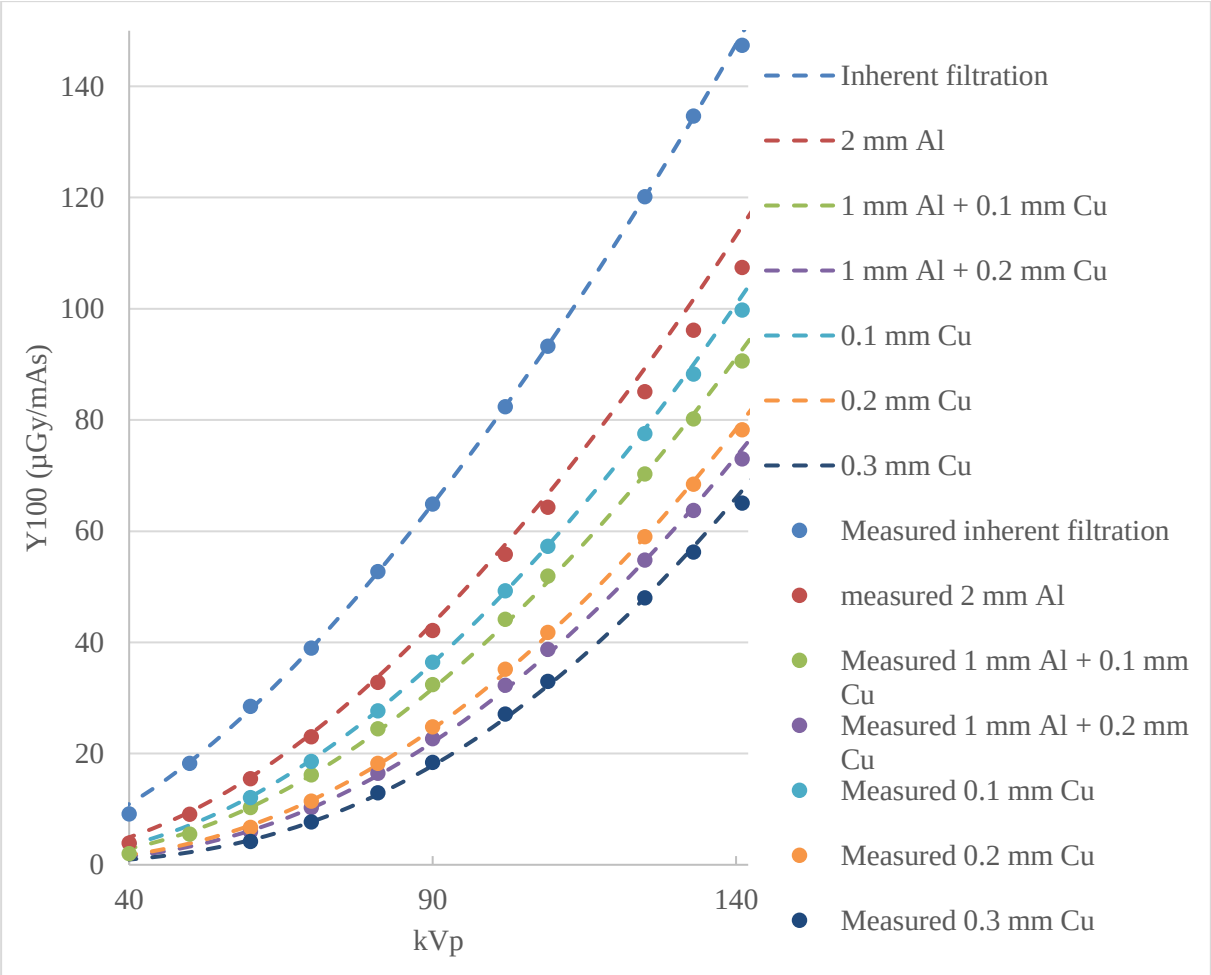

Figure 58 – Estimated (dashed line) and measured (points) Y_{100} for different filtrations. Estimations based on measurements at 70, 90 and 125 kVp for the inherent filtration, and 70 and 125 kVp for the filters (1 mm Al + 0.1 mm Cu and 0.3 mm Cu).

kVp	*Inherent filtration*	*2 mm Al*	*1 mm Al+0.1 mm Cu*	*1 mm Al+0.2 mm Cu*	*0,1 mm Cu*	*0,2 mm Cu*	*0,3 mm Cu*
40	19.67	26.78	46.65	x	x	x	x
50	1.75	4.93	8.34	x	x	x	x
60	-1.73	2.02	0.72	2.94	1.25	1.25	6.75
70	0.01	2.40	0.02	1.07	1.44	1.44	0.00
81	-0.19	3.09	1.73	2.35	0.40	0.40	1.93
90	0.00	3.06	2.29	2.67	0.37	0.37	3.03
102	0.15	3.23	1.86	2.30	0.28	0.28	2.63
109	0.19	3.72	1.88	2.02	0.29	0.29	2.26
125	0.00	5.05	0.01	0.06	1.15	1.15	0.01
133	-0.16	5.80	1.14	1.00	2.02	2.02	1.72
141	1.44	6.91	2.21	2.46	2.59	2.59	3.50

Table 50 – Errors in percent between the estimated and measured Y_{100}

The model is also tested for filtrations higher than these for which measurements are available. In the following, output for 0.4 and 0.6 mm Cu are estimated from measurements up to 0.3 mm Cu. Results are shown in Figure 59. The same inputs as previously were used. Table 51 shows the errors between estimated and measured Y_{100} for these two filtrations. For 0.4 mm Cu, only 4 points have been measured (at 70, 90 and 109 kVp), which explains why some errors could not be calculated, and are thus marked with 'X' (at 81, 102 and 125 kVp). Even though the values are interpolated, the errors remain lower than 10%, except for the point at 70 kVp and 0.6 mm Cu. The interpolation is thus efficient in this case.

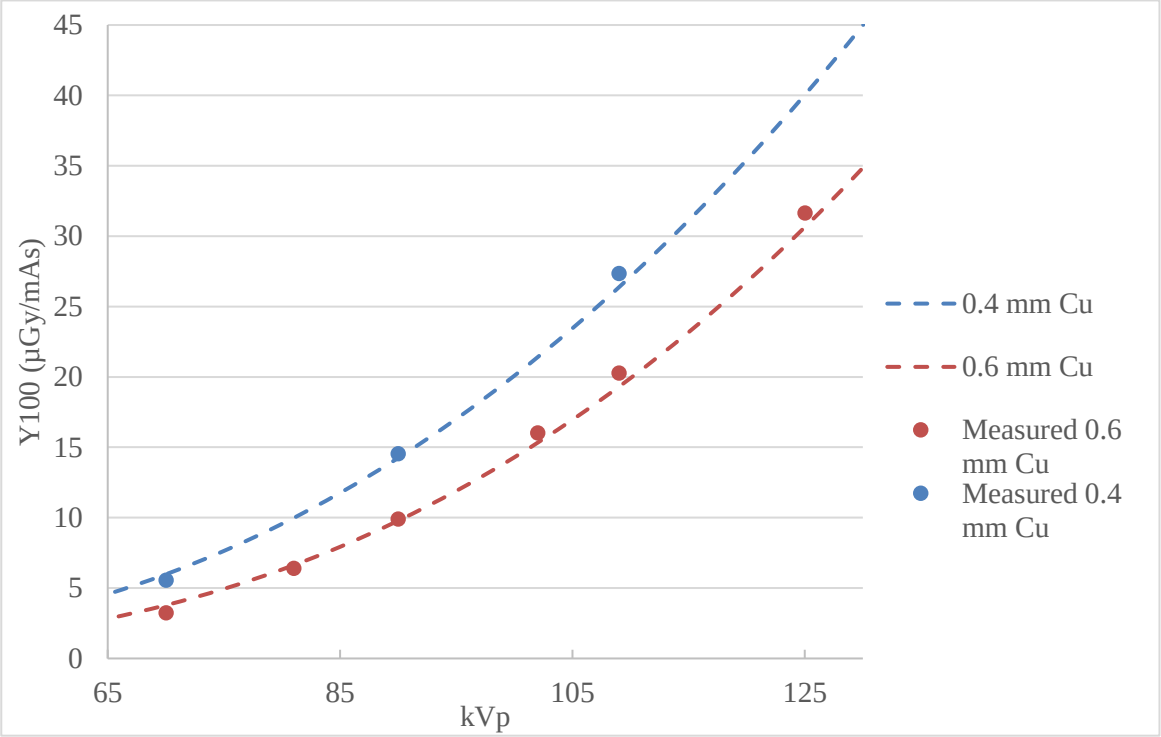

Figure 59 – Y_{100} estimated (dashed line) and measured (points) for higher filtrations

kVp	*0.4 mm Cu*	*0.6 mm Cu*
70	7,83	17.41
81	X	3.73
90	2,01	1.04
102	X	4.35
109	3,56	4.75
125	X	3.18

Table 51 – Errors in percent between estimated and measured Y_{100}

It can also happen that only one measurement point is available. In this case, the user has to use either the generic or the limited dataset model (with DRF from TASMICS). Table 52 shows the errors between estimated and measured Y_{100} for both of these models. To calculate the error at 121 kVp between the

generic model and the measurements, the measured dose output had to be interpolated, as no measurement has been done at this kVp. No generic DRF are available at 40 kVp for 2 mm Al filtration and 40 and 50 kVp for 1 mm Al + 0.1 mm Cu, so the DRF from TASMICS are used. It results in higher errors, as it is known that TASMICS is not precise enough. For the other results, this table shows that the generic model is much more appropriate, as the limited dataset model has errors up to -18%, against maximum -9% for the generic model. One can notice that the errors for the inherent filtration are low for the limited model, but high when a filtration is added. It means that DRF calculated with TASMICS are not appropriate for this system. DRF from the generic model could thus be used to improve the results, as it has been shown that they are more accurate than DRF calculated with TASMICS.

kVp	*Inherent filtration*		*2 mm Al*		*1 mm Al + 0.1 mm Cu*		*1 mm Al + 0.2 mm Cu*		*0.1 mm Cu*		*0.2 mm Cu*		*0.3 mm Cu*	
	Generic	Limited dataset	Generic	Limited dataset	Generic	Limited dataset	Generic	Limited dataset	Generic	Limited dataset	Generic	Limited dataset	Generic	Limited dataset
40	-4,18	11,74	-12,63	1,88	-23.82	-11,17	X	X	X	X	X	X	X	X
50	-3,42	0,78	-3,36	-6,19	-20.33	-16,86	X	X	X	X	X	X	X	X
60	-2,52	-1,29	0,61	-6,30	-7,45	-15,54	-9,13	-18,39	-1,96	-9,91	-3,88	-13,02	-3,08	-14,41
70	0,33	0,00	2,90	-6,14	-0,62	-13,43	-0,94	-16,74	3,61	-8,26	3,15	-12,52	3,14	-13,56
81	0,08	-3,07	2,94	-8,50	1,24	-15,92	2,34	-17,97	4,72	-11,11	5,57	-14,87	5,96	-15,17
90	0,31	-0,82	2,91	-5,92	-0,29	-12,37	0,43	-13,37	3,24	-8,25	3,77	-10,19	3,81	-10,84
102	-8,89	-4,73	-6,71	-10,03	-8,93	-15,39	-8,15	-16,86	-6,73	-11,98	-6,13	-14,22	-5,15	-15,13
109	2,08	0,24	4,35	-3,84	1,33	-8,67	2,14	-9,20	4,33	-4,93	4,89	-6,21	5,12	-6,98
121*/125**	1.55	-2,12	2.76	-4,77	1.85	-8,38	2.66	-9,49	1.65	-5,81	1.57	-7,23	-0.65	-7,90
133	-0,65	-6,43	-0,02	-8,63	-2,07	-11,94	-3,04	-13,77	-1,22	-9,61	-2,63	-11,56	-2,45	-12,34

Table 52 – Errors in percent between measured and estimated Y_{100} (generic and scaling models).: for generic model, **: for limited dataset model*

Table 53 shows the errors between the measurements and the limited dataset model with generic DRF. As foreseen, the errors are reduced compared to Table 52 (max 12%). Except for high kVp, they are also lower than the errors of the generic model. For this system, the user is thus advised to use the limited dataset model with the generic DRF.

	40	*50*	*60*	*70*	*81*	*90*	*102*	*109*	*125*	*133*
Inherent filtration	11.74%	0.78%	-1.29%	0.00%	-3.07%	-0.82%	-4.73%	0.24%	-3.58%	-6.43%
2 mm Al		0.85%	1.88%	2.56%	-0.30%	1.75%	-2.45%	2.48%	-2.58%	-5.84%
1 mm Al+0.1 mm Al			-6.28%	-0.95%	-1.95%	-1.41%	-4.76%	-0.50%	-6.90%	-7.76%
1 mm Al+0.2 mm Cu			-7.98%	-1.26%	-0.88%	-0.70%	-3.95%	0.31%	-7.70%	-8.68%
0.1 mm Cu			-0.72%	3.27%	1.43%	2.08%	-2.47%	2.46%	-5.12%	-6.96%
0.2 mm Cu			-2.67%	2.81%	2.25%	2.60%	-1.84%	3.00%	-6.20%	-8.29%
0.3 mm Cu			-1.86%	2.80%	2.63%	2.64%	-0.82%	3.22%	-6.21%	-8.12%

Table 53 - Errors between the measurements and the limited dataset model with generic DRF. Empty cases: no generic DRF available or no measurement available to calculate the errors.

4.5 Comparison of Austrian standards and generic model developed in this work

The Austrian standards are usually used to estimate the Y_{100} of an x-ray system (ÖNORM S 5234-10, 2005). It gives a set of parameters (a, b, c) which estimate the Y_{100} according to:

$$Y_{100} = a * U^2 + b * U + c$$

Coefficients	*Additional filtration*						
	0 mm Al	0.5 mm Al	1.5 mm Al	2.5 mm Al	0.1 mm Cu	0.2 mm Cu	0.3 mm Cu
a	0.0037	0.0045	0.0055	0.0060	0.0069	0.0076	0.0076
b	1.38	1.09	0.66	0.38	0.22	-0.20	-0.39
c	-41.51	-36.30	-27.10	-20.00	-16.50	-3.80	3.35

Table 54 – Coefficients estimating Y_{100} according to (ÖNORM S 5234-10, 2005)

The generic model and the Austrian standards are compared in Table 55. It shows the errors relative to the measurements for system 1, 3 and 7. It results that the Austrian standards always have very large errors (min 20%), whereas the generic model highly depends on the system. For system 7, the max error is 9%, whereas it is 44.6% for system 3. Nevertheless, even when the errors are high, they always remain lower than the errors from the Austrian standards. The user is thus advised to always use the generic model rather than the Austrian standards.

	Inherent filtration						*0.1 mm Cu*					
System	1		3		7		1		3		7	
	Generic	Standard	Generic	Standard	Generic	Standard	Generic	Standard	Generic	Standard	Generic	Standard
40	-23,6%	71,4%	44,6%	224,0%	-4,2%	114,8%	-20,8%	260,3%	X	X	X	X
50	-20,6%	65,8%	35,1%	182,1%	-3,4%	101,7%	-16,9%	121,3%	X	X	X	X
60	-19,0%	59,4%	30,7%	157,4%	-2,5%	91,9%	-15,25	77,6%	X	X	-2,0%	105,4%
70	-18,6%	52,4%	29,7%	142,8%	0,3%	87,9%	-13,2%	52,3%	22,1%	114,3%	3,6%	81,9%
81	-17,4%	48,0%	26,7%	126,9%	0,1%	79,3%	X	X	21,3%	89,5%	4,7%	63,6%
90	-16,5%	44,5%	24,7%	115,9%	0,3%	73,7%	-11,7%	31,4%	18,2%	75,8%	3,2%	53,5%
102	X	X	10,8%	103,4%	-8,9%	67,2%	X	X	X	X	-6,7%	45,7%
109	-14,9%	36,8%	20,5%	96,3%	2,1%	64,0%	-10,8%	22,4%	15,2%	61,1%	4,3%	43,2%
125	-14,5%	34,4%	20,4%	89,0%	-0,4%	57,2%	X	X	9,8%	55,9%	-2,0%	39,1%
133	-15,1%	31,7%	21,6%	88,6%	-0,7%	54,1%	-14,6%	19,6%	X	X	-1,2%	38,4%
	0.2 mm Cu						0.3 mm Cu					
System	1		3		7		1		3		7	
	Generic	Standard	Generic	Standard	Generic	Standard	Generic	Standard	Generic	Standard	Generic	Standard
70	-11,5%	45,4%	20,1%	97,4%	3,2%	69,6%	-10,0%	50,5%	18,3%	97,8%	3,1%	72,4%
81	X	X	20,4%	86,7%	5,6%	63,8%	X	X	18,8%	87,9%	6,0%	67,5%
90	-10,4%	38,6%	16,7%	80,5%	3,8%	60,5%	-9,2%	41,7%	15,4%	80,2%	3,8%	62,0%
102	X	X	X	X	-6,1%	56,1%	X	X	X	X	-5,2%	57,4%
109	-9,5%	36,7%	13,7%	71,8%	4,9%	54,9%	-8,1%	35,6%	12.3%	69.8%	5,1%	55,1%
133	-13,3%	35,3%	X	X	-2,6%	52,1%	-13,5%	35,4%	X	X	-2,4%	52,8%

Table 55 – Comparison of the errors of the generic model and the Austrian standards.

4.6 Limitations of the study

4.6.1 Actual vs nomial filter's thickness

Table 13 shows that the actual thickness of the filter differs from the nominal thickness. TASMICS has been used to estimate the impact of using the nominal thickness instead of the actual. The absolute dose output has been calculated for the nominal thickness and for actual thickness according to the values in Table 13. The results are shown in Table 56 and Figure 60 plots the errors that appear when using the nominal thickness instead of the actual. In this example the nominal thickness is 0.1 and three larger thicknesses have been tested: 0.102 mm Cu, 0.105 mm Cu and 0.107 mm Cu. One can see that the errors rise up to 5% in the worst case.

	60	*70*	*80*	*90*	*100*	*110*	*120*	*130*
0.1 mm Cu	13,31	20,83	30,04	40,80	52,98	66,49	81,27	97,41
0.102 mm Cu	13,12	20,57	29,71	40,40	52,52	65,96	80,69	96,76
0.105 mm Cu	12,84	20,19	29,23	39,83	51,84	65,19	79,82	95,81
0.107 mm Cu	12,65	19,95	28,92	39,45	51,40	64,69	79,26	95,19

Table 56 – Nominal vs actual thickness – Absolute dose output.

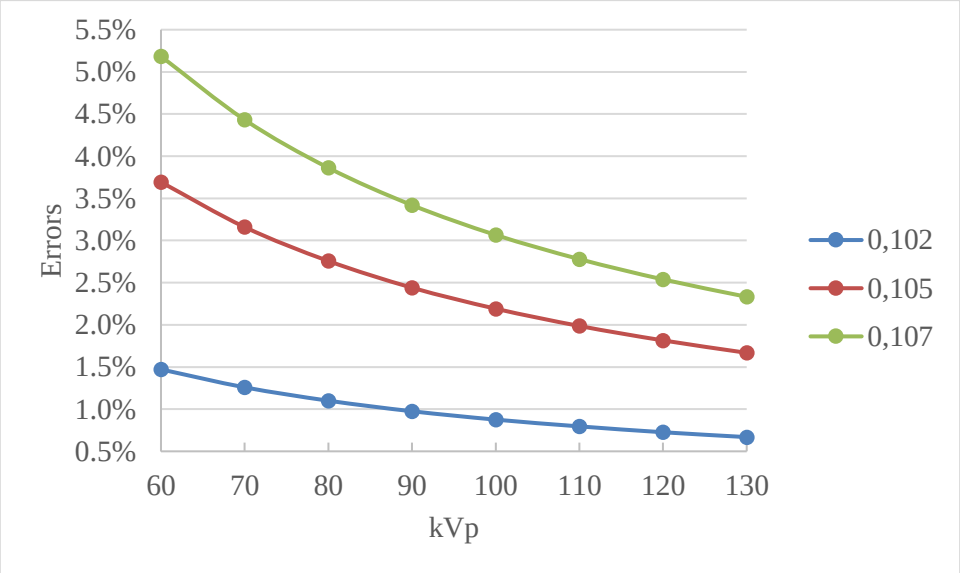

Figure 60 – Error - Nominal filter thickness (0.1 mm Cu) vs actual thicknesses.

The simulation have been run for other thicknesses, the results are plotted in Figure 61, Figure 62, Figure 63 for a nominal thickness of respectively 0.3 mm Cu, 0.8 mm Cu and 1 mm Al. The filter can be one large sheet of copper/Aluminum, but it can also be a superposition of thin sheets of copper/Aluminum. In this case, the actual thicknesses add up and the difference between the nominal and the total actual

thickness can be large. This explains why an actual thickness of 0.82 mm Cu has been tested. It results in high error (5%), which should not be neglected.

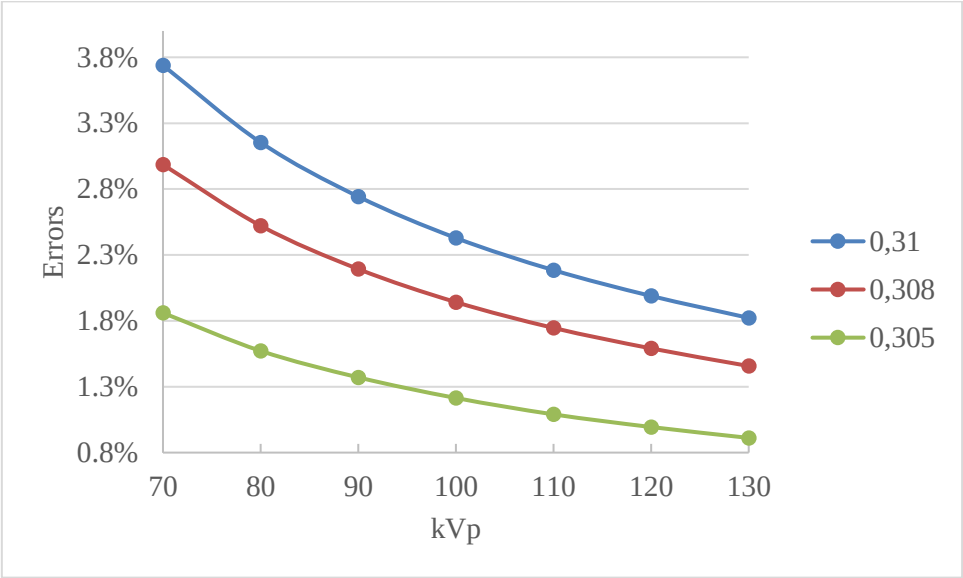

Figure 61 - Error - Nominal filter thickness (0.3 mm Cu) vs actual thicknesses.

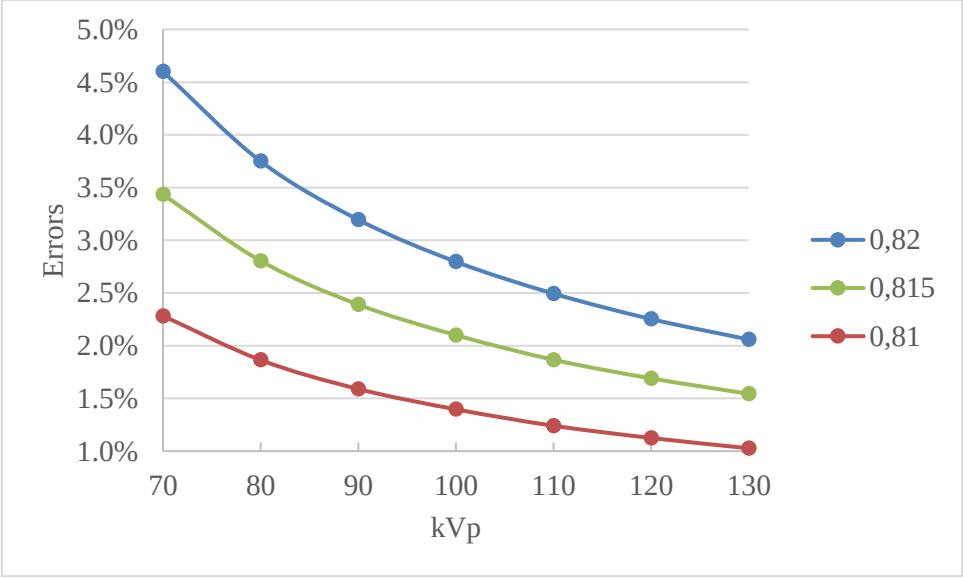

Figure 62 - Error - Nominal filter thickness (0.8 mm Cu) vs actual thicknesses.

Contrary to the copper filters, the Aluminum filters used for the measurements were a bit thinner than the nominal thickness (minimum 0.991 mm Al). Figure 63 shows that the errors from the nominal thickness are this time small, and can be neglected.

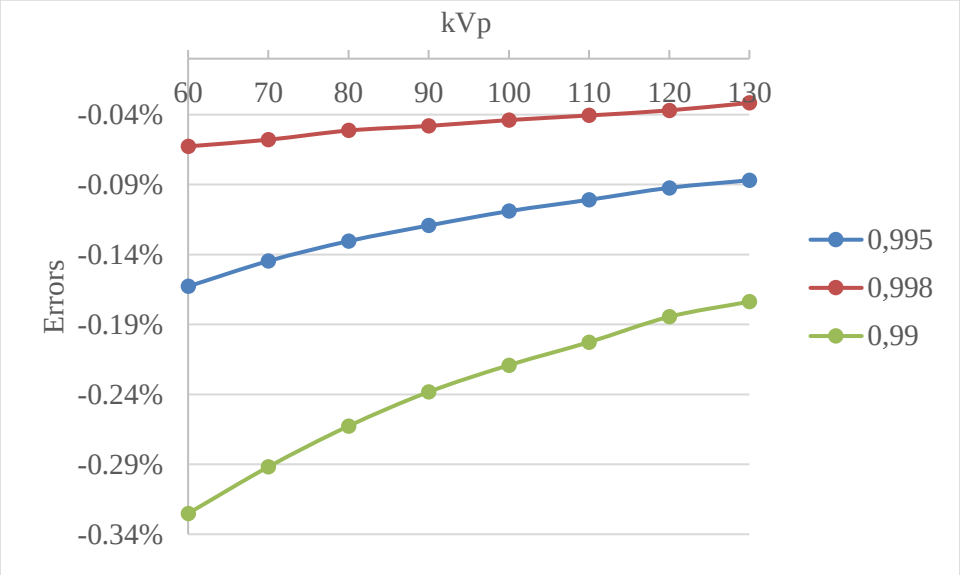

Figure 63 - Error - Nominal filter thickness (1 mm Al) vs actual thicknesses.

From these figures, one sees that the higher the filtration is and the lower the kVp is, the higher the error will be. The user should thus be careful with the results when using the model in these conditions.

4.6.2 Shot to shot variation

From one shot to the other, systems do not give the same output. Each measurement has been realised three times on system 9 to characterize these variations. Table 57 shows the standard deviations that result from these three shots. The cases marked with 'X' indicate that no measurement has been done for this kVp value, and thus no standard deviation can be measured. The higher the standard deviation is, the more the data varies. From this table, one can see that, although there are some variations in the results, the standard deviations are very low (maximum 0.62 for the higher kVp), so these variations canbe neglected. Shot to shot variations is thus not a limitation.

kVp	*Inherent filtration*	*0.1 mm Cu*	*0.2 mm Cu*	*0.3 mm Cu*	*0.4 mm Cu*	*0.5 mm Cu*	*0.6 mm Cu*	*0.7 mm Cu*	*0.8 mm Cu*	*0.9 mm Cu*	*1 mm Al*	*2 mm Al*	*1 mm Al+0.1 mm Cu*	*1 mm Al+0.2 mm Cu*
40	0.06	0.03	0.01	0.01	X	X	X	X	X	X	0.08	0.03	0.03	0.01
45	0.10	0.11	0.04	0.01	X	X	X	X	X	X	0.09	0.08	0.01	0.02
50	0.09	0.05	0.06	0.05	0.02	0.02	0.00	0.03	X	X	0.28	0.16	0.06	0.04
55	0.14	0.24	0.10	0.02	0.01	0.01	0.03	0.01	0.01	0.01	0.06	0.17	0.04	0.03
60	0.19	0.20	0.05	0.01	0.03	0.06	0.09	0.02	0.03	0.01	0.08	0.28	0.10	0.10
70	0.42	0.07	0.08	0.11	0.04	0.06	0.05	0.06	0.03	0.02	0.26	0.19	0.26	0.10
81	0.10	0.07	0.27	0.06	0.03	0.04	0.03	0.07	0.03	0.01	0.41	0.11	0.18	0.19
90	0.14	0.34	0.09	0.19	0.12	0.04	0.06	0.02	0.05	0.12	0.45	0.05	0.14	0.20
99	0.47	0.12	0.42	0.17	0.24	0.10	0.08	0.05	0.10	0.03	0.54	0.05	0.10	0.15
109	0.31	0.60	0.29	0.35	0.13	0.05	0.19	0.07	0.14	0.17	0.48	0.51	0.55	0.43
121	0.47	0.25	0.35	0.13	0.26	0.19	0.07	0.07	0.14	0.29	0.82	0.27	0.25	0.18
133	0.60	0.21	0.38	0.42	0.28	0.22	0.05	0.42	0.30	0.40	1.39	0.45	0.62	0.12

Table 57– Standard deviation for Y100 between the three shots performed for each measurement on system 9.

4.7 Recommendations

To sum up, the user is advised to

- use TASMICS rather than XCompW
- use the generic model rather than the Austrian standards
- if measurement points are available, use the Matlab model rather than the generic model
- when using the Matlab model, use three measurement points for the inherent filtration. If possible, the user should use 81 as reference kVp. For the additional filtrations, the user should use as many measurement points as he has.

Conclusion

A new model to estimate the dose output of x-ray systems has been developed. It is based on two major steps: first it determines the absolute dose output of the system for the inherent filtration, and then it calculates a dose reduction factor to estimate the dose output of the system when a filtration is applied. The distinctive characteristic of this new program is that it is based on some measurements, so that the results are characteristic of each system.

The program has been tested on different machines from different brands and with different filtrations. Depending on which measurements are performed and how many of them, the accuracy of the results might change, but for filters up to 0.6 mm Cu, one can expect errors lower than 10% for every kVp. For higher filtrations, errors for low kVp might be higher. In any case, the deviations are always lower than those obtained when using the Austrian standards and should thus always be preferred.

Acknowledgments

First I would like to express my thankfulness to my supervisor Dr.techn. Peter Homolka for giving me the opportunity to work on this project, for introducing me to the field of medical physics and for always being free for me when I had questions.

From the Center of Medical Physics and Biomedical Engineering, I would like to thank Dr. Michael Figl for helping me with Matlab and providing me some support for the statistics part and Ms. Angela Taubeck for helping me with the measurements.

Finally, I am grateful to Ms. Martina Dünkelmeyer and Mr. Fuchs for helping finding different x-ray systems and letting me work with them.

Bibliography

B.W. SOOLE 1976. A method of x-ray attenuation analysis for approximating the intensity distribution at its point of origin of Bremsstrahlung excited in a thick target by incident electrons of constant medium energy. *Phys Med Biol,* 21**,** 369 - 389.

BIRCH R. & MARSHALL M. 1979. Computation of bremsstrahlung X-ray spectra and comparison with spectra measured with a Ge(Li) detector. *Phys Med Biol,* 24**,** 505-17.

E. L. NICKOLOFF, H. L. B. 1993. Factors Affecting X-ray Spectra. *RadioGraphics,* 13**,** 1337 - 1348.

FAO, IAEA, ILO, OECD/NEA, PAHO & WHO 1996. International Basic Safety Standards for Protection against Ionizing Radiation and for the Safety of Radiation Sources. Vienna.

GREEN M. & COSSLETT V.E. 1968. Measurements of K, L and M shell x-ray production efficiencies. *Br. J. Appl. Phys.,* 1**,** 425.

H. A. KRAMERS 1923. On the theory of x-ray absorption and of the continuous x-ray spectrum. *Philos. Mag.,* 46**,** 836 - 871.

HERNANDEZ A. M. & BOONE J. M. 2014. Tungsten anode spectral model using interpolating cubic splines: unfiltered x-ray spectra from 20 kV to 640 kV. *Med Phys,* 41**,** 042101.

IAEA 2000a. Absorbed Dose Determination in External Beam Radiotherapy: An International Code of Practice for Dosimetry based on Standards of Absorbed Dose to Water. Vienna.

IAEA 2000b. Radiological Protection for Medical Exposure to Ionizing Radiation. Vienna: IAEA Safety Standards Series No. RS-G-1.5.

IAEA 2007. Dosimetry in diagnostic radiology: an international code of practice. IAEA technical report series 457. Vienna.

IAEA 2014. *Diagnotic Radiology Physics - A Handbook for Teachers and Students*.

ICRU REPORT 74 2006. Patient Dosimetry for X Rays Used in Medical Imaging. International Commission on Radiation Units and Measurements.

IEC 2005. IEC 61267. Medical Diagnostic X-Ray Equipment – Radiation Conditions for Use in the Determination of Characteristics. Geneva: IEC.

ILES W. J. 1987. The computation of the bremsstrahlung x-ray spectra over an energy range 15keV to 300keV.

NICKOLOFF E. L. & BERMAN H. L. 1993. Factors affecting x-ray spectra. *Radiographics,* 13**,** 1337-48.

ÖNORM S 5234-10 2005. Klinische Dosimetrie - Teil 10: Verfahren zur Ermittlung der Patientendosis in der Röntgendiagnostik. Wien.

RTI ELECTRONICS AB. 2010. *Conversion Tables between HVL and Total Filtration. Application Note 1-AN-52020-11* [Online]. Sweden. Available: http://rtigroup.com/content/downloads/application-notes/Piranha%20-%20HVL%20and%20TF%20-%20AN011.pdf [Accessed].

SIEMENS 2005. *Imaging Systems for Medical Diagnostics - Fundamentals, technical Solutions and Applications for Systems Applying Ionizing Radiation, Nuclear Magnetic resonance and Ultrasound,* Germany.

SILBERSTEIN L. 1932. Determination of the spectral composition of x-ray radiation from filtration data. *Opt. Soc. Am.,* 22**,** 265 - 280.

TUCKER D. M., BARNES G. T. & CHAKRABORTY D. P. 1991. Semiempirical model for generating tungsten target x-ray spectra. *Med Phys,* 18**,** 211-8.

UNSCEAR 2000. Sources and Effects of Ionizing Radiation (Report to the General Assembly with Scientific Annexes). New York: Scientific Committee on the Effects of Atomic Radiation, UN.

VÖLK M., HAMMER O.W. , FEUERBACH S. & STROTZER M. 2004. Dose reduction in skeletal and chest radiography using a large area flat-panel detector based on amorphous silicon and thallium-doped cesium iodide: technical background, basic image quality parameters, and review of the literature. *Eur. Radiol.,* 14**,** 827 - 834.

WHO 1982. Quality Assurance in Diagnostic Radiology. Geneva: World Health Organization.

WIKIPEDIA, C. 2018. *Dosimetry* [Online]. Wikipedia, The Free Encyclopedia. Available: https://en.wikipedia.org/w/index.php?title=Dosimetry&oldid=836986581 [Accessed]. (18.04.2018)

Appendix

Values of Figure 31 and Figure 32

kVp	*0,01*	*0,02*	*0,03*	*0,06*	*0,1*	*0,2*	*0,3*	*0,4*	*0,5*	*0,6*	*0,7*	*0,8*	*0,9*
40	0,4	0,8	0,8	4,1	12,8	X	X	X	X	X	X	X	X
50	0,4	0,9	0,4	0,2	3.0	X	X	X	X	X	X	X	X
60	0,2	0,6	0,3	0,4	0,4	X	X	X	X	X	X	X	X
70	0,01	0,2	0,03	0,2	0,01	2,0	4,8	8,3	12,2	16,5	21,1	26,1	31,3
80	0,1	0,09	0,1	0,04	0,1	0,2	0,9	1,8	3.0	4,4	5,9	7,5	9,3
90	0,1	0,2	0,2	0,04	0,2	0,5	0,8	1.0	1.0	0,8	0,5	0,2	0,3
100	0,1	0,2	0,1	0,08	0,1	0,7	1,3	1,9	2,3	2,7	2,9	3,1	3,2
110	0,1	0,2	0,1	0,09	0,04	0,6	1,2	1,8	2,3	2,8	3,2	3,5	3,8
120	0,1	0,2	0,05	0,09	0,06	0,2	0,6	1,1	1,5	1,9	2,3	2,6	2,9
125	0,09	0,2	0,02	0,06	0,08	0,08	0,3	0,7	1.0	1,3	1,6	1,9	2,1
130	0,06	0,2	0,03	0,03	0,07	0,04	0,08	0,3	0,5	0,7	0,9	1,1	1,3

Table 58 – Errors in percent shown in Figure 31 and Figure 32.

Measurements with clinical systems

For system 1 to 8, the field size is 15*15 cm. It is 12*12 cm for system 9.

System	*1*	*2*	*3*	*4*	*5*	*6*	*7*	*8*	*9*
FDD (cm)	100.15	98.6	104.3	101.7	100	98.6	107.5	106.05	95

Filtration	*kVp*	*40*	*50*	*60*	*70*	*81*	*90*	*109*	*121*	*133*
Inherent filtration	mAs	20	20	20	20	20	20	20	20	10
0.1 mm Cu	mAs			20	20		20	20	20	20
0.2 mm Cu	mAs				20		20	20	20	10
0.3 mm Cu	mAs				20		20	20	20	20
0.4, 0.5, 0.6, 0.7, 0.8 and 0.9 mm Cu	mAs				20	20	20	20	20	20

Table 59 – Filtrations and mAs used for the measurements on system 1

Filtration	*kVp*	*40*	*50*	*60*	*70*	*81*	*90*	*102*	*110*
Inherent filtration	mAs	20	20	20	20	20	20	20	20
0.1 mm Cu	mAs			20	20	20	20	20	20
0.2 to 0.9 mm Cu and 1 mm Al and 1 and 2 mm Al + 0.1 mm Cu and 1 mm Al + 0.2 mm Cu	mAs				20	20	20	20	20

Table 60 - Filtrations and mAs used for the measurements on system 2

Filtration	*kVp*	*40*	*50*	*60*	*70*	*81*	*90*	*102*	*110*	*125*	*133*
Inherent filtration	mAs	10	10	10	10	10	10	10	10	10	10
0.1 to 0.9 mm Cu and 1 mm Al and 1 mm Al + 0.1 mm Cu and 1 mm Al + 0.2 mm Cu	mAs				10	10	10		10	10	

Table 61 - Filtrations and mAs used for the measurements on system 3

Filtration	*kVp*	*40*	*50*	*60*	*70*	*81*	*90*	*102*	*109*	*125*	*133*
Inherent filtration	mAs	10	10	10	10	10	10	10	10	10	10
0.1 to 0.9 mm Cu and 1 mm Al and 1 mm Al + 0.1 mm Cu and 1 mm Al + 0.2 mm Cu	mAs				10	10	10		10	10	

Table 62 - Filtrations and mAs used for the measurements on system 4

Filtration	*kVp*	*40*	*50*	*60*	*70*	*81*	*90*	*109*	*121*	*133*
Inherent filtration	mAs	20	20	20	10	10	10	10	5	5
0.1 mm Cu	mAs			20	10		10	10	5	5
0.2 and 0.3 mm Cu	mAs				10		10	10	5	5

Table 63 - Filtrations and mAs used for the measurements on system 5

Filtration	*kVp*	*40*	*50*	*60*	*70*	*81*	*90*	*102*	*110*
Inherent filtration	mAs	20	20	20	20	20	20	20	20
0.1 mm Cu	mAs			20	20	20	20	20	20
0.2 to 0.9 mm Cu and 1 mm Al and 1 and 2 mm Al + 0.1 mm Cu and 1 mm Al + 0.2 mm Cu	mAs				20	20	20	20	20

Table 64 - Filtrations and mAs used for the measurements on system 6

Filtration	*kVp*	*40*	*50*	*60*	*70*	*81*	*90*	*102*	*109*	*125*	*133*	*141*
Inherent filtration and 2 mm Al	mAs	5	5	5	5	5	5	5	5	5	5	5
0.1 mm Cu	mAs			5	5	5	5	5	5	5	5	5
1 mm Al + 0.1 mm Cu	mAs	10	10	10	10	10	10	10	10	10	10	10

1mm Al + 0.2 mm Cu, 0.2 and 0.3 mm Cu	mAs		10	10	10	10	10	10	10	10	10
0.4 mm Cu	mAs			25		25		25			
0.6 mm Cu	mAs			25	25	25	25	25	25		

Table 65 - Filtrations and mAs used for the measurements on system 7

Filtration	*kVp*	*40*	*50*	*60*	*70*	*81*	*90*	*100*	*109*	*121*	*125*
Inherent filtration and 0.1 mm Cu	mAs	10	10	10	10	10	10	10	10	10	10
2 mmAl	mAs		10	10	10	10	10	10	10	10	10
1 mm Al + 0.1 mm Cu and 1 mm Al + 0.2 mm Cu	mAs			10	10	10	10	10	10	10	10
0.2 and 0.3 mm Cu	mAs				10	10	10	10	10	10	10
0.4 mm Cu	mAs			20	20	20	20	20	20	20	20
0.5 and 0.6 mm Cu	mAs				20	20	20	20	20	20	20
0.7, 0.8 and 0.9 mm Cu	mAs				25	25	25	25	25	25	25

Table 66 - Filtrations and mAs used for the measurements on system 8

Filtration	*kVp*	*40*	*45*	*50*	*55*	*60*	*70*	*81*	*90*	*99*	*109*	*121*	*133*
Inherent filtration, 0.1, 0.2 and 0.3 mm Cu, 1 and 2 mm Al, 1 mm al +0.1 mm Cu and 1 mm Al + 0.2 mm Cu	mAs	10	10	10	10	10	10	10	10	10	10	10	10
0.4, 0.5, 0.6 and 0.7 mm Cu	mAs			10	10	10	10	10	10	10	10	10	10
0.8 and 0.9 mm Cu	mAs				10	10	10	10	10	10	10	10	10

Table 67 - Filtrations and mAs used for the measurements on system 9

Precision of the measurements with system 9

Three shots have been taken for the measurements with system 9 to ensure the precision of the system. Table 68 shows the dose output for the inherent filtration for all shots. The results do not vary a lot between the shots, the system is thus precise enough.

kVp	*Shot 1*	*Shot 2*	*Shot 3*
40	91,67	92,36	91,19
45	138,1	140,1	139,3
50	187,7	186,1	186,3
55	261,7	262,2	259,6
60	324,3	320,6	322,9
70	454,3	454,6	447,2
81	607,8	607,2	605,8
90	728,9	730,3	731,7
99	893,8	888,3	884,5
109	1066	1062	1068
121	1313	1304	1306
133	1527	1532	1539

Table 68 - Dose output for the inherent filtration in µGy for system 9 for three different shots.

User guide for the Matlab program

This appendix gives a description of how to use the Matlab file to obtain the dose output of one clinical system. The user needs to fill only the part named 'Inputs', the rest of the program (starting from 'Program') must not be changed. In this Inputs part, the user has to enter the results of his measurements on the clinical system.

First the measurements for the inherent filtration have to be given. The kVp values at which they are performed have to be written in the vector 'kV', on the fourth line in Figure 64. The corresponding absolute dose output are to be given in the vector 'gy', line 5. The order of the values are important. If the measurement at kVp_i is the i^{th} value of kV, then the absolute dose output at kVp_i has to be the i^{th} value of the vector 'gy'. The second value of kV is the reference kVp, it should thus be chosen wisely. (70, 80 or 90 kVp seems to be the best choices)

Then the results of the measurements with additional filtrations have to be given. First the user has to fill in the vectors mmCu_filter and mmAl_filter, which define respectively the thickness of copper and of Aluminum that have been used. The i^{th} value of each vector defines the thickness of copper and Aluminum of the i^{th} filter. In Figure 64, the filters used for the measurements are thus 0.2 mm Cu and 0.6 mmCu. If one wants to use 2 mm Al as first filter, 1 mm Al and 0.1 mm Cu as second filter and 0.3 mm Cu as third filter, the vectors have to be defined in the following way:

mmCu_filter = [0; 0.1; 0.3];

mmAl_filter = [2; 1; 0];

The semi-colon are necessary and must not be forgotten.

```
1   %% Inputs
2
3   % without filtration
4   kV = [40 80 130];
5   gy = [12.5 62.5 154];
6
7   % Filtration measured, at least 2
8   mmCu_filter = [0.2; 0.6];
9   mmAl_filter = [0; 0];
10
11  kVfilter = [70 110; 70 110];
12  GY1 = [12.3 47.8; 3.26 22.2];
13
14  % Filtration that needs to be estimated
15  filtration_Al = 1;
16  filtration_Cu = 0.2;
```

Figure 64 - Screenshot - Inputs that should be given to Matlab.

The kVp used for the measurements have to be written in 'kVfilter' (line 11). The number of values between each semi-colon needs to be the same. The i^{th} set of values represents the kVp values that have been used to perform the measurements with the i^{th} filter. The corresponding absolute dose outputs are to be given in 'GY1' (line 12). Once again, the order of the value matters. So in the example of Figure 64, two filters have been used: for 0.2 mm Cu, the measurements at 70 kVp gave an absolute dose outputs of 12.3 µGy/mAs and the one at 110 kVp gave 47.8 µGy/mAs. For 0.6 mm Cu, the measurements at 70 kVp gave an absolute dose outputs of 3.26 µGy/mAs and the one at 110 kVp gave 22.2 µGy/mAs. More than two filters can be inserted, a semi-colon needs then to be inserted between the sets of values (as in between the first and second filter sets).

Finally, the user has to define which filtration he/she is interested in. The thickness of Aluminum needs to be given in 'filtration_Al' (line 15), and the one of copper in 'filtration_Cu' (line16). If no Aluminum is used, give zero as input for filtration_Al, and vice versa if no copper is used.

Once everything is filled, run the program (green arrow in Matlab). At least four graphs appears. Figure 1 shows Y_{100} for the inherent filtration, the last figure shows Y_{100} for the filtration the user is interested in, and the other figures are Y_{100} for the filters used for the measurements. To get the parameters of the equations, type:

- a, b, c and d to get the parameters a, b, c and d of $Y_{100,0}$
- x_1 to get x_1, x_2 and x_3 defining the correction function of $Y_{100,0}$
- B to get the parameters of the DRF of the filters. B(i,1) gives the parameter B for filter i, B(i,2) gives the parameter C for filter i.
- b2 and c2 to get respectively the parameters B and C of the DRF of the filtration the user is interested in.

NB: a, b c and d give the relative dose output. To get the absolute dose output, multiply the relative with the second value of 'gy'.

List of Tables

Table 1 - radiation qualities for calibrations of diagnostic dosimeters (adapted from (IAEA, 2007)).. 12
Table 2 - Characterization of radiation quality series RQR used for unattenuated beams (according to (IEC, 2005)). 12
Table 3 - Binding energies and H radiation energies of common anode materials (IAEA, 2014)..... 18
Table 4 - RQR quality standard..... 25
Table 5 - Inherent filtrations resulting in HVLs according to RQR qualities with XcompW..... 26
Table 6 - Inherent filtrations resulting in HVLs according to RQR with SPEKTR 3.0 for TASMICS 26
Table 7 – Estimation of equivalent copper thickness for Aluminum filter 31
Table 8 – Values of A in the various copper filter thickness ranges 37
Table 9 - Matrix used in Matlab to parametrize A 39
Table 10 - Additional inputs of the first model 43
Table 11 – Additional inputs of the second model..... 50
Table 12 – Clinical systems..... 52
Table 13 - Nominal and actual thicknesses of the filters used 53
Table 14 - Actual filter thicknesses used. Empty case: no measurement performed for this filtration. 55
Table 15 - Parameters describing Y_{100} calculated for the inherent filtration..... 56
Table 16 - Minimum, average and maximal deviations in percent for relative dose output between clinical systems and XCompW, or TASMICS, respectively. Numbers in brackets indicate which system has the minimal / maximal deviations. 57
Table 17 - Absolute dose outputs of clinical systems and TASMICS 59
Table 18 – Maximum negative, average and maximum positive deviations in percent for the individual systems. Inherent filtration, XCompW or TASMICS used to run the Matlab program, respectively. Max. negative deviation was always seen at 50 kVp. Max. positive at 90(*), 100 or 102 (#), 109 ($^{@}$) or 121($^{\&}$) kVp 60
Table 19 - Parameters describing $Y_{100,0}$ for the different systems 61
Table 20 - DRF measured at 70 kVp for clinically used filtrations and TASMICS 64
Table 21 - DRF measured at 109 or 110 kVp for clinically used filtrations and TASMICS 65
Table 22 - Parameter A describing the DRFs of all systems..... 67
Table 23 - Parameter B describing the DRF. 67
Table 24 - Parameter C describing the DRF 68
Table 25 - Differences between measured and calculated DRF at 70 kVp. 69
Table 26 - Differences between measured and calculated DRF at 109/110 kVp. 69
Table 27 – Generic Y_{100} 70
Table 28- Parameters for the generic dose output of the inherent filtration..... 70
Table 29 - Errors in percent between generic data and fit function. 71

Table 30 - Generic DRFs from measurements. Empty cases: not enough measurements available to calculate the central value. 72
Table 31 – DRF calculated with TASMICS..... 73
Table 32 - Parameter B..... 75
Table 33 - Parameter C..... 76
Table 34 - Parameter D 77
Table 35 - (min, average, max) errors (in %) for the two models 80
Table 36 – Minimal, average and maximal errors in percent for inherent filtration for different reference kVp. The minimum error is always at 50 kVp. Maximum varies between 90 kVp (*), 100 or 102 kVp (#), 109 kVp (@) and 121 or 125 kVp (&). 81
Table 37- Errors in percent for measurements at 40 or 70 kVp, 81 and 133 kVp..... 83
Table 38 – Errors in percent depending on the number of measurement points. 84
Table 39 – Errors in percent for the system 1 depending on the kVp chosen for the measurements.... 85
Table 40 - Errors in percent for the system 3 depending on the kVp chosen for the measurements. ... 85
Table 41 - Errors in percent for the system 7 depending on the kVp chosen for the measurements. ... 85
Table 42 – Errors in percent depending on the number of measurement points. X: no measurement done for this kVp value. 87
Table 43 – Influence on the number of filters used for the measurements 89
Table 44 – Errors in percent – Comparison of the different method to calculate Y_{100}..... 93
Table 45 - Y_{100} for a filtration of 0.3 mm Cu determined with the limited dataset used with generic DRF – Errors between this model and the measurements. 94
Table 46 – Errors between measurements and scaled limited dataset model, when a measurement is done at 0.3 mm Cu, 90 kVp (used for scaling). 95
Table 47 - Errors between measurements and scaled limited dataset model with generic DRF, when a measurement is done at 0.3 mm Cu, 90 kVp (used for scaling)..... 95
Table 48 – Errors in percent between the estimated and measured Y_{100} 97
Table 49 – Errors in percent between estimated and measured Y_{100} for the Matlab and the generic model 98
Table 50 – Errors in percent between the estimated and measured Y_{100} 99
Table 51 – Errors in percent between estimated and measured Y_{100} 100
Table 52 - Errors between the measurements and the generic or limited dataset model.....102
Table 53 - Errors between the measurements and the limited dataset model with generic DRF 104
Table 54 – Coefficients estimating Y_{100} according to (ÖNORM S 5234-10, 2005) 105
Table 55 – Comparison of the errors of the generic model and the Austrian standards..... 106
Table 56 – Nominal vs actual thickness – Absolute dose output. 107
Table 57– Standard deviation for Y100 between the three shots performed for each measurement on system 9..... 110

Table 58 – Errors in percent shown in Figure 31 and Figure 32. 116
Table 59 – Filtrations and mAs used for the measurements on system 1 117
Table 60 - Filtrations and mAs used for the measurements on system 2 117
Table 61 - Filtrations and mAs used for the measurements on system 3 118
Table 62 - Filtrations and mAs used for the measurements on system 4 118
Table 63 - Filtrations and mAs used for the measurements on system 5 118
Table 64 - Filtrations and mAs used for the measurements on system 6 118
Table 65 - Filtrations and mAs used for the measurements on system 7 119
Table 66 - Filtrations and mAs used for the measurements on system 8 119
Table 67 - Filtrations and mAs used for the measurements on system 9 119
Table 68 - Dose output for the inherent filtration in µGy for system 9 for three different shots. 120

List of Figures

Figure 1 - Cross-sectional diagram of a silicon diodes. From: (IAEA, 2014)..... 10
Figure 2 - Cross-sectional section of a MOSFET (IAEA, 2014) 11
Figure 3 – International Measurement System for radiation dosimetry. The calibration can either be done directly in a PSDL or via a SSPD which is linked to the BIPM, a PSDL or the IAEA/WHO network of SSDLs. The dashed lines indicate intercomparisons of primary and secondary standards (IAEA, 2000a). 11
Figure 4 - Components of an x-ray tube (IAEA, 2014) 13
Figure 5 - (a) Distribution of the energy fluence for a thin target bombarded with electrons of kinetic energy T. (b) Triangular spectrum obtained if a thick target is considered as a superposition of thin targets. From: (IAEA, 2014). 17
Figure 6 - (a) Ideal bremsstrahlung spectrum for a Tungsten anode and a tube voltage of 90 kVp, (b) actual spectrum includind characteristic x-rays for an inherent filtration of 1mm Be, (c) spectrum filtered with 2.5mm Al eq. From: (IAEA, 2014)..... 18
Figure 7 - X-ray spectra for different tube voltages. From: (IAEA, 2014) 19
Figure 8 - X-ray spectra for various tube voltage ripple at 70 kVp. From: (IAEA, 2014)..... 20
Figure 9 - X-ray spectra for different anode angles. From: (IAEA, 2014)..... 20
Figure 10- X-ray spectra for different filtrations (IAEA, 2014)..... 21
Figure 11- XCompW window. (A) X-ray tube settings. (B) Plotting. (C) Spectrum characteristics.... 23
Figure 12 - SPEKTR 3.0 window. (A) Plotting. (B) X-ray tube settings. (C) Added filtration. (D) Spectrum characteristics. (E) File operations. (F) Reset all. Image from (Punnoose J. et al., 2016).... 24
Figure 13 - HVL simulated and measured for the inherent filtration. 27
Figure 14 - Y_{100} simulated and measured with kVp dependent inherent filtrations resulting in HVLs according to RQR..... 27
Figure 15 - HVL measured and simulated for a total filtration of 2.41mm Al for XCompW and 2.55mm Al for TASMICS..... 28
Figure 16 - Y_{100} measured and simulated for a total filtration of 2.41mm Al for XCompW and 2.55mm Al for TASMICS..... 28
Figure 17 – Low kVp (A) – High kVp (B). Blue points: Y_{100} calculated for inherent filtration 29
Figure 18 - DRF calculated depending on kVp and thickness of copper..... 32
Figure 19 - AF calculated depending on kVp and thickness of copper..... 32
Figure 20 – Surface: AF estimated; blue points: data. 33
Figure 21 - Surface: DRF estimated; blue points: data. 34
Figure 22 - Errors in percent between the DRF calculated and the fit 34
Figure 23 - Dependence of B on filter thickness. 35
Figure 24- Dependence of C on filter thickness. 35

Figure 25 - $A*U^{-C}$ depending on kVp for range 1(A), 2 (B), 3 (C) and 4 (D). Blue points: data, black line: power fit. 36
Figure 26 - Values of A depending on the thickness of copper at 40 kvp (A), 50 kVp (B), 70 kVp (C), 90 kVp (D), 110 kVp (E), 130 kVp (F) and 150 kVp (G). 38
Figure 27 – Blue points: values of log(A); dark line: fit 39
Figure 28 – Exponential fit for A 40
Figure 29 - Dependence of B on filter thickness 41
Figure 30 - Dependence of C on filter thickness 41
Figure 31 – Errors between the simulated values and the fit for low filtrations and kVp ranging from 40 to 125 kVp when A is fixed (A) and when A is described with (25) (B) 42
Figure 32 – Errors between the simulated values and the fit for high filtrations and kVp ranging from 70 to 125 kVp when A is fixed (C) and when A is described with (25) (D) 42
Figure 33 - Dependence of dose output on filter thickness at 70kVp 44
Figure 34 - Dependence of dose output on filter thickness at U_1=70 kVp (A), U_2 = 110 kVp (B). Blue points: data; dashed line: fit from equation (29) for A and from equation (30) for B. 44
Figure 35 –Homogeneity coefficient simulated. 46
Figure 36 - Estimated function for h depending on HVL and kVp 46
Figure 37 - Error in percent between the simulated homogeneity coefficient and the fit. 46
Figure 38 - DRF simulated. 47
Figure 39 - Surface: DRF estimated; blue points: data. 48
Figure 40 - Errors in percent between the fit and the simulated data. 48
Figure 41- Errors for low filtrations,40 to 125 kVp. 48
Figure 42- Errors for high filtrations,70 to 125 kVp. 48
Figure 43 - Errors for low filtrations, A fixed,40 to 125 kVp. 49
Figure 44 - Errors for high filtrations, A fixed, 70 to 125 kVp. 49
Figure 45 - Dependence of HVL calculated on filter thickness at 70 kVp. Blue circles: simulation's values; red line: fitted power function. 51
Figure 46 - Dependence of HVL calculated on filter thickness at 70 kVp. Blue circles: simulation's values; red line: fitted power function. 51
Figure 47 - Relative dose output calculated with TASMICS and XcompW along with those measured on the clinical systems. 57
Figure 48 - Absolute dose output calculated with TASMICS and XcompW along with those measured on the clinical systems. 58
Figure 49 – Y_{100} for the inherent filtration of the clinical systems. Dashed line: estimation from Matlab program; points: measurement data; red points: input of the Matlab program. 62
Figure 50 – Function for generic output. Points: generic data; dashed line: fit of the generic data; bars: uncertainties. 71

Figure 51 – Generic Y_{100} compared with measurement for 0.3 mm Cu. 90
Figure 52 – Y_{100} obtained from scaling the TASMICS values, inherent filtration. 91
Figure 53 – Y_{100} obtained from scaling the TASMICS values, 0.3 mm Cu. 91
Figure 54 – Y_{100} calculated with Matlab, 0.3 mm Cu. 92
Figure 55 – Comparison of generic and limited dataset model. 93
Figure 56 – Estimated (dashed line) and measured (points) Y_{100} for different filtrations. Estimations based on measurements at 50, 70, 81 and 121 kVp 96
Figure 57 – Y_{100} estimated (dashed line) and measured (points) for higher filtrations 97
Figure 58 – Estimated (dashed line) and measured (points) Y_{100} for different filtrations. Estimations based on measurements at 70, 90 and 125 kVp for the inherent filtration, and 70 and 125 kVp for the filters (1 mm Al + 0.1 mm Cu and 0.3 mm Cu). 99
Figure 59 – Y_{100} estimated (dashed line) and measured (points) for higher filtrations 100
Figure 60 – Error - Nominal filter thickness (0.1 mm Cu) vs actual thicknesses. 107
Figure 61 - Error - Nominal filter thickness (0.3 mm Cu) vs actual thicknesses. 108
Figure 62 - Error - Nominal filter thickness (0.8 mm Cu) vs actual thicknesses. 108
Figure 63 - Error - Nominal filter thickness (1 mm Al) vs actual thicknesses. 109
Figure 64 - Screenshot - Inputs that should be given to Matlab. 121